EARLY CHLORIDE CORROSION OF REINFORCING STEEL IN CONCRETE(Dissertation_全文)

AUTHOR(S):

Miyagawa, Toyoaki

EARLY CHLORIDE CORROSION OF REINFORCING STEEL IN CONCRETE

February 1985

TOYOAKI MIYAGAWA

EARLY CHLORIDE CORROSION OF REINFORCING STEEL IN CONCRETE

February 1985

TOYOAKI MIYAGAWA

CONTENTS

Chapter Page

LIST OF ABBREVIATIONS

ACI : American Concrete Institute

ASCE : The American Society of Civil Engineers

ASTM : American Society for Testing and Materials

CAJ : The Cement Association of Japan

CCA : Cement and Concrete Association

CEB : Comite Euro-International du Beton

CIRIA : Construction Industry Researchand Information Association

CP : Code of Practice

DNV : Det Norske Veritas

FIP : Federation Internationale de la Precontrainte

HRR : Highway Research Record

IABSE : International Association for Bridge and Structural Engineering

ICE : The Institution of Civil Engineers

JCI : Japan Concrete Institute

JPCEA : Japan Prestressed Concrete Engineering Assiciation

JSCE : The Japan Society of Civil Engineers

JSMS : The Society of Materials Science, Japan

NCHRP : National Cooperative Highway Research Program

RILEM : The International Union of Testing and Research Laboratories for Materials and Structures

SCI : Society of Chemical Industry

TRB : Transportation Research Board

1 INTRODUCTION

1.1 General

Land of Japan consists of a plenty of islands surrounded by seas. Many concrete structures have been constructed in marine environment. And, the sea sand having salt is being increasingly used as fine aggregate for concrete, particularly in Kansai area. Consequently, various kinds of reinforced concrete structures in Japan are more or less under chloride attack .

It is well known that the reinforcing steel in concrete has a tendency of corroding in chloride environment, although concrete is inherently durable. As a result, the corrosion of reinforcing steel is one of the most critical problems from the viewpoint of durability of concrete structures.

Generally, the ultimate strength of reinforced concrete member with corroded reinforcement will not be lowered so much. But, splitting, spalling or scaling of cover concrete due to expansion of corroded reinforcing steel give critical damage to reinforced

concrete structure. Once subjected to these deterioration, the reinforcement corrosion accelerates damage of the structures, followed by the reduction of load carrying capacity.

On the other hand, the design procedure for concrete structures is being shifted to the limit state design method in Japan. Under these situations, it is essentially needed to make clear the long term performance of reinforced concrete in chloride atmosphere.

1.2 Objective and Scope

In this thesis, systematical investigations on early chloride corrosion of reinforcing steel embedded in concrete are carried out to establish the base of durability design against chloride corrosion.

The objective and the scope of this study are as follows.

(1) In Chapter 2, the chloride corrosion mechanisms are reviewed, and the main factors influencing the chloride corrosion of reinforcing steel are discussed.

(2) In Chapter 3, the accelerated corrosion tests on reinforcing steel in concrete are carried out to examine its applicability and the influences of chloride content and crack width on the corrosion.

(3) In Chapter 4, the rate of chloride corrosion in cracked concrete is investigated to assess the influences of crack width.

(4) In Chapter 5, the mechanism of chloride corrosion in cracked

concrete is investigated. And then, influences of water cement ratio and crack width on corrosion are discussed.

(5) In Chapter 6, influences of cover concrete on chloride corrosion are determined. And, the effects of water cement ratio, thickness of concrete cover and arrangement of reinforcing steel are also examined.

(6) Chapter 7 discusses the corrosion monitoring method for reinforced concrete structures. Particularly, the half cell potential method is examined through both the laboratory and field tests. And macrocell corrosion rate is estimated by using the numerical model analysis.

2 STATE OF THE ART ON CHLORIDE CORROSION OF REINFORCING STEEL

2.1 Introduction

Reinforced concrete can be used efficiently for a wide range of structures in saline environment as typically represented by offshore structures. Durability of reinforced concrete structures in chloride environment has been of great concern of concrete engineers.

It is considered that the corrosion of reinforcing steel in concrete is the most critical limit state from the viewpoint of the durability of reinforced concrete structures, especially, in marine environment. "Recommendations for Prevention against Deterioration of Offshore Concrete Structures (JCI Committee 202)" is established on the basis of experiences of corrosion damages resulting from not only marine environment but also sea sand and de-icing salts.

2.2 Durability of Reinforced Concrete Structures

Reinforced concrete is inherently a durable composite material. When properly designed for the environment to be exposed and carefully constructed, reinforced concrete is capable of giving maintenance-free performance. However, when unintentionally are used the unproper materials such as sea sand having much salt together with poor controlled quality, or the concrete are placed in highly aggressive environment such as marine atmosphere, the durability is one of the most significant concerns of concrete.

Recently, many reseachers in Japan (2.1-2.3) have reported on the premature deterioration of reinforced concrete bridges due to chloride corrosion of reinforcing steel. These deteriorations were caused either by using sea sand or by penetration of sea salt. Particularly, in the latter case, many kinds of reinforced concrete structures in the marine environment suffered from damages due to premature chloride corrosion. The most feasible cause of damages results from an unsufficient assessment of attack of marine environment in the design of concrete sea structures. Its attack mechanisms, therefore, should be made clear.

2.3 Reinforced Concrete Structures in Marine Environment

When discussing the durability of reinforced concrete structures in marine environment, two problems must be dealt (2.4).

(1) Deterioration of concrete.

(2) Corrosion of reinforcing steel.

These two problems are related each other. When reinforcing steel rusts, the corrosion products generally occupy considerably more volume (2.5, 2.6) than that of the original steel. This expansion makes covering concrete cracked and spalled. Then the rate of corrosion is increasingly accelerated.

Chloride penetrating through cover concrete to reinforcing steel breaks the passivation of reinforcement to initiate corroding. The corrosion due to carbonation of cover concrete is of secondary effect in marine atmosphere.

2.4 Chloride Corrosion of Reinforcing Steel

2.4.1 Corrosion Reaction of Reinforcing Steel

Mechanism of metal corrosion depends on whether water takes part in the corrosion reaction or not. The former case is called wet corrosion and the latter dry corrosion. In the marine environment, concrete is rarely situated in the perfect dry condition. Thus as to corrosion of reinforcing steel in concrete,

only wet corrosion is needed to be discussed here.

The corrosion of reinforcing steel in concrete results from an electrochemical process accompanied by anodic and cathodic reactions. In the anodic reaction, iron is transferred into solution as hydrated ions with two electrons left in the reinforcing steel (eq.-1). These two electrons are transferred to the cathode to assimilate in the cathodic reaction (eq.-2).

$$Fe = Fe^{2+} + 2e^{-} \qquad \text{(eq.-1)}$$

$$O_2 + 2H_2O + 4e^{-} = 4OH^{-} \qquad \text{(eq.-2)}$$

This cathodic reaction is active in alkaline solution such as pore solution of concrete and its rate-determining step is diffusion of oxygen (2.7). Equilibrium potentials of these reactions can be calculated using the Nernst equation, but in corroding, the anodic and cathodic potentials change respectively with electric current. Usually the anode and cathode areas are unequal, but the corrosion current is common to both the anodic and cathodic reactions.

Electrochemical corrosion cells are built up by heterogeneities of media. Two types of corrosion cells may exist corresponding to the prevailing conditions. The first type, called the microcell, is characterized by microscopic distance separating the anode and cathode. In the second type known as the macrocell, both the anodic and cathodic reactions frequently take place in different places some distance apart. The potential difference between the anode and cathode of a macrocell is larger than that of a microcell. The corrosion reaction in the former is rapider than the latter. In the

microcell, only the mixed potential at the anode and cathode can be measured, but in the macrocell, each potential and macrocell corrosion current can be measured using the appropriate methods. Thus, the potential itself from equilibrium potential should be measured in order to study the polarization of corrosion reaction. At the same time the potential difference, which is considered as electromotive force of macrocell corrosion, should be measured to investigate the corrosion rate.

2.4.2 Mechanism of Macrocell Corrosion

In concrete, macrocell corrosion frequently proceeds first (2.8). Since concrete is a macro-heterogeneous material, differential concentrations of oxygen and chloride may exist therein, and corrosion, sufficiently severe to cause spalling, may occur in a macrocell, the poles of which can be separated as far as several feet (2.9). Stratfull (2.10) relates the half cell potential measurements to the observed conditions of corroded bridge slabs by showing the cumulative frequency distribution of potential (as shown in Fig. 2.1). In the bridge deck that required replacement, about 94% of all of the potential values showed that the steel was active or corroding. In a deck that was repaired, only 30% of the measurements were shown to be active, and the new deck had no active potentials. These reports are examples of macrocell corrosion of reinforcing steel in concrete.

The mechanism of macrocell corrosion is shown diagramatically

in Fig. 2.2. Lewis and Copenhagen (2.11) demonstrated the effect of factors on corrosion rate, such as quality of concrete, concrete permeability and environment of concrete structures, and discussed on five models of corrosion cell. The model giving the most corrosion current is shown as follows.

	Permeable concrete low pH high Cl^-		Less permeable concrete high pH low Cl^-	
Steel (anode)				Steel (cathode)

Formations of anodic and cathodic areas are not necessarily permanent, especially as far as the latter is concerned. As this process continues, various kinds of deposits accumulate on either the anode or the cathode. These deposits can greatly affect the process. Furthermore many factors may combine to cause a change in the potential difference between steel areas, which in turn lead to a change in the macrocell corrosion activity (2.12).

2.4.3 Factors Influencing Chloride Corrosion

Chloride corrosion of reinforcing steel results from the reaction between reinforced concrete and environmental condition. Thus, there are a plenty of factors influencing the chloride corrosion. In this chapter, main factors which remarkably influence on the chloride corrosion are described.

Permeability of Concrete--Fundamental corrosion protection method is to assure sufficient cover with concrete of low permeability. The permeability of concrete is dependent primarily upon those of aggregates and cement paste binder. Particularly, the cement paste binder is an important factor in selecting the mix proportion of concrete.

In order to assure the concrete cover of low permeability, concrete mix of low water content and low water cement ratio (see Fig. 2.3), using appropriate air-entraining agent or water-reducing agent, should be casted with good compaction and curing (2.13, 2.14). Typical permeabilities are shown in Table 2.1 (2.15).

The most feasible factor to reduce the permeability of concrete is to keep the water cement ratio as low as possible. But, the actual water cement ratio shows local variation within the structure. For instance, Kanda (2.16) reported that the actual water cement ratio in the upper part of concrete member was higher than that in the lower part due to bleeding. And, he also stated that the variation in actual water cement ratio was at most 13% in a 200 cm high column made of high water cement ratio concrete.

Corrosion inhibiting mechanism due to low permeability of cover concrete is considered to retard the penetration of water and chloride into concrete and then inhibit disolving of hydrated iron ions.

Chloride--Many code requirements and design standards specify the permissible chloride content in the constitutive materials of concrete for corrosion protection. For instance, in "Standard Specification for Concrete Structures (JSCE)", the permissible sodium chloride content for oven dried sea sand is limited to less than 0.1% for reinforced concrete structures. And ACI 318-83 specifies the permissible chloride content as listed in Table 2.2.

Berman (2.17) measured the electrical half cell potentials of reinforcing steel in saturated calcium hydroxide solution contaminated with sodium chloride, and concluded as follows; (1) Corrosion in saturated calcium hydroxide solution exposed to air occurred at sodium chloride concentration as low as 0.03 molar, (2) This threshhold concentration was raised up to 1.0 molar when oxygen was excluded. However, saturated calcium hydroxide solution can not entirely simulate the actual environment in concrete.

Part of the chloride in concrete can be chemically bound by the cement to form the so-called "Friedel salt". This chemically bound chloride is of a harmless nature as far as the corrosion of reinforcing steel is concerned. Approximately 0.4% of the chloride related to the weight of cement may be bound to form Friedel salt. But, the ability to bind 0.4% of the chloride chemically decreases with sulfate ion and will be lost after the concrete has been carbonated (2.18).

The chloride in the concrete materials, such as sea sand or

chemical agent, can be chemically bound, while, the chloride penetrating through hardened concrete cann't be expected to be bound.

Stratfull (2.10) surveyed the bridge deck deterioration due to chloride corrosion, and found that the threshold value of chloride was about 1.5 lb/yd^3 ($\fallingdotseq$ 0.89 kg/m^3). Stewart (2.12) reported that about 2 lb/yd^3 ($\fallingdotseq$ 1.2 kg/m^3) of concrete was usually accepted as the minimum chloride content required to cause the serious steel corrosion. These values of chloride content are a little smaller than the chemically binding value as described above.

Crack and Clear Cover--Cracks in reinforced concrete structures not only permit air, salt and other impurities to penetrate to reinforcing steel, but also make reinforced concrete so heterogeneous as to form macrocell. The region near a crack may become an anode as suggested by Lewis and Copenhagen (2.11). As a measure of corrosion protection, many codes of practice and design regulations provide checks for permissible crack widths, depending on aggressivity of the environment as shown in Table 2.3. There seems to exist general agreement between codes on what these limits should be. But, influence of cracks on corrosion reaction of steel in concrete has not yet been made clear sufficiently to determine these limits.

Akatsuka, Seki et al. (2.19) investigated the probability of corrosion of reinforcement embedded in cracked concrete immersed in

sea water, and concluded that the permissible crack width corresponding to corrosion probability of 0.50 was 0.1 mm.

When the crack width is kept constant, the probability of corrosion occurrence decreases with increasing thickness of cover. Fujii, Kobayashi et al. (2.20) reported on the influence of cover resulted from the specimens placed in the marine atmospheric zone as illustrated in Fig. 2.4. Many codes of practice require to maintain the minimum cover, corresponding to various environmental conditions. For example, CP 110 requirements for cover are listed in Table 2.4.

Moreover, Attimtay (2.21) reported that both the bar size (ϕ) and the thickness of cover (c) must be considered together, as the c/ϕ ratio, and stated that c/ϕ ratios of 3.0 for stressed bars and 2.5 for unstressed bars may provide enough resistance to longitudinal splitting and thus established a case of self-healing corrosion.

Environmental Condition--Environmental condition is one of the most important factors influencing corrosion of reinforcing steel. Many reseachers (2.22, 2.23) reported that significant corrosion could occur in the wetting and drying or the splash zone.

"Recommendations for the Design and Construction of Concrete Sea Structures (FIP)", states that following three types of exposure should be considered in marine environment.

(a) In the submerged zone, attention should be paid to:

(i) prevention of chemical deterioration of concrete;

(ii) prevention of corrosion of embedded steel;

(iii) abrasion.

(b) In the splash zone, attention should be paid to:

(i) freezing and thawing;

(ii) prevention of chemical deterioration of concrete;

(iii) prevention of corrosion of embedded steel.

(c) In the atmospheric zone, attention should be paid to:

(i) freezing and thawing;

(ii) prevention of corrosion of embedded steel;

(iii) fire hazards.

And, it is considered that macrocell is formed due to environmental difference in a concrete structure when locally exposed to various environmental conditions at the same time (2.24, 2.25).

Moreover, it is well known that the severe chloride corrosion damages were experienced in the concrete bridges constructed in the coastal region along the Nihon Sea, where a seasonal wind is blowing mainly from the sea in winter (2.1).

2.5 References

(2.1) Iwamatsu, S., "Durability and maintenance of prestressed concrete structures", Jour. of JPCEA, Vol. 25, No. 5, pp. 10-15, Sept.-Oct. 1983

(2.2) Ohta, T. and Gushi, Y., "Corrosion of steel reinforcement in concrete", Concrete Journal, Vol. 19, No. 3, pp. 29-32, March 1981

(2.3) Ohshiro, T., Igei, S. and Uezu, S., "Deterioration of RC bridge due to chloride content", Trans. of JCI, Vol. 6, (in printing)

(2.4) Okada, K., "Reinforcement corrosion in concrete structure", Report of the Corrosion and Corrosion Inhibition Committee, JSMS, Vol. 14, No. 74, Part 1, Jan. 1976

(2.5) Hachemi, A. A., Murat, M. and Cubaud, J. C., "Recherches sur la corrosion accélerée des aciers dans le béton", Revue Des Matériaux de Construction, No. 702, pp. 285-290, May 1976

(2.6) Crumpton, C. F. and Jayaprakash, "Scanning rust crystals and salt crystals with electron microscope", TRB 860, pp. 45-49, 1982

(2.7) Tomashov, N. D., "Theory of Corrosion and Protection of Metals" Macmillan, New York, 1966

(2.8) Task Group on Steel Corrosion in Concrete, "Testing of corrosion of reinforcing steel in concrete", Jour. of JSMS, Vol. 27, No. 302, pp. 1064-1067, Nov. 1978

(2.9) Browne, R. D. and Domone, P. L. J.,"The long-term performance of concrete in the marine environment", Off-shore Structures, ICE, pp. 49-59, 1975

(2.10) Stratfull, R. F., "Corrosion autopsy of a structurally

unsound bridge deck", HRR 433, pp. 1-11, Dec. 1973

(2.11) Lewis, D. A. and Copenhagen, W. J., "Corrosion of reinforcing steel in concrete in marine atmospheres" Corrosion, Vol. 15, pp. 382-388, July 1959

(2.12) Stewart, C. E., "Considerations for repairing salt damaged bridge decks", ACI Journal, Vol. 72, No. 12, pp. 685-713, Dec. 1975

(2.13) Murata, J., "Studies on the permeability of concrete", Trans. of JSCE, No. 77, pp.69-103, Nov. 1961

(2.14) Powers, T. C., Copeland, L. E., Hays, J. C. and Mann, H. M., "Permeability of Portland cement paste", ACI Journal, Vol. 51, pp. 285-298, Nov. 1954

(2.15) Browne, R. D., "Mechanism of corrosion of steel in concrete in relation to design, inspection, and repair of offshore and coastal structures", ACI SP-65, pp. 169-204, Aug. 1980

(2.16) Kanda, M. and Yoshida, H., "Distribution of water cement ratio in section of concrete member after cast", Cement & Concrete, No. 357, pp. 38-43, Nov. 1976

(2.17) Berman, H. A., "Sodium chloride, corrosion of reinforcing steel and the pH of calcium hydrooxide solution", ACI Journal, Vol. 72, No. 4, pp. 150-157, Apr. 1975

(2.18) Richartz, W., "Die binding von Chlorid bei der Zementerhartung", Zement-Kalk-Gips, Heft 10, S. 447-456, 1969

(2.19) Akatsuka, Y., Seki, H. and Asaoka, K., "Crack width and reinforcement corrosion of reinforced concrete attacked by sea water", Cement & Concrete, N. 266, pp. 38-43, Jan. 1966

(2.20) Fujii, M., Kobayashi, S., Okazaki, S., Kanai, S. and Kanai, K., "Reinforcement corrosion in concrete using sea water as mixing

water", Annual Meeting of Kansai Branch of JSCE, pp. V.14-15, May 1976

(2.21) Atimtay, E., "Chloride corrosion of reinforced concrete", The University of Texas, Austin, May 1976

(2.22) Brook, K. M. and Stillwell, J. A., "Exposure tests on concrete for offshore structures", Corrosion of Reinforcement in Concrete Construction, SCI, 1983

(2.23) Mehta, P. K.,"Durability of concrete in marine environment--A review" ACI SP-65, pp. 1-20, Aug. 1980

(2.24) Finley, H. F., "Corrosion of reinforcing steel in concrete in marine atmospheres", Corrosion, pp. 104-108, March 1961

(2.25) Willkins, N. J. M. and Lawrence, P. F., "Fundamental mechanisms of corrosion of steel reinforcements in sea-water", *Concrete in the ocean 6, CIRIA/UEG-CCA-Dept. of Energy*, 1980

(2.26) Gerwick, Jr.,B. C., "Considerations and problem areas in design and construction of concrete sea structures", Proc. of the FIP Symposium, Concrete Sea Structures, pp. 129-140, Sept. 1972

(2.27) Verbeck, G. J., "Mechanisms of corrosion of steel in concrete", ACI SP-49, pp. 21-38, Nov. 1975

(2.28) Cady, P. D., "Corrosion of reinforcing steel in concrete - A general overview of the problem", ASTM STP629, pp. 3-11, 1977

(2.29) Gerwick, Jr., B. C., "Prestressed concrete in offshore construction", Developments in Prestressed Concrete - 2, pp.43-66, Applied Science Publishers Ltd., London, 1978

(2.30) Browne, R. D. and Baker, A. F., "The performance of structural concrete in a marine environment", Developments in Concrete Technology - 1, pp. 111-150, Applied Science Publishers

Ltd., London, 1979

(2.31) Loe, J. A. and Griffin, L. J.,"The contribution of research to bridge inspection in the U. K.", Bridge Maintenance and Rehabilitation Conference, pp. 1-20, ASCE-TRB-IABSE-WVDOH, Aug. 1980

(2.32) Locke, C. E. and Siman A., "Electrochemistry of reinforcing steel in salt-contaninated concrete", ASTM STP713, pp. 3-16, 1980

(2.33) Browne, R. D., "Design prediction of the life for reinforced concrete in marine and other chloride environments", Durability of Building Materials, Vol. 1, No. 2, pp. 113-126, July 1982

(2.34) Popovics, S., Simeonov, Y., Bozhinov, G. and Barovsky, N., "Durability of reinforced concrete in sea water", Corrosion of Reinforcement in Concrete Construction, SCI, pp. 19-38, 1983

(2.35) Seki, H., "Concrete sea structures", pp.1-161, Sankaido, Tokyo, Dec. 1983

(2.36) Stewart, C. F. et al. "Bridge decks:Maintenance and repair", ACI Journal, Vol. 72, No. 12, pp. 685-713, Dec. 1975

(2.37) TRB, "Bridge deck repairs", NCHRP RRD85, 22p, March 1976

(2.38) TRB, "Durability of concrete bridge decks", NCHRP SHP57, 61p, May 1979

(2.39) ACI Committee 546, " Guide for repair of concrete bridge superstructures", Concrete International, Vol. 2, No. 9, pp. 69-88, Sept. 1980

(2.40) CEB Task group Durability, "Durability of Concrete structures - state-of-art report -", Bulletin d'Information, CEB, No. 148, Fev. 1982

(2.41) FIP, "Recommendations for the design and construction of concrete sea structures", 1977

(2.42) DNV, "Rules for the design, construction and inspection of offshore structures", 1977

(2.43) ACI, "Guide for the design and construction of fixed offshore concrete structures", 1978

(2.44) JCI Comittee 202, "Recommendations for prevention against deterioration of offshore concrete structures", 1983

(2.45) Okada, K. and Miyagawa, T.,"Chloride corrosion of reinforcing steel in concrete", Concrete Journal, Vol. 17, No. 9, pp. 1-10, Sept. 1979

Table 2. 1 Typical coefficients of permeability

10^{-10} m/sec.	- Permeability recorded for an air-dried slip-formed concrete
10^{-12} m/sec.	- Permeability of a high quality concrete
10^{-14} m/sec.	- Permeability of an ulta-high quality wet cured concrete

Table 2. 2 Maximum chloride ion content for corrosion protection

Type of member	Maximum water soluble chloride ion (Cl^-) in concrete, percent by weight of cement
Prestressed concrete	0.06
Reinforced concrete exposed to chloride in service	0.15
Reinforced concrete that will be dry or protected from moisture in service	1.00
Other reinforced concrete construction	0.30

Table 2. 3 Permissible crack width

	Crack width(mm)	
ACI 318	0.40	In door
	0.33	Out door
BS CP110	0.30	
	$0.004d_c$	Particularly aggressive environment dc:nominal cover to the main reinforcement
CEB	0.40	Mild exposure
	0.20	Moderate exposure
	0.10	Severe exposure
JSCE*	0.005c	Moderate environment
	0.004c	Aggressive environment
	0.0035c	Particularly aggressive environment

* Recommendations for limit state design of concrete structure

Table 2. 4 Nominal cover to reinforcement

Condition of exposure	Nominal cover				
	Concrete grade				
	20	25	30	40	50 and over
	mm	mm	mm	mm	mm
Mild:e.g. completely protected against weather, or aggressive conditions, except for brief period of exposure to normal weather conditions during construction	25	20	15	15	15
Moderate:e.g. sheltered from severe rain and against freezing whilst saturated with water. Buried concrete and concrete continuously under water	—	40	30	25	20
Severe:e.g. exposed to driving rain, alternate wetting and drying and to freezing whilst wet. Subject to heavy condensation or corrosive fumes	—	50	40	30	25
Very severe:e.g. exposed to sea water or moorland water and with abrasion	—	—	—	60	50
Subject to salt used for de-icing	—	—	50*	40*	25

* Only applicable if the concrete has entrained air

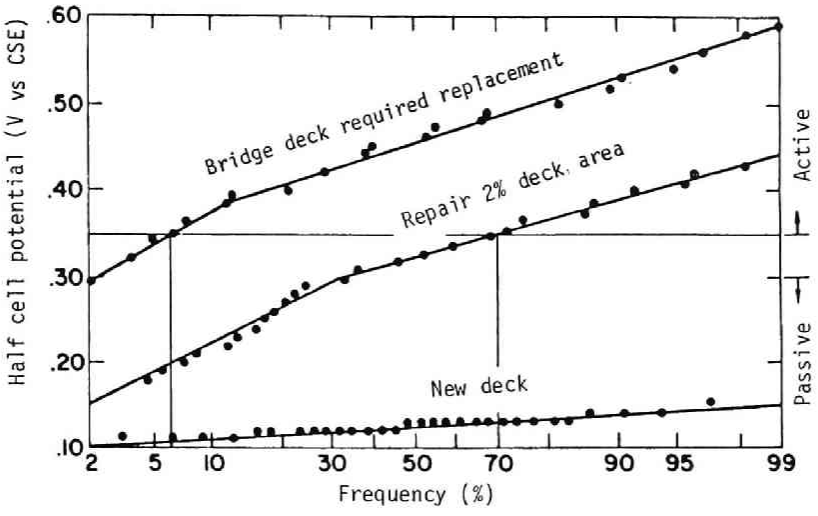

Fig. 2. 1--Distribution of half cell potentials

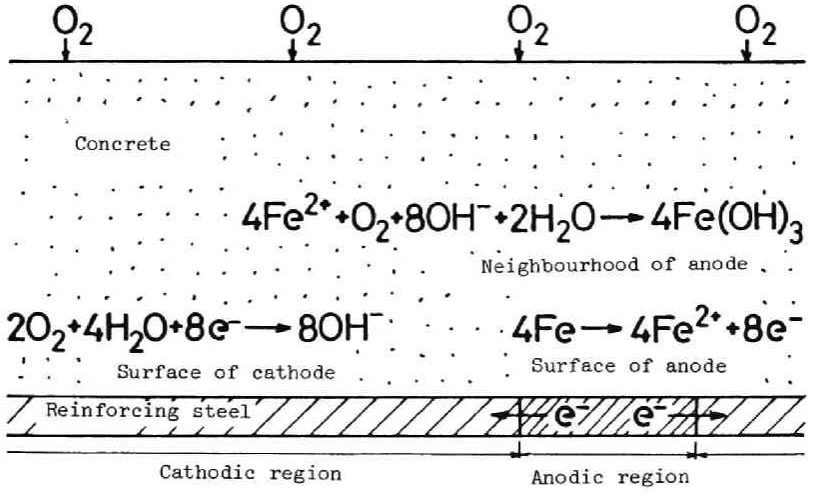

Fig. 2. 2--Macrocell corrosion

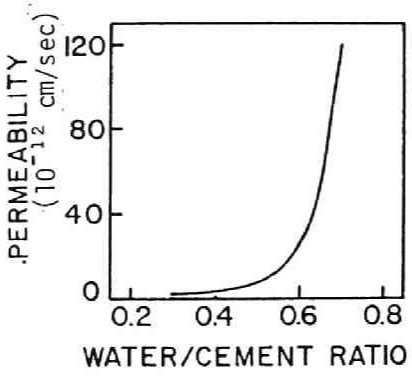

Fig. 2. 3--Effect of water-cement ratio on permeability of hydrated paste to water

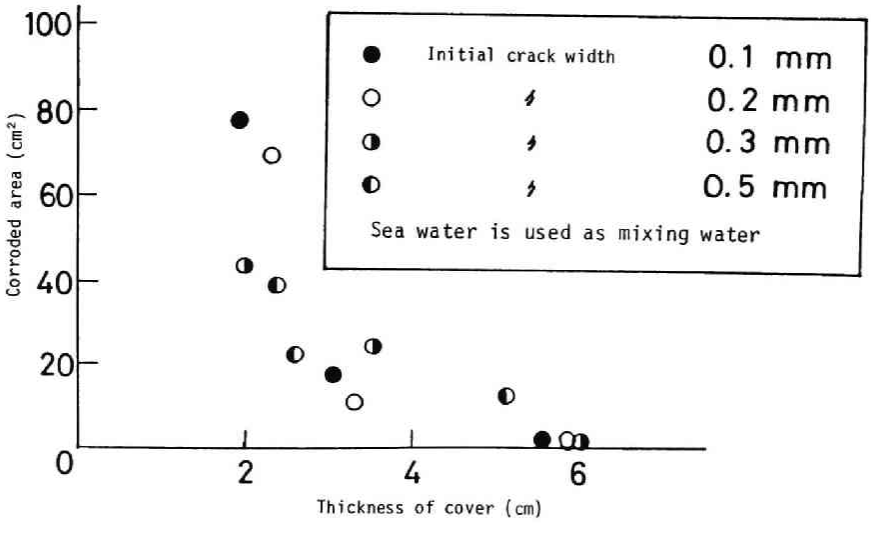

Fig. 2. 4--Effect of cover thickness on crack corrosion

3 ACCELERATED CORROSION TEST OF REINFORCING STEEL IN CONCRETE AT RAISED TEMPERATURE

3.1 Introduction

As described in Chapter 2, the diffusion of oxygen is generally considered to be an essential step controlling the corrosion reaction, and the cracks of cover concrete permit the oxygen, moisture and carbon dioxide to penetrate to the reinforcing steel in concrete. As the corrosion of reinforcing steel frequently proceeds in the form of macrocell, corrosion problems should be discussed using not only corrosion rates but corrosion mechanisms due to heterogeneous properties of concrete, for instance, cracks.

In this chapter, the accelerated corrosion tests of reinforcing steel as proposed in 3.2 are conducted and the influences of test variables, such as salt concentration in mixing water, crack width in cover concrete and surface condition of reinforcing steel, on its corrosion rate and mechanism are investigated from a view point of macrocell corrosion mechanism due to crack.

3.2 Accelerated Corrosion Test

In analyzing the corrosion process of reinforcing steel in concrete, the most reliable method is to test the reinforcing steel under the actual conditions that the structures would be exposed to. However, this method takes a very long time to obtain the test results. In order to shorten the time of testing, various accelerated corrosion test methods have been proposed.

Principal requirements for accelerated corrosion test are as follows.

(1) The corrosion mechanism of test method is to simulate the actual corrosion mechanism of reinforcing steel in field.

(2) The effect of acceleration is to be high.

(3) The applicability is to be wide.

(4) The test is to be conducted relatively easily.

Though it is difficult to satisfy all of these requirements, several test methods, for example, wetting and drying method, higher temperature and humidity method and autoclave method, have been developed.

3.2.1 Wetting and Drying Method

In this accelerated test, the repeated cycles of wetting and drying are applied on the reinforced concrete specimens. During the wetting period (60 - 80°C, 90 - 95% R.H.), water as electrolyte penetrates into cover concrete and corrosion rate is accelerated

under raised temperature. On the other hand, during the drying period (10 - 20°C, 30 - 50% R.H.), oxygen is supplied so that the thick water layer may inhibit the oxygen to reach the reinforcing steel surface. This method is considered to simulate the corrosion condition for the actual reinforced concrete structures.

3.2.2 Higher Temperature and Humidity Method

The rate of electrochemical corrosion is usually increased with raised temperature. This method is based on the concept of temperature dependence of corrosion rate, and corresponds to the wetting part in the wetting and drying test as mentioned above. As shown in Fig. 3.1 (3.1), the corrosion rate of open system increases with raised temperature until 80°C. This test is usually conducted under the condition of 40 - 80°C and about 90% R.H.. This method, particularly, has an advantage of simplicity in test procedures.

3.2.3 Autoclave Method

The corrosion reaction can be accelerated by higher temperature and higher pressure vapor as obtained by means of autoclave vessel (180°C, 10 a.t.m.). As the autoclave vessel is of highly closed system, the solubility of oxygen is not reduced, and also the corrosion rate doesn't decrease even beyond 80°C. Using this method, however, the micro structures of concrete may change due to thermal and humid shocks.

In this chapter, the simple accelerated corrosion test under both the raised temperature and humidity was carried out to minimize a damage of concrete quality during the acceleration process.

3.3 Test Program

Test variables chosen for this test are shown in Table 3.1. In the open system, the corrosion rate controlled by diffusion of oxygen shows the maximum value at 80°C, but there remains some probability that very high temperature deteriorates the concrete matrix. Therefore, the accelerated test in this experiments were conducted at 40°C and 60°C, while the standard level of temperature was 20°C. The relative humidity was 90% in all of the test conditions. Four levels of crack width due to bending moment were chosen as the test variables, in which "0+" means a small crack width which can be detected using a micro scope (x20). And, the surface conditions of deformed reinforcing steel were changed as follows, although the reinforcing steels of surface level 0 were only used in 3.6.1 - 3.6.5.

Level 0: Good mill scale.

Level 1: Mill scale with thin rust layer.

Level 2: Mill scale having mounted red rust.

Level 3: Washed with water after immersed in HCl sol. (1N) and NaOH sol. (1N).

Level 4: Polished using the mechanical buffer after immersed in HCl sol. (10N) for 2 hours.

3.4 Materials and Test Specimens

3.4.1 Materials

Ordinary Portland cement, Yasu river sand for fine aggregate (Specific gravity = 2.58, F.M. = 2.97) and Kurama crushed gravel for coarse aggregate (Specific gravity = 2.61, Maximum size = 10 mm) were used in the concrete mix. Sodium chloride, as the chloride parts of sea water, and magnesium sulfate, as the sulfate parts of sea water, were used. And, one kind of deformed reinforcing steel (D10, SD35) was used.

3.4.2 Mix Proportion

In accordance with "Chapter 29 Sea Structure, Standard Specification for Concrete Structures (JSCE)", the water cement ratio and design slump were chosen as 0.50 and 12±2 cm, respectively. The mix proportion of concrete is shown in Table 3.2.

3.4.3 Specimens

The test specimen is shown in Fig. 3.2. A reinforcing steel was placed vertically at center of 5x5x40 cm prism using mortar spacers. 10ϕx20 cm cylinders for compressive test, 15ϕx15 cm cylinders for splitting test and 10x10x40 cm prisms for flexural test were prepared. One day after casted, all of the test specimens were stripped and stored in the water of about 20°C for 4 weeks

until the accelerated tests were started.

A day before the commencement of test, 3 pointed loading was applied to introduce the required residual crack width of flexural cracks.

3.5 Test Procedures

The specimens for accelerated tests at 40°C and 60°C were stored in the temperature and humidity controlled box (90% R.H.), while the test specimens at 20°C were sored in the curing room of 20°C and 90% R.H.. The weight of specimens were measured at both the start and the end of accelerated test to calculate their water content.

After the end of corrosion test, the specimens were longitudinally splitted along the reinforcing steel embedded in concrete. The carbonation depth was also measured by means of a micrometer, after being sprayed with phenol phthalane 1% sol. on the splitting plane. The weight loss of reinforcing steel due to corrosion was considerably small, and therefore the corroded area was measured as follows. The local corroded area ratio was assessed as 1, 3/4, 2/4, 1/4 or 0 in each of the local area 1, 2 and 3 as shown in Fig. 3.3 respectively. The corroded surface area could be determined by summation of each local corroded area ratio multiplying the square measure of each of local areas 1, 2 and 3.

And, the corroded area (%) could be expressed by the percentage of the corroded surface area to the nominal surface area of reinforcing steel.

3.6 Results and Discussions

Strengths, elastic moduli and poisson's ratios of concrete at the begining of corrosion test are listed in Table 3.3. Salts in mixing water had little influence on the mechanical properties of concrete.

Typical water content of test specimens are shown in Table 3.4. all specimens contained the water as electrolyte, and the electrochemical corrosion of reinforcing steel could proceed. The water contents of specimens of salt concentration level 3 at 60°C decreased until 6 months' duration and increased after that. This may be caused by the absorption of water by corrosion products.

Typical ultimate splitting loads of test specimens are listed in Table 3.5. The splitting load was lowered with increased corrosion damages. Especially, the ultimate loads of test specimen having longitudinal cracks due to corrosion were very small. And, the extension of longitudinal crack increased with acceleration period.

The carbonated area could not be determined except for the

cracking plane.

3.6.1 Time Dependence

Total corroded areas are shown in Figs. 3.4 - 3.6. Typically, in the case of 60°C, the total corroded area increased sharply after a certain period of time, so called, incubation period of corrosion. This period is one of the typical phenomena of electrochemical corrosion (3.2) or/and the phenomenon due to change of corrosion mode as explained later in 3.6.4 and 3.6.5.

The total corroded areas at temperature level of 20°C are shown in Figs. 3.7 and 3.8. The corroded area (in the area of cracked region as shown in Fig. 3.3) - time relations at temperature level of 20°C are shown in Fig. 3.9 and 3.10. The corroded area increased with elapsed time, but the corroded area after 3 years' duration was found to be rather smaller than after 2 months' duration at 60°C and after 12 months' at 40°C. And, even after 3 years' duration, there were no longitudinal cracks on the specimen at temperature level of 20°C.

3.6.2 Influence of Temperature Rise

The relations between total corroded area and temperature are shown in Figs. 3.11 - 3.13. It was shown that the total corroded area increased with raised temperature, and that especially the acceleration under the 60°C conditon was very remarkable. The

longitudinal cracks occurred after 6 months on the specimens tested at the temperature level 60°C and salt concentration level 3 . Thus, it was difficult to assess their corroded area. For the nearly constant values of total corroded area, the corrosion appearance rarely change among the corresponding specimens. Therefore, it was concluded from these findings that the acceleration method at higher temperature and humidity used in this test was reasonable.

The period during which the total corroded area increased from 0% to 10%, being calculated from the test results in Figs. 3.4 - 3.6, decreased with increasing temperature. The corrosion rate at the temperature level of 60°C was increased up to 4 - 6 times the corrosion rate at that of 40°C. Comparing with the corroded area obtained at 20°C as given in 3.6.1, the acceleration ratio obtained at 60°C to 20°C was not less than 18 and that of 40°C not less than 3. Skaperdas et al. (3.3) reported that the corrosion rate controlled by the diffusion of oxygen increased twice with increase in temperature 30°C. The acceleration ratio obtained from this test was much higher than that from Skaperdas et al.. This may be caused by heterogeneous properties of concrete such as micro cracks, and by increasing salt concentration accompanied by water loss due to temperature rise.

3.6.3 Influence of Salt Content

The relations between the total corroded area and the salt

concentration level are shown in Figs. 3.14 - 3.16. And, Figs. 3.17 - 3.18 show the relationships between the corroded area in the area of cracking region and the salt concentration level. Generally, the corroded areas at the salt concentration levels 2 and 3 were larger than those at levels 0 and 1. In particular, the corroded areas of specimens having wide cracks together with high salt concentration level were very remarkable. Therefore, considering the scattering of test results, this accelerated test implied that the critical chloride contents, which caused the remarkable steel corrosion, was between the salt concentration level 1 (0.29% : NaCl/Oven dried sand weight, 2.5 kg/m^3 : Cl/Concrete) and level 2 (0.58% :NaCl/Oven dried sand weight, 5.0 kg/m^3 : Cl/Concrete). This critical value was much higher than that as described in Chapter 2. This may be due to the relative short period of accelerated test.

3.6.4 Influence of Crack Width

The relations between total corroded area and crack width are shown in Figs. 3.19 - 3.21. The increase in crack width had little influence on the total corroded area, when the temperature level was 40°C or 60°C. The crack width chosen in this test was relatively narrow. It was thought that the influence of crack width on total corroded area was relatively small. After 3 years' duration, however, the total corroded area of specimens tested at temperature level 20°C and salt concentration level 3 was influenced by the crack width, although the value of total corroded area was not so large.

Figs. 3.22 - 3.24 show the relationship between the corroded area in the area of cracked region and crack width. It was cleary indicated that the corroded area in the area of cracked region increased with increasing crack width. Especially, in case of crack level 3, the corroded area in the area of cracked region was found to be considerably large. But, in case of 60°C and salt concentration level 3, the corroded area became so large after 6 or 12 months that the influence of crack width became remarkably small.

The typical ralation between the corroded area in the area of cracked region and the total corroded area of salt concentration level 3 is shown in Fig. 3.25, in which the diagonal line means that the corroded area in the area of cracked region equals to the total corroded area. The specimens of crack level 0 and 1 were plotted near the diagonal line, and then the corrosion reaction occurred all over the surface of reinforcing steel. On the other hand, in the case of crack levels 2 and 3, plotted points were on the considerably upper side of the diagonal line, and therefore, the corroded area in the area of cracked region was larger than the total corroded area. This phenomena means that the corrosion reaction occurred locally near the cracks. When neglecting very small values of corroded area, the corroded area in the area of cracked region was larger than the total corroded area at early stage of corrosion, and thereafter these two values became nearly equal gradually. It is considered that the corrosion mechanism mode changed from the local corrosion in which cracks and bondless area near cracks became anode, to the nearly uniform corrosion or the

anode area moved.

3.6.5 Influence of Bleeding

The bleeding ratio of tested concrete was about 20%. There existed porous parts beneath the reinforcing steel due to bleeding. The ratio of the corroded surface area on lower half surface of steel to the total corroded surface area (ξ) is shown in Fig. 3.26. Although the ratio, ξ, was large at early stage of corrosion process, it decreased gradually with increasing total corroded area and finally became to close 50%. This may be caused by the change in corrosion mechanism. In other words, the electrochemical defect beneath reinforsing steel due to bleeding was anode at early stage of corrosion.

3.6.6 Influence of Surface Condition of Reinforcing Steel

The influence of steel surface levels on corrosion properties, such as total corroded area, the corroded area at cracking and the ratio are shown in Figs. 3.27 - 3.29, respectively. In this test, it was not clear whether the mill scale of reinforcing steel influenced either the corrosion rate or mechanism.

3.7 Conclusions

In this chapter, the accelerated corrosion tests at higher temperature and humidity were carried out on the reinforced concrete specimens. The conclusions in this chapter are summarized as follows;

(1) At raised temperature ranging from 40°C to 60°C, the time needed to corrode the reinforcing steel embedded in concrete becomes much shorter than that at normal temperature (20°C). The accelerated method using in this chapter is quite effective for shortening the time of testing.

(2) The amount of corrosion of reinforcing steel embedded in concrete can be estimated from the ratio of the corroded surface area to the total surface area. Cracks narrower than 0.06 mm have little influence on the whole corrosion, although distinct influence just around the cracks.

(3) The corroded area of embedded steel is larger on the lower surface than on the upper surface, particularly, at early stage of corrosion process.

(4) According to the accelerated corrosion test used here, the critical chloride content, which causes the remarkable steel corrosion, is between 2.5 and 5.0 kg/m^3.

3.8 References

(3.1) Speller, F., "Corrosion, Cause and Prevention", MacGraw-Hill, New York, 1951

(3.2) Tomashov, N. D., (Translated by Tytell, B. H. et al.) "Theory of Corrosion and Protection of Metals", Macmillan, New York, 1966

(3.3) Uhlig, H. H., "Corrosion and Corrosion Control", John Wily & Sons, New York, 1971

(3.4) Okada, K., Koyanagi, W. and Miyagawa, T., "Accelerated corrosion test of reinforcing steel in concrete at raised temperature", Jour. of JSMS, Vol. 26, No. 290, pp. 1110-1116, Nov. 1979

(3.5) Miyagawa, T., Hatamura, H. and Okada, K., "Chloride corrosion and stress corrosion of prestressing tendon", Annual Meeting of JSCE, Vol. 35-5, pp. 347-348, Sept. 1980

Table 3. 1 Test Program

Factor \ Level		0	1	2	3	4	5
Salt Concentration (%:mixing water)	NaCl	0	1.04	2.09	3.13*)	—	
	$MgSO_4$	0	0.11	0.22	0.33	—	
Temperature(°C) **)		20	40	60	—		
Crack width(mm)		0	0+	0.03	0.06	—	
Steel surface condition		0	1	2	3	4	—
Elapsed Time (month)		0	1	2	6	12	36

*) Sea water level : NaCl/Oven dry weight of sand=0.87%
Cl^-/m^3(Concrete)=3.7kg/m^3

**) Relative humidity = 90%

Table 3. 2 Mix proportion of concrete

Slump (cm)	Air content (%)	Water cement ratio (%)	Absolute fine aggregate ratio (%)	Unit weight(kg/m^3)			
				Water	Cement	Sand	Gravel
12±2	2±0.5	50	41	196	391	714	1048

Table 3. 3 Properties of concrete

Salt concentration level	Compressive strength (kg/cm^2)	Tensile strength (kg/cm^2)	Flexural strength (kg/cm^2)	Elastic modulus (×10^5kg/cm^2)	Poisson's ratio
0	471	34.9	54.8	3.43	0.23
1	449	40.0	57.6	3.03	0.21
2	444	38.8	58.0	3.39	0.22
3	417	37.2	50.5	3.46	0.20

Table 3. 4 Change of water content in concrete from test start.

(%)

Salt concentration level	Temperature (°C)	Crack width level	Time (Month)			
			1	2	6	12
3	60	0	-25.1	-27.0	-23.2	-13.5
		1	-25.1	-25.1	-21.2	-10.0
		2	-25.1	-29.0	-15.4	-12.7
		3	-25.1	-25.1	-21.2	-11.2
	40	0	-3.9	-15.4	-3.9	-2.9
		1	-3.9	-13.5	-3.9	-2.7
		2	-3.9	-17.4	-3.9	-3.1
		3	-1.9	-15.4	-1.9	-2.5
	20	0			-5.8	-1.0
		1			-5.8	4.2
		2			-5.8	-1.5
		3			-7.7	-2.3
2	20	0			3.1	1.5
		1			2.3	3.9
		2			4.2	3.7
		3			6.0	4.2
1	20	0			3.7	1.0
		1			1.7	2.9
		2			6.6	3.1
		3			7.3	4.8
0	20	0			4.4	1.5
		1			4.1	-0.6
		2			2.5	-0.2
		3			2.5	1.2

Table 3. 5 Ultimate splitting load. (ton)

Salt concentration level	Temperature (°C)	Crack width level	Time (Month)	
			6	12
3	60	0	10.7	7.67
		1	10.6 *	6.57 *
		2	10.2	6.37
		3	12.2	7.20
	40	0	14.8	12.6
		1	12.8	13.5
		2	12.8	12.4
		3	12.0	12.2
	20	0	11.5	13.4
		1	11.1	12.2
		2	11.2	9.87
		3	11.0	12.4
2	20	0	10.5	10.7
		1	11.1	11.6
		2	11.6	14.9
		3	10.9	12.7
1	20	0	10.6	12.9
		1	12.1	10.2
		2	11.2	13.7
		3	11.4	13.3
0	20	0	11.4	15.1
		1	12.6	14.7
		2	11.4	12.8
		3	11.4	13.5

* With longitudinal cracks

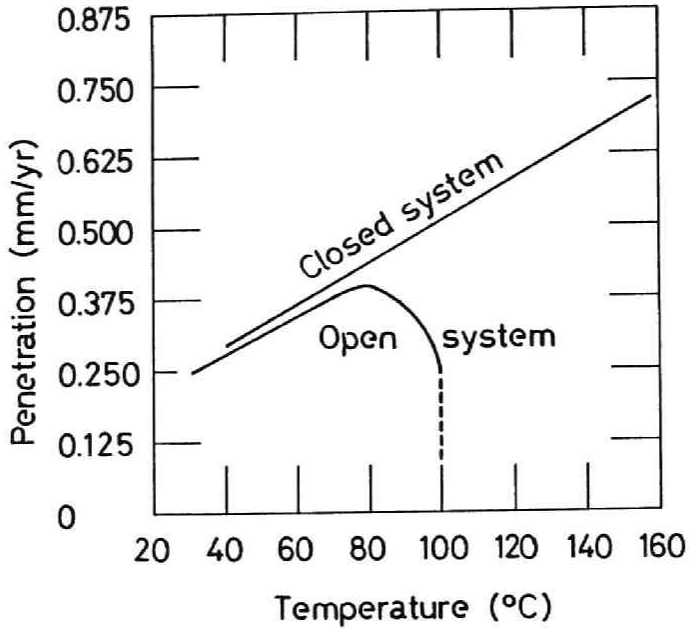

Fig. 3. 1--Temperature dependence of corrosion rate of iron in water

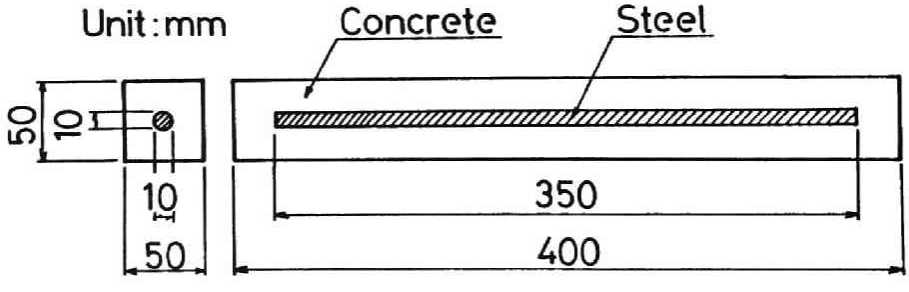

Fig. 3. 2--Test specimen

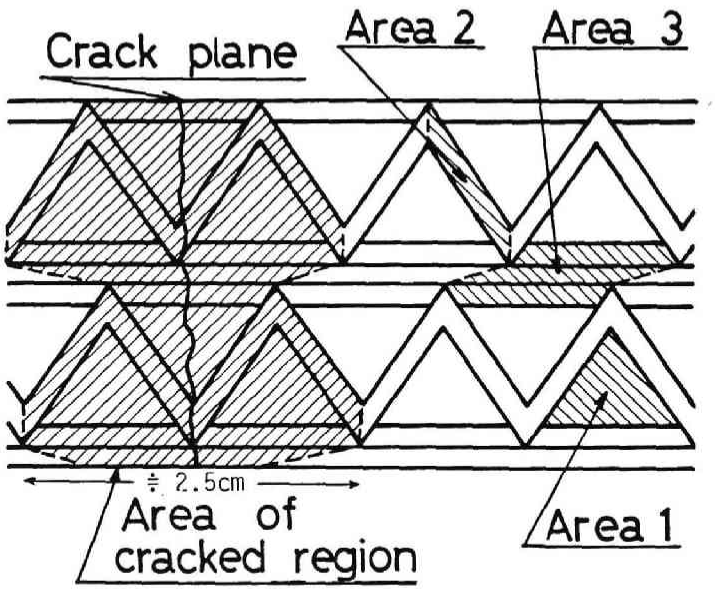

Fig. 3. 3--Schematic view of steel surface

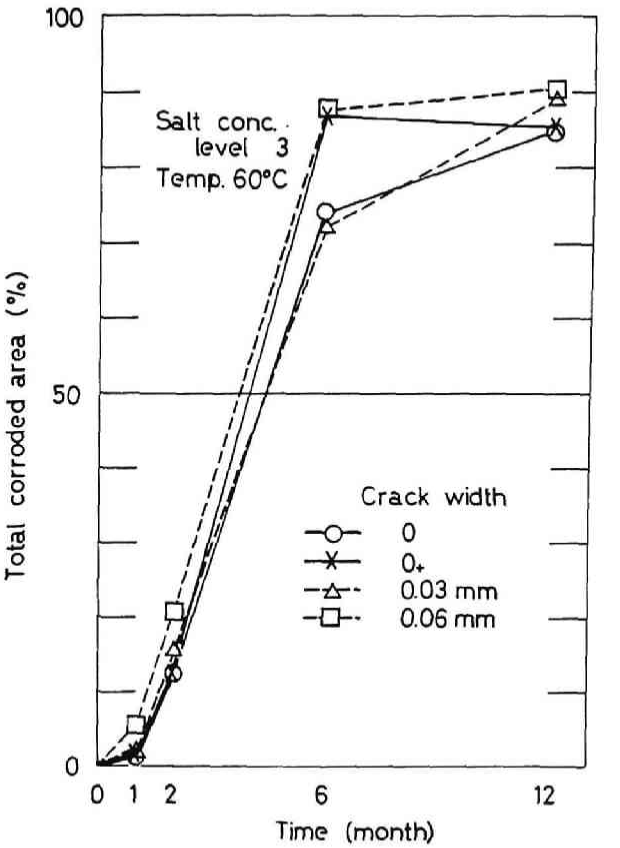

Fig. 3. 4--Total corroded area (60°C)

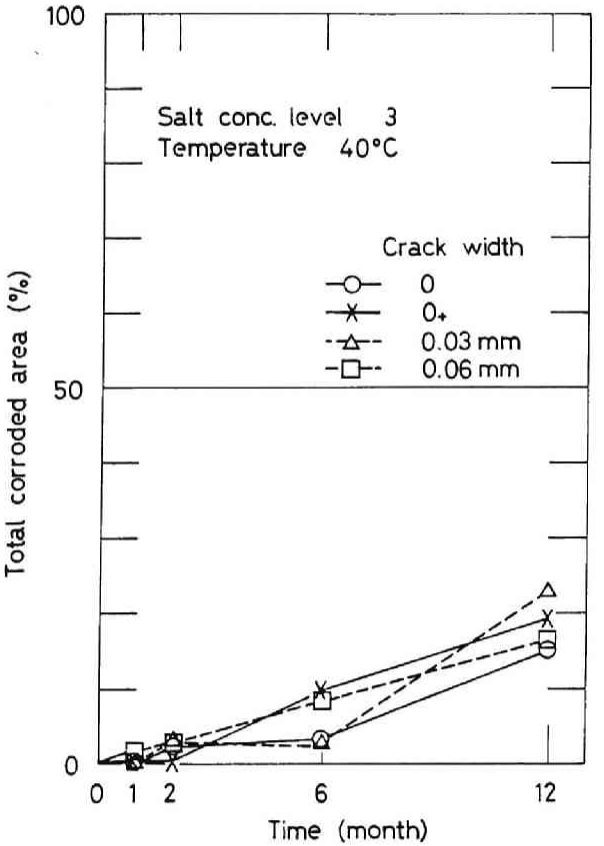

Fig. 3. 5--Total corroded area (40°C)

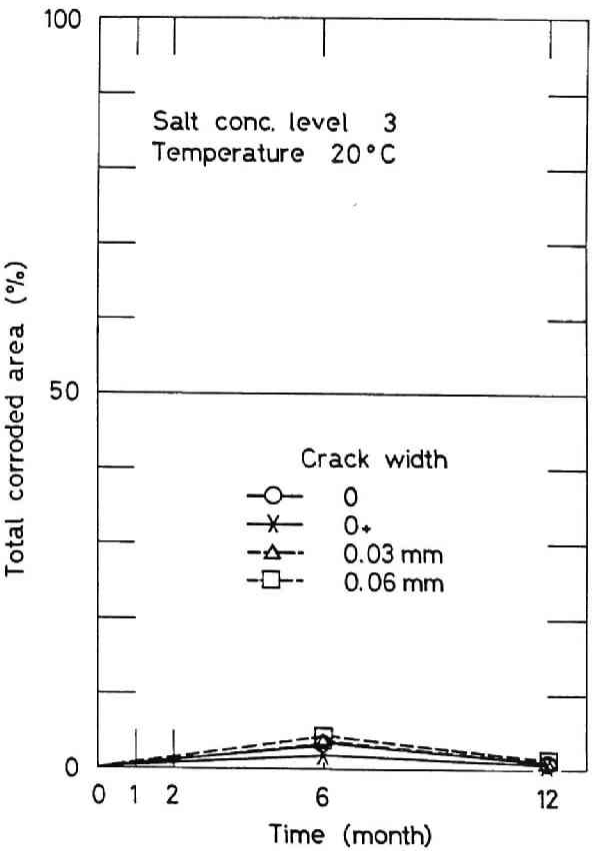

Fig. 3. 6--Total corroded area (20°C)

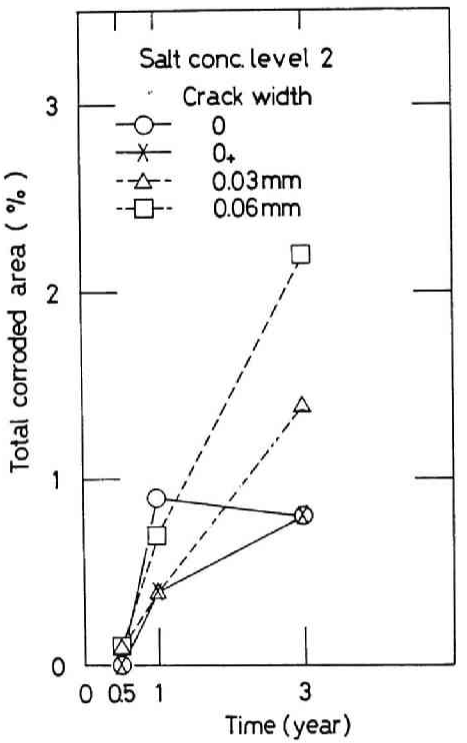

Fig. 3. 7--Total corroded area
(20°C, salt concentration level 2)

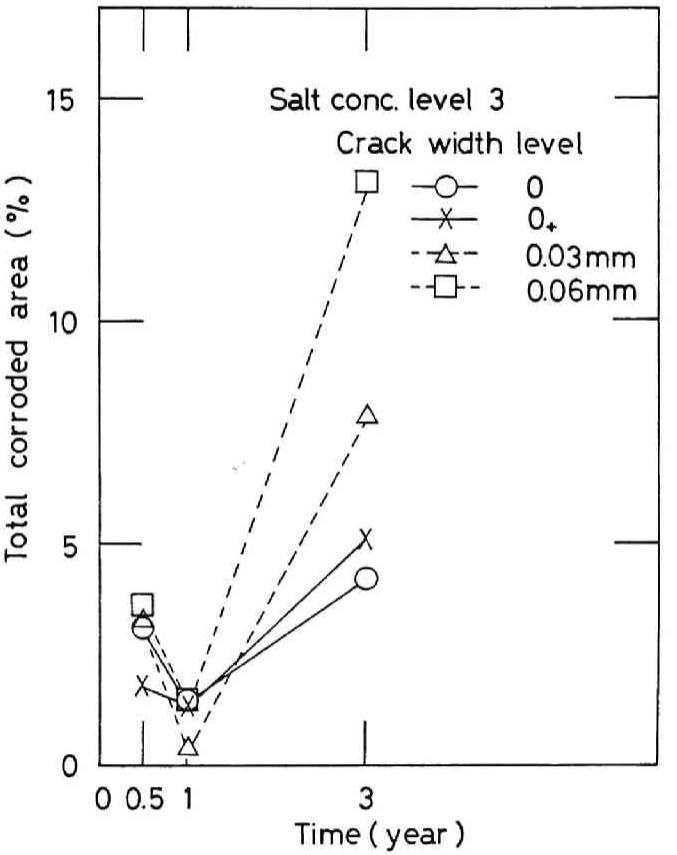

Fig. 3. 8--Total corroded area
(20°C, salt concentration level 3)

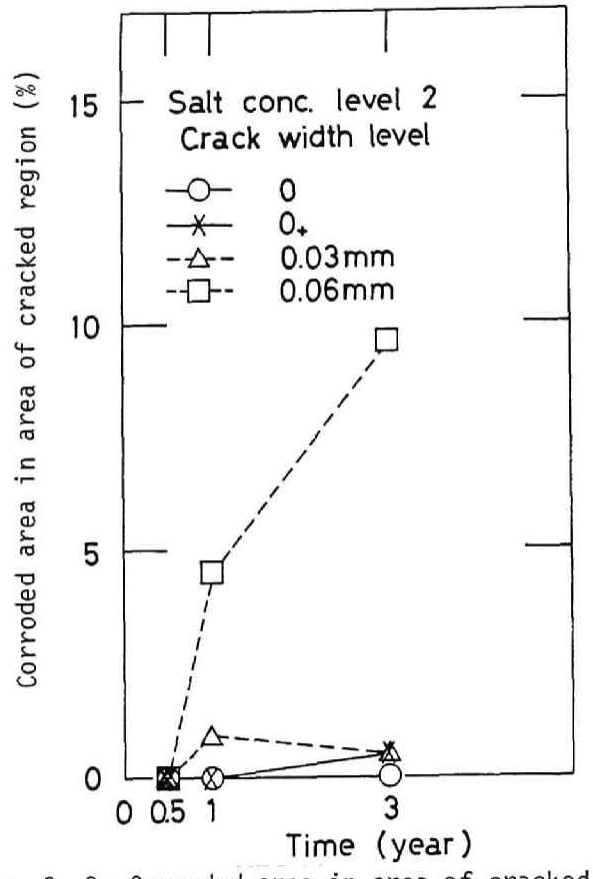

Fig. 3. 9--Corroded area in area of cracked region (20°C, salt concentration level 2)

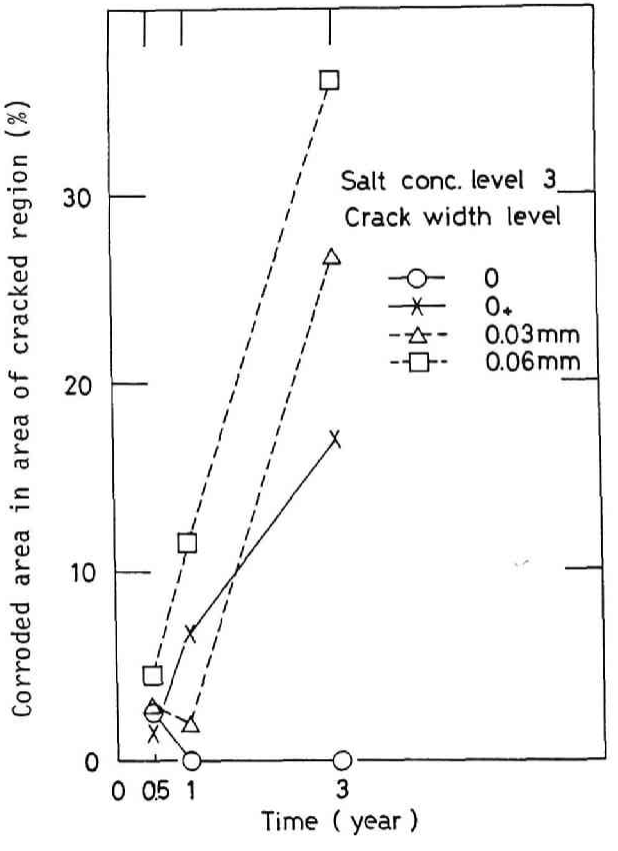

Fig. 3. 10--Corroded area in area of cracked region (20°C, salt concentration level 3)

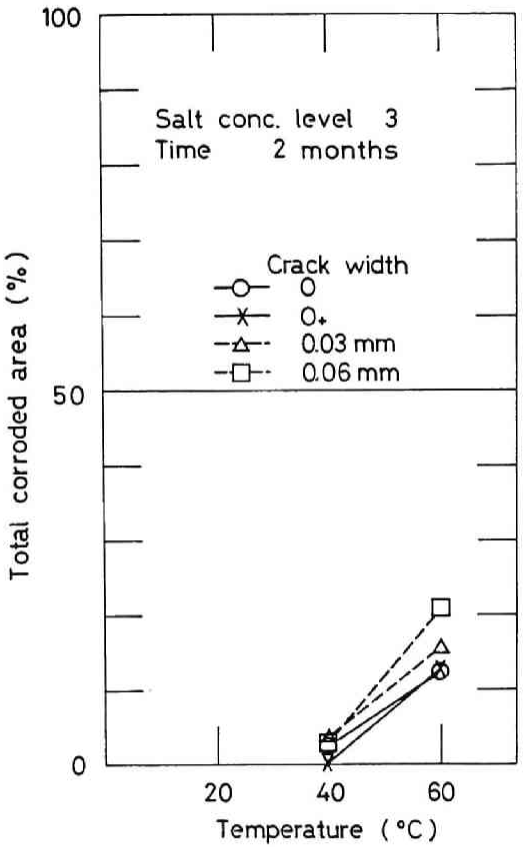

Fig. 3. 11--Relation between total corroded area and temperature (at 2 months)

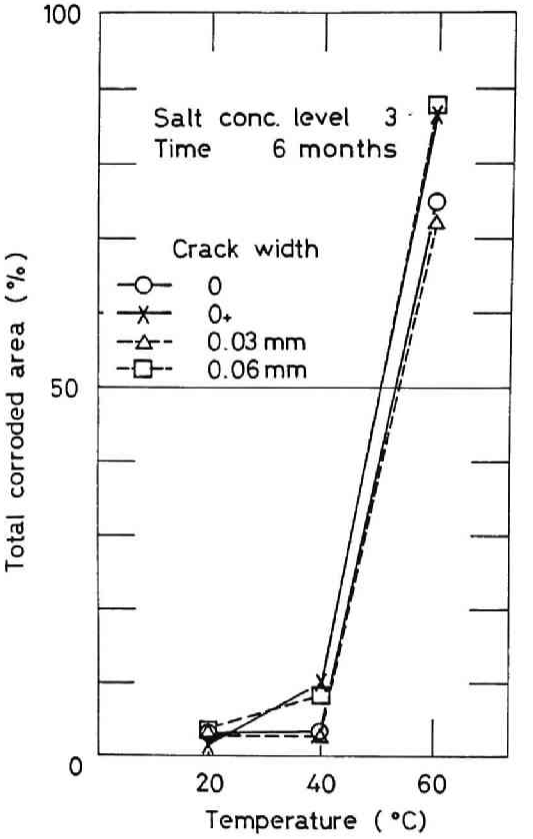

Fig. 3. 12--Relation between total corroded area and temperature (at 6 months)

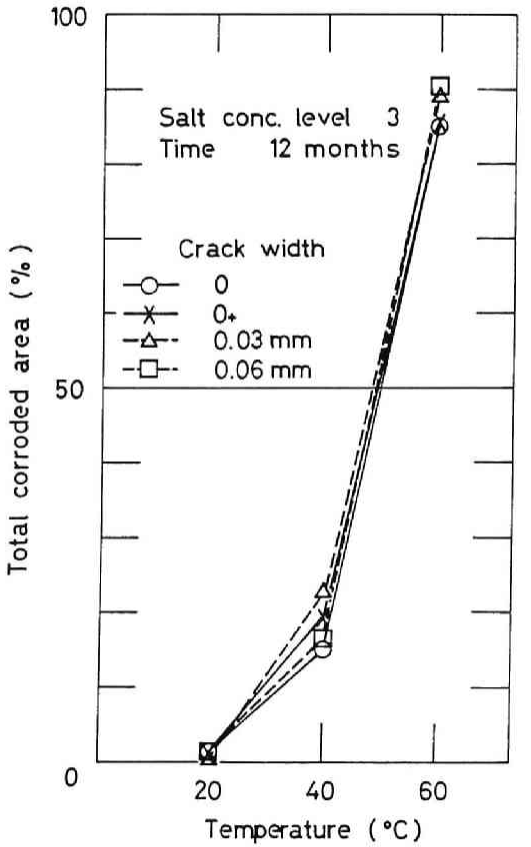

Fig. 3. 13--Relation between total corroded area and temperature (at 12 months)

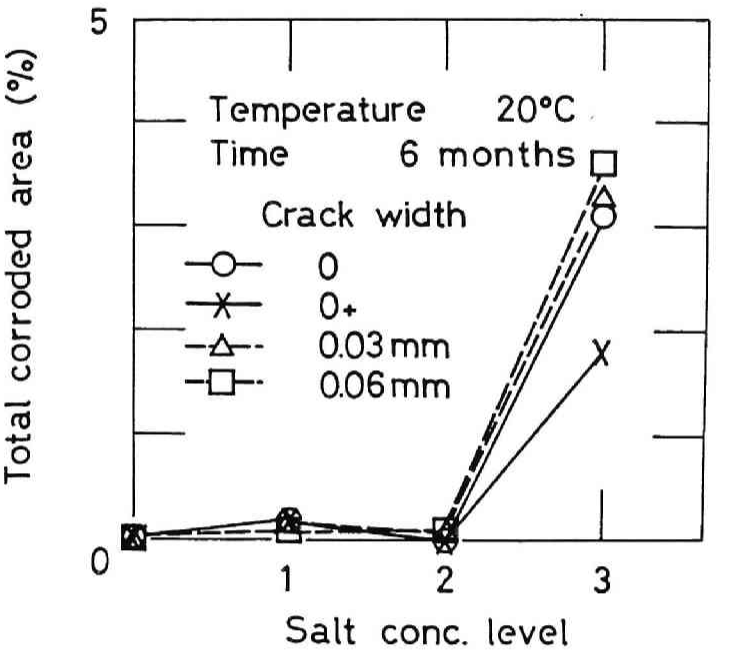

Fig. 3. 14--Influence of salt concentration level (at 6 months)

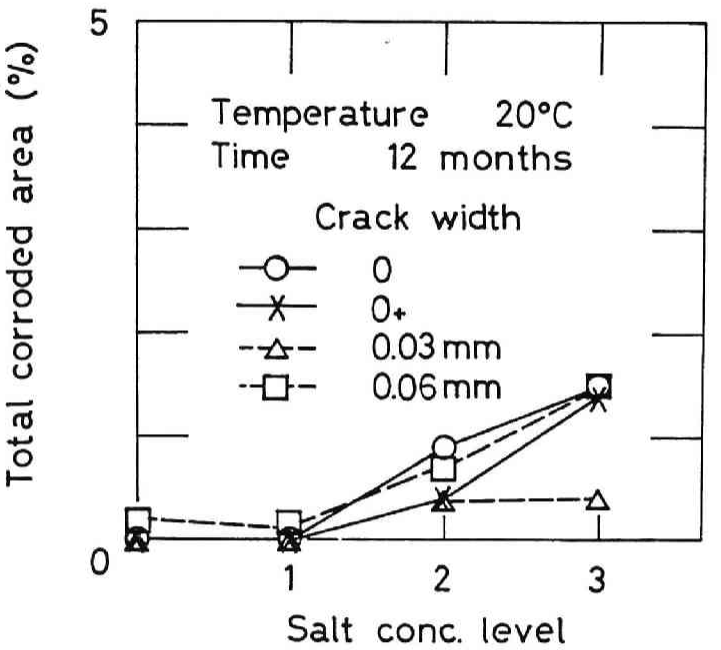

Fig. 3. 15--Influence of salt concentration level (at 1 year)

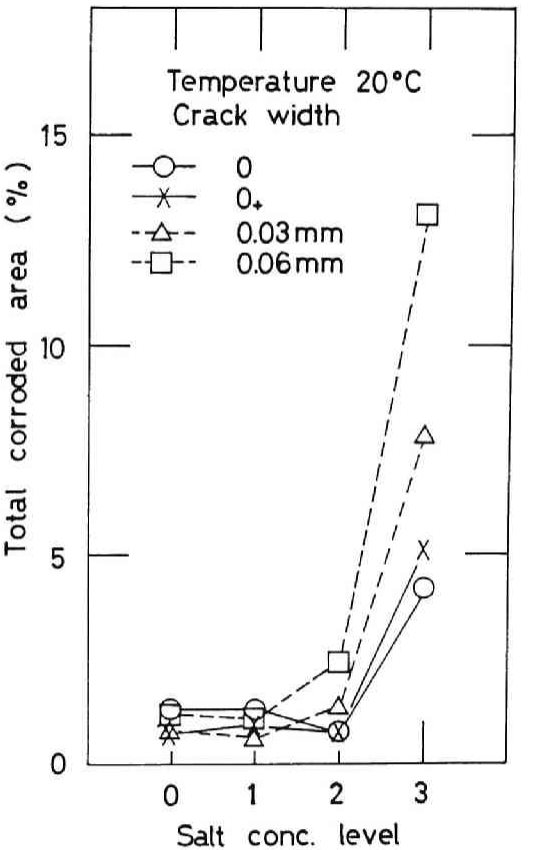

Fig. 3. 16--Influence of salt concentration level (at 3 years)

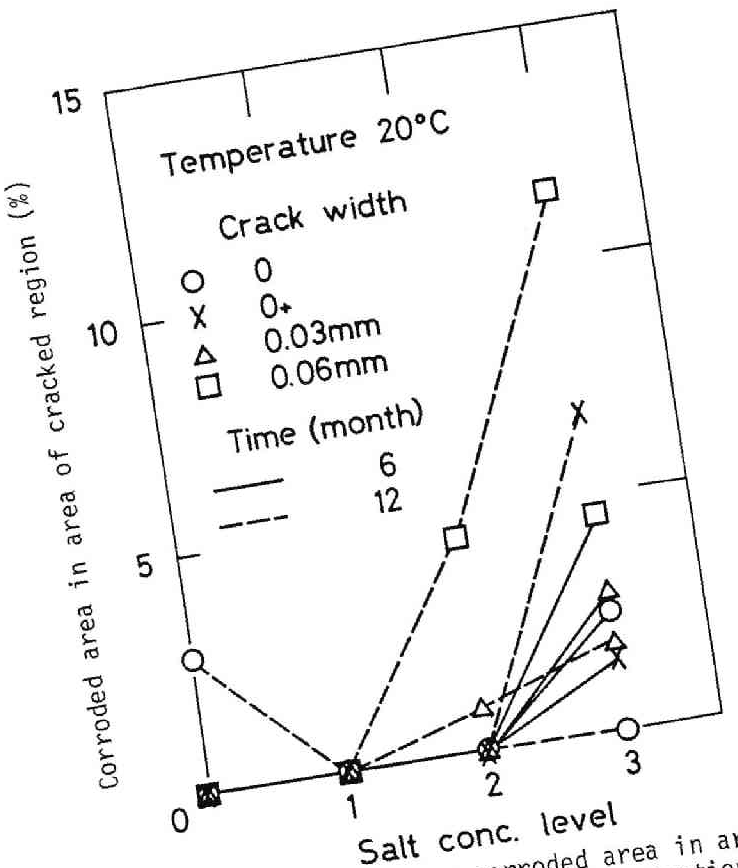

Fig. 3. 17--Relation between corroded area in area of cracked region and salt concetration level (at 6 and 12 months)

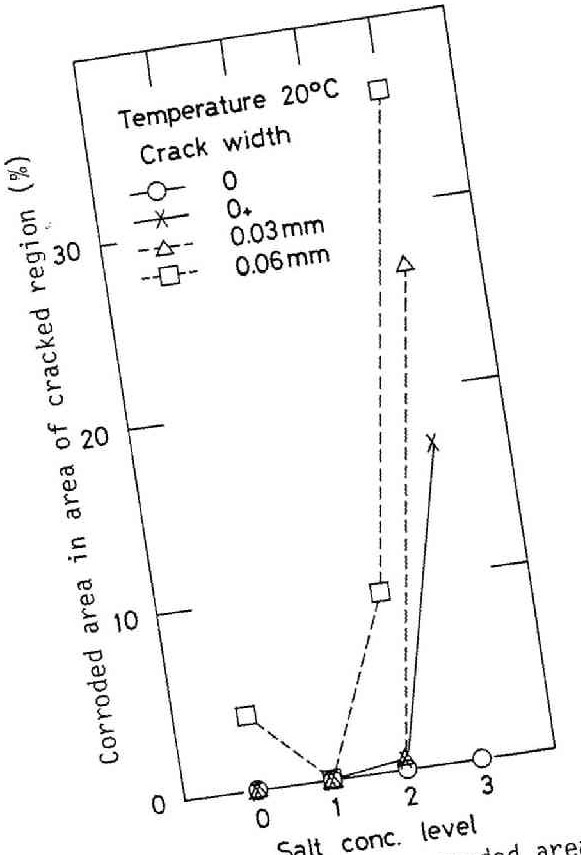

Fig. 3. 18--Relation between corroded area in area of cracked region and salt concetration level (at 3 years)

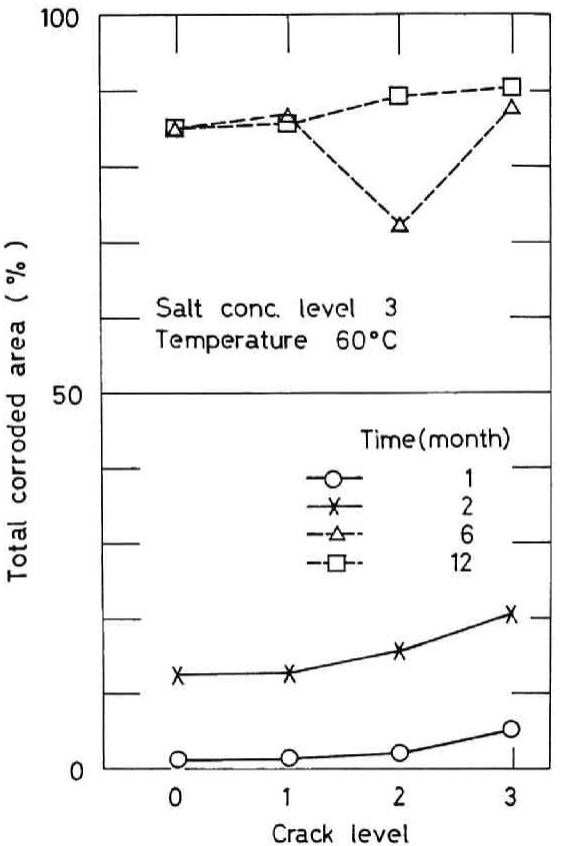

Fig. 3. 19--Relation between total corroded area and crack level (at 60°C)

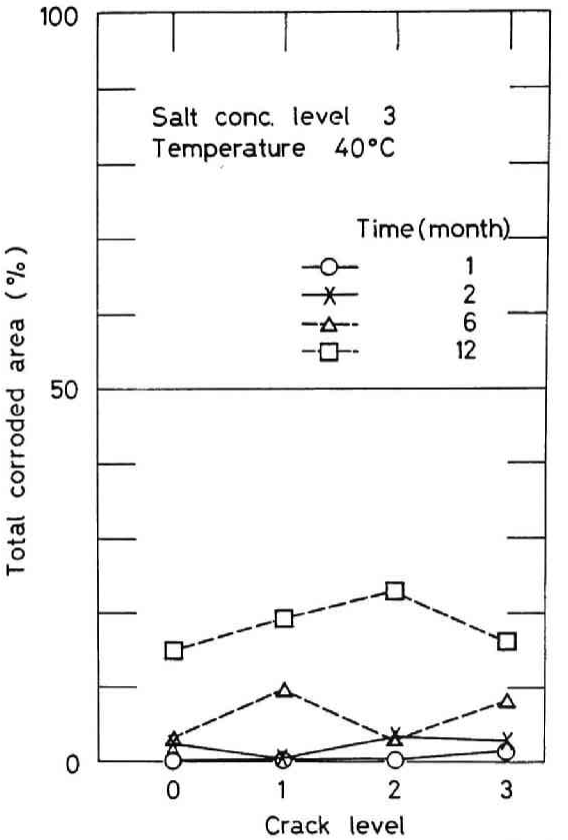

Fig. 3. 20--Relation between total corroded area and crack level (at 40°C)

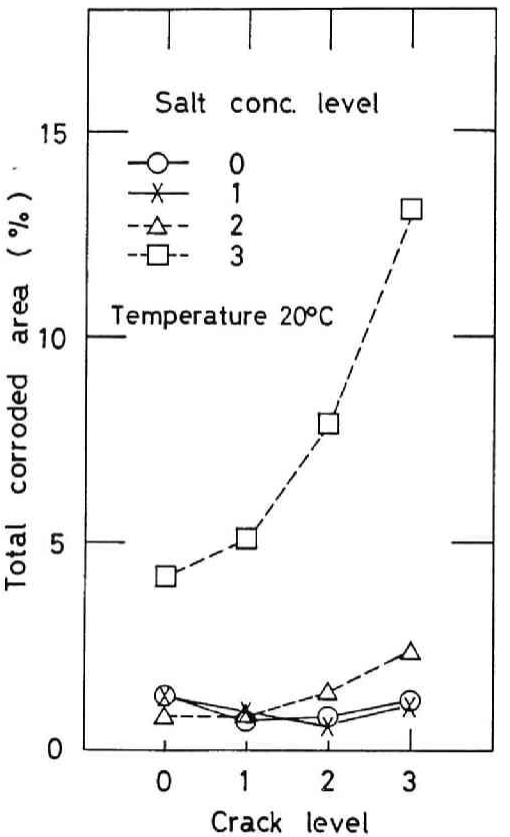

Fig. 3. 21--Relation between total corroded area and crack level (at 20°C, 3 years)

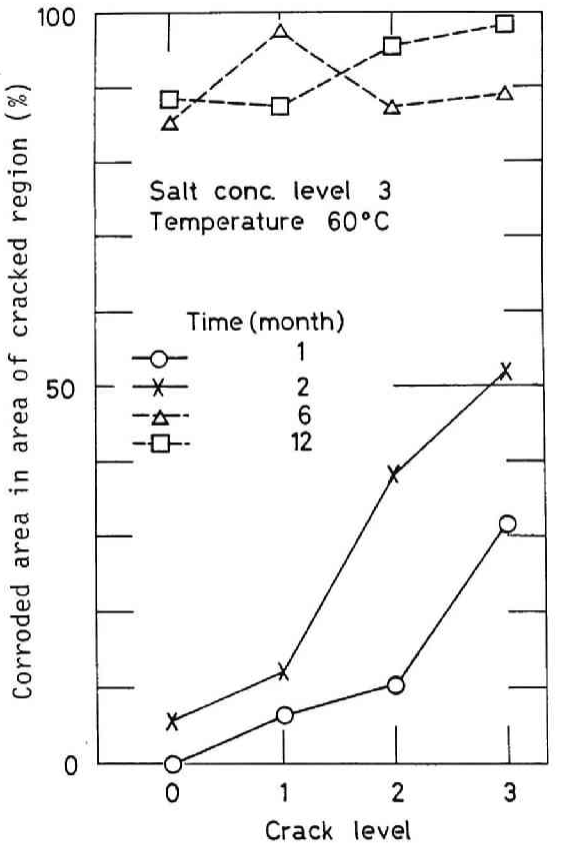

Fig. 3. 22--Influence of crack level (at 60°C)

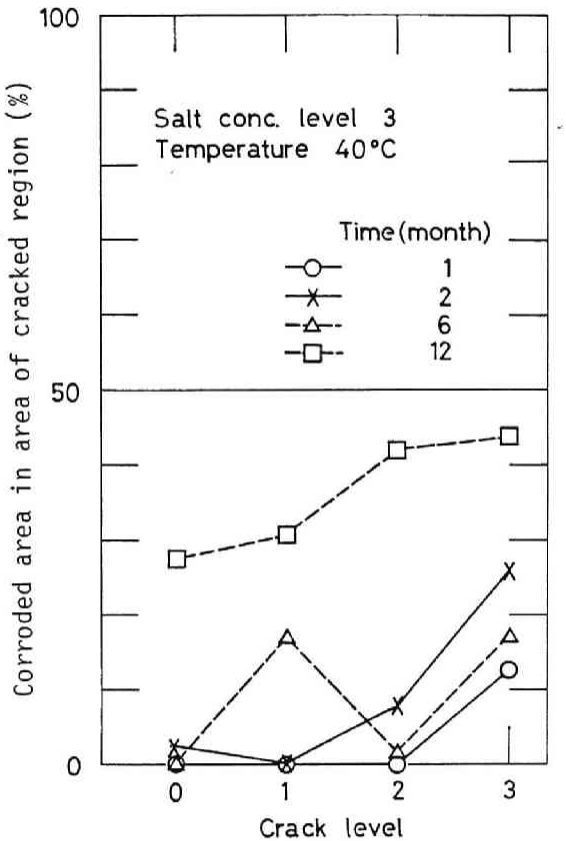

Fig. 3. 23--Influence of crack level (at 40°C)

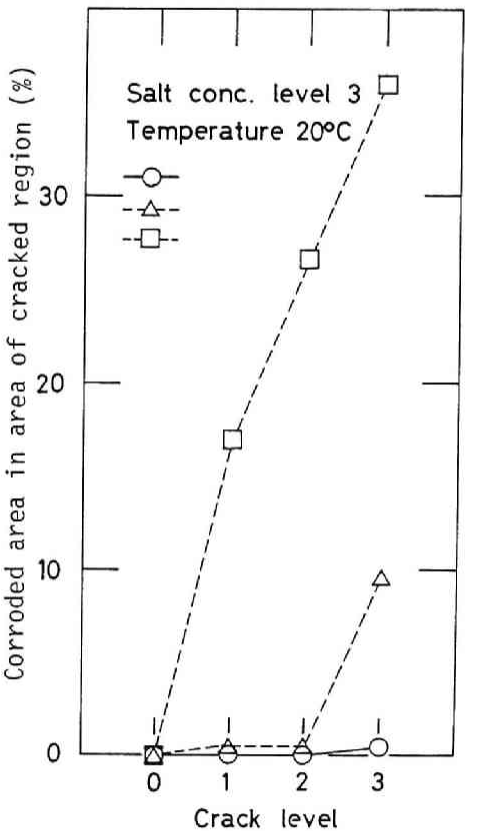

Fig. 3. 24--Influence of crack level (at 20°C)

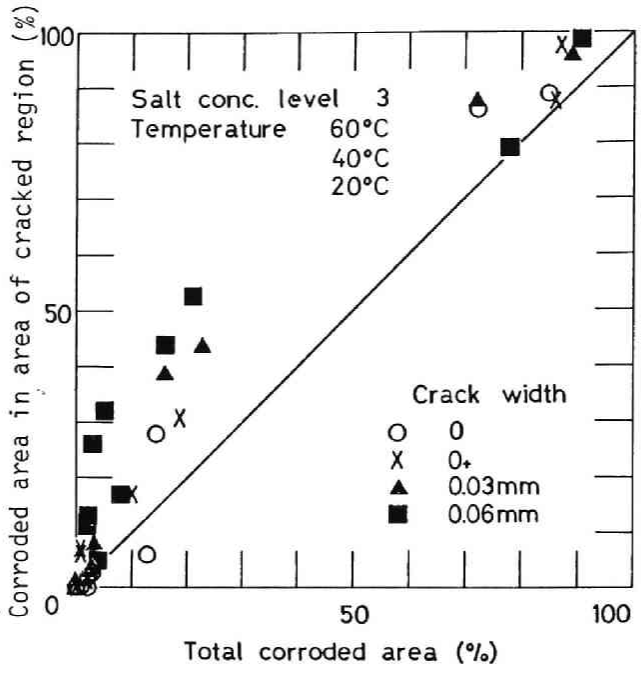

Fig. 3. 25--Relation between corroded area in area of cracked region and total corroded area

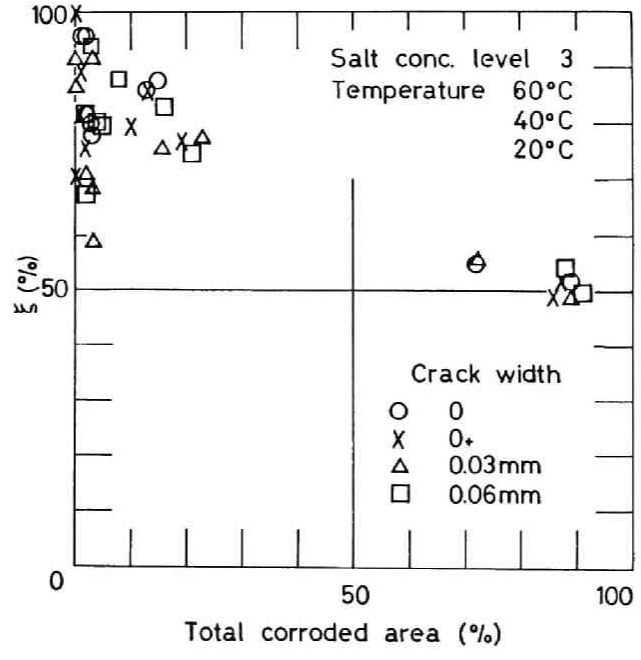

Fig. 3. 26--Relation between ξ and total corroded area

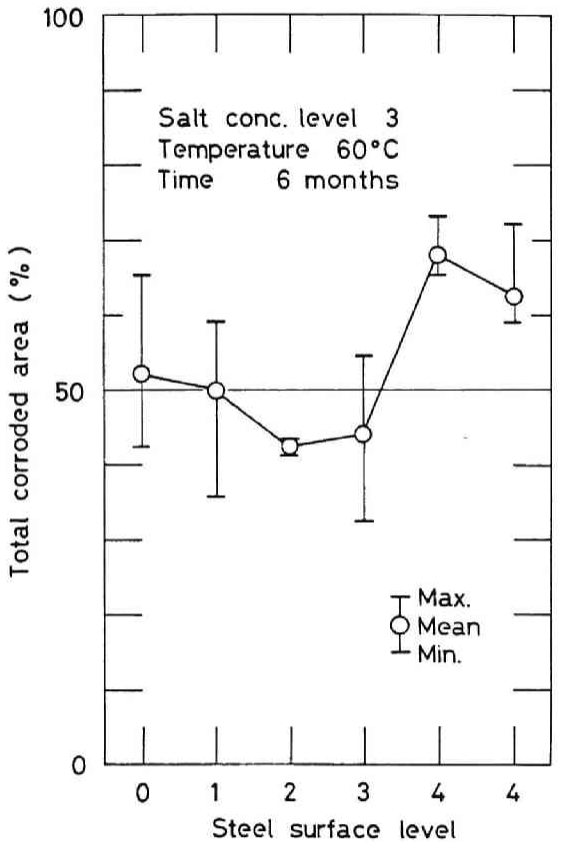

Fig. 3. 27--Relation between corroded area and steel surface level

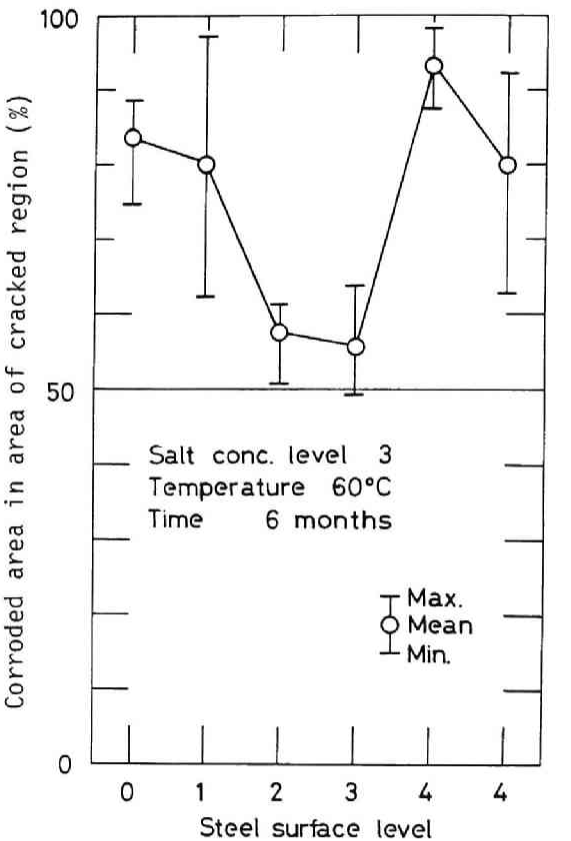

Fig. 3. 28--Relation between corroded area in area of cracked region and steel surface level

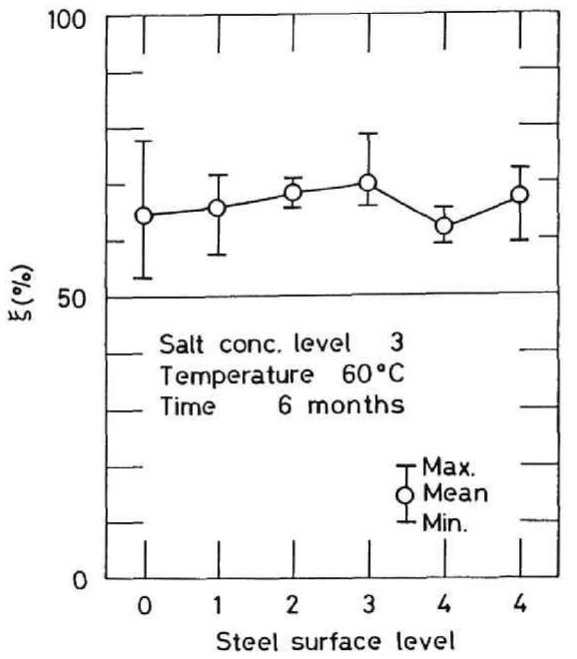

Fig. 3. 29--Relation between ξ and steel surface level

4 RATE OF CHLORIDE CORROSION OF REINFORCING STEEL IN CRACKED CONCRETE

4.1 Introduction

As discussed in Chapter 3, owing to occurrence of cracks reinforced concrete becomes heterogeneous as such a extent to result in forming macrocell. In a case of narrow cracks, however, there is such a high probability in the actual exposure conditions that fine cracks are healed and a passive film due to high alkalinity of concrete surrounds the exposed surface of reinforcing steel. Thus, the corrosion due to relatively wide cracks should be investigated to discuss on the cracked concrete in situ. Referring to the permissible crack width specified in many codes of practice and design regulations for aggressive exposure conditions, wide cracks were used in this chapter.

Macrocell corrosion proceeds continually on the reinforcing steel in widely cracked structures. Therefore, it is necessary to measure the rate of macrocell corrosion, and to compare it with the rate of microcell corrosion. The purpose of this chapter is to

point out that electrochemical measurements are useful as nondestructive methods for detecting corrosion, and how cracks effect upon the rate of corrosion.

4.2 Influence of Cracks on Corrosion Damage

When concrete materials contain little chloride when casting, the deterioration of reinforced concrete made of the materials due to chloride corrosion may proceed as shown schematically in Fig. 4.1 (4.1). The interaction of factors relating corrosion such as crack width defines the time at which the steel becomes active (t_0), i.e. it will start to corrode, and the rate at which corrosion then takes place, the time at which damage becomes visible (t_1) and the nature of resulting damage. When the cover concrete is contaminated with much chloride or has wide cracks, t_0 becomes zero. Thus the corrosion problem accompanied by wide cracks results in the crack corrosion rate during the period t_1. And, when the regions near cracks become an anode, other parts play a cathode. As a result, transferring of hydrated iron ions is controlled by oxygen supply at cathode (4.2).

4.3 Test Programs

As to the corrosion at cracks, following two items should be discussed. One is whether the corrosion reaction due to existence

of cracks proceeds or not, and another is how cracks affects the rate of corrosion while the crack corrosion is proceeding. This chapter deals with mainly the latter item.

Tests were carried out using various electrochemical methods. The mechanism and rate of corrosion are accurately obtained by measuring the electric potential and current. Then, in order to confirm the expected corrosion reaction experimentally, other methods such as visual inspection, measurement of weight loss etc. have to be employed.

Tests were conducted on three series of reinforced concrete specimens. In Series 1, the influence of cracks on potential distribution was investigated. In Series 2, relation between potential difference along the reinforcing steel and macrocell current was examined. And, finally in Series 3, study was made on the influence of cracks on macrocell current.

4.4 Test Series 1

-Influence of Cracks on Potential Distribution-

4.4.1 Test Program

While reinforced concrete beams were loaded to form flexural cracks wider than 0.06 mm used in Chapter 3, sodium chloride solution (NaCl 3.13% sol.) was injected through cracks, and the half

cell potential (vs Ag/AgCl electrode) of the reinforcing steel was measured. Then, cracked beams were immersed in the sodium chloride solution (NaCl 3.13% sol.) of about 25°C, and their potentials were measured intermittently for 43 days.

In this test, corrosion levels of reinforcing steel were defined as follows.

Level H : Red rust was mounted.

Level M : Between H and L.

Level L : Trace of rust.

4.4.2 Materials and Test Specimens

Materials--Ordinary Portland cement, Yasu river sand for fine aggregate (Specific gravity = 2.58, F.M. = 2.97) and Kurama crushed gravel for coarse aggregate (Specific gravity = 2.61, Maximum size = 10 mm) were used in concrete mix. Deformed bars (D10, SD35) with mill scale were used for reinforcing steel.

Mix Proportion--The high water cement ratio of 0.65 was used to accelerate corrosion process, and the design slump was 10±2 cm. The mix proportion of concrete in Series 1 is shown in Table 4.1.

Test Specimens--The test specimens in Series 1 is indicated in Fig. 4.2, and Table 4.2 shows the variations of specimens. The thickness of cover for reinforcing steel was 15 mm in all of the test specimens. The 10ø x 20 cm cylinders for compressive test,

15ø x 15 cm cylinders for splitting test and 10x10x40 cm prisms for flexural test were prepared. One day after casted, all of the test specimens were stripped and covered with wet burlaps for 4 weeks until the tests were started.

4.4.3 Test Procedures

Test setup of half cell potential measurements is shown in Fig. 4.2. Spacing between measurements during immersion was about 5 cm. Half cell potentials were measured along the reinforcing steel on the cover concrete surface using Ag/AgCl reference electrode and voltmeter of input impeadance 10^{11} ohm.

4.4.4 Results and Discussions

Strengths of concrete are listed in Table 4.3.

Half cell potentials at Point 1 shown in Fig. 4.2 are given in Fig. 4.3. Potential differences between the half cell potentials at Point 1 and Point 2 are shown in Figs. 4.4 - 4.6. During the injection of sodium chloride solution, the potential scarcely changed and the potential difference could be rarely recognized in case of crack width of less than 0.1 mm.

Typical relations between the potential distributions and the conditions of rust are shown in Figs. 4.7 - 4.12. The tendency that the potential became less noble at the location of cracks could be

recognized remarkably at 30 min. after loaded. After immersion in the sodium chloride solution, the potential became less noble and the potential difference became small. And at the location of cracks, the reinforcing steel was corroded. This phenomenon showed that the macrocell corrosion reaction proceeded, in which the anode was near the crack and the cathode in the concrete. Decrease in potential difference was mainly due to corrosion deposits formed at the anode and to consumption of oxygen at the cathode. Thus influence of macrocell became smaller and on the other hand that of microcell larger. All of potentials of reinforcing steel after 43 days' immersion were active, because of large water cement ratio and small clear cover for reinforcing steel.

4.5 Test Series 2

-Relation between Potential Difference and Macrocell Current-

4.5.1 Test Program

Potential and its difference are considered as the capability of corrosion and the electromotive force of macrocell corrosion, respectively. As the anode and cathode exist apart in macrocell, separation of the anode and cathode can be made experimentally. On the cracked model specimens as shown in Fig. 4.13, which were immersed in the sodium chloride solution (NaCl 3.13% sol.) of about 25°C, the distribution of potentials on the long reinforcing steel was measured, and then the difference between the maximum and

minimum potentials was calculated. Electric current flowing from the short reinforcing steel embedded in concrete to that exposed at the crack was also measured.

4.5.2 Materials and Test specimens

Materials and Mix Proportion--Materials and mix proportions of concrete were similar to those described in Series 1.

Test Specimens--The test specimens in Series 2 are indicated in Fig. 4.13, and Table 4.4 shows the variations of specimens. The thickness of cover for reinforcing steel was 15 mm. One day after casted, all of the test specimens were treated in the similar manner to Series 1.

4.5.3 Test Procedures

Half cell potentials were measured at about 5 cm spacings in the same manner as described in Series 1. Electric currents flowing from the short reinforcing steel embedded in concrete to that exposed at the crack were also measured using zero-shunt amperemeter.

4.5.4 Results and Discussions

The maximum potentials could be measured near the model crack and the minimum ones apart from the crack.

Fig. 4.14 shows the relation between the potential difference and the period of immersion. The potential difference decreased with elapsed time. When the sodium chloride solution was used as mixing water, potential difference was smaller at first stage and later larger than when tap water was used. The effect of mill scale on the potential difference was not clear.

Fig. 4.15 shows the typical relation between the current density and the period of immersion. The current density decreased with elapsed time. The sodium chloride solution as mixing water, gave current density larger than the tap water. Mill scale of reinforcing steel gave the current density smaller at first, but later had no effects.

The time dependence of the potential difference and the current are shown in Figs. 4.16 - 4.20. As the potential difference decreased, the current became smaller. Therefore, it became clear that the potential difference was the electromotive force giving rise to the measured current as macrocell corrosion. When the model crack was not fabricated, the current was very small because the anodic process was inhibitted. The current was not in proportion to the potential difference. This phenomenon is caused by physical and chemical factors, such as no existence of model crack and the nonlinear relation between the potential and the current of the corrosion reaction.

The relation between the current density and the crack width is

shown in Fig. 4.21. The current density decreased with increasing width of model crack. This may be caused by the availability of oxygen at cathode.

4.6 Test Series 3

-Influence of Cracks on Macrocell Current-

4.6.1 Test Program

It is considered that macrocell corrosion rate is controlled by both the availability of oxygen at the cathode and the electrical resistance of the concrete between the anode and the cathode (4.2). Thus the macrocell corrosion rate depends on the ratio of the cathodic area (Ac) to the anodic area (Aa).

To intensify the macrocell corrosion, the crack model specimens were subjected to the cycles of wetting (immersed in the sodium chloride solution : NaCl 3.13% sol.) and drying (in the air). The half cell potentials of reinforcing steel were measured. The macrocell current and the depth of damage due to corrosion were also measured.

4.6.2 Materials and Test Specimens

Materials--The similar materials those described in Series 1 were used.

Mix Proportion--The water cement ratio was 0.70 to highly accelerate corrosion process and the design slump was 15±2 cm. The mix proportion of concrete in Series 3 is shown in Table 4.5.

Test Specimens--The test specimens in Series 3 are shown in Fig. 4.22, and Table 4.6 shows the variations of specimens. The thickness of cover for reinforcing steel was 20 mm. 10ø x 20 cm cylinders for compressive test, 15ø x 15 cm cylinders for splitting test and 10x10x40 cm prisms for flexural test were prepared. One day after casted, all of the test specimens were treated in the similar manner to Series 1.

4.6.3 Test Procedures

Half cell potentials and macrocell currents were measured in the same manner as described in Series 2.

4.6.4 Results and Discussions

Strengths of concrete are shown in Table 4.7.

The relation between the potential and the current density had the same tendency as in case of test Series 2. As shown in Figs. 4.23 and 4.24, the current density decreased with the period of immersion, and increased after drying. This may be caused by the supply of oxygen. It was clear that the wetting and drying cycle gave the corrosion rate higher than the continuous immersion only.

The observed corrosion depth due to macrocell according to pickling method are compared in Fig. 4.25 and Table 4.8 with that calculated from the quantity of electricity using Faraday's law. The close agreement between two was noticed. Thus, it was confirmed experimentally that measured current density means macrocell corrosion rate.

Fig. 4.26 shows the relation between the current density (the maximum value during the second wetting period) and the ratio of Ac/Aa. As the ratio of Ac/Aa increased, the macrocell current density and the corrosion rate became larger. In case of actual cracks, the ratio of Ac/Aa affects on macrocell corrosion rate when the crack width is large enough.

4.7 Conclusions

In this chapter, three series of tests were carried out on various types of reinforced concrete specimens to make clear the influence of cracks on potential distribution, the relation between potential difference and macrocell current, and the influence of cracks on macrocell current. The conclusions relating the effects of cracks on the corrosion rate obtained in this chapter are summarized as follows;

(1) Cracks, wider than the critical crack width of 0.1 mm or more, in the reinforced concrete structures will form the macrocell corrosion of reinforcing steel.

(2) The testing method, based on half cell potential and macrocell current measurements, for the relation between crack width and corrosion process used in this chapter is applicable to determine the crack corrosion of reinforced concrete members.

(3) The potential difference between macro anode and cathode can be considered as the electromotive force giving rise to the macrocell corrosion.

(4) As the ratio of cathodic area to anodic area (Ac/Aa) increases, the macrocell current density and the corrosion rate at cracks become larger.

4.8 References

(4.1) Browne, R. D., "Mechanism of corrosion of steel in concrete in relation to design, inspection and repair of offshore and coastal structures", ACI SP-65, pp. 169-204, Aug. 1980

(4.2) Beeby, A. W., "Cracking and Corrosion", Concrete in the Ocean Technical Report No. 1, CIRIA/UEG-CCA-Dept. of Energy, 1978

(4.3) Okada, K., Koyanagi, W. and Miyagawa, T., "Chloride corrosion of reinforcing steel in cracked concrete", Proc. of JSCE, No. 283, pp. 75-87, Jan. 1979

(4.4) Okada, K., Koyanagi, W. and Miyagawa, T., "Chloride corrosion of reinforcing steel in cracked concrete", Int. Symposium on Offshore structures, RILEM-FIP-CEB, Brazil Offshore '79, Vol. 1 I-4, Aug. 1979

(4.5) Okada, K., Koyanagi, W. and Miyagawa, T., "Chloride corrosion

of reinforcing steel in cracked concrete", Offshore Structures, pp. 1.61-1.78, Pentech Press, London, 1980

Table 4. 1 Mix proportion of concrete

Slump (cm)	Air content (%)	Water cement ratio (%)	Absolute fine aggregate ratio (%)	Unit weight (kg/m^3)			
				Water	Cement	Sand	Cravel
10±2	2	65	40	195	300	718	1097

Table 4. 2 Variations of concrete specimens for Series 1

Specimen	Mixing water	Surface condition of reinforcing steel
M - 1 2	Tap water	With mill scale
SM - 1 2	Sodium chloride solution	With mill scale
P - 1 2	Tap water	Polished

Table 4. 3 Strengths of concrete (Series 1 & 2)

Mixing water	Compressive strength (kg/cm^2)	Tensile strength (kg/cm^2)	Flexural strength (kg/cm^2)
Tap water	314	28.3	44.2
Sodium chloride sol.	292	27.8	47.3

Table 4. 4 Variation of specimens for Series 2

Specimen	Width of model crack(mm)	Mixing water	Surface condition of reinforcing steel
M - 0	0	Tap water	With mill scale
M - 5	5	Tap water	With mill scale
M - 10	10	Tap water	With mill scale
M - 25	25	Tap water	With mill scale
SM - 0	0	Sodium chloride solution	With mill scale
SM - 25	25	Sodium chloride solution	With mill scale
P - 25	25	Tap water	Polished

* Every type of specimens consist of two specimens.

Table 4. 5 Mix proportion of concrete

Slump (cm)	Air content (%)	Water cement ratio (%)	Absolute fine aggregate ratio (%)	Unit weight (kg/m^3)			
				Water	Cement	Sand	Gravel
15±2	2	70	50	210	300	900	924

Table 4. 6 Variations of specimens for Series 3

Specimen	Type of model	Length of anode a**(cm)	Length of cathode c**(cm)	Ratio of Ac/Aa
C - 30	Crack model	3	90	30
C - 19		3	56	19
H - 30	Half model	1.5	45	30
H - 19		1.5	28	19
S - 300	Separate model	1	300	300
S - 100		1	100	100
S 30		1	30	30
S - 10		1	10	10
S - 0		1	0	0

* Every type of specimens consist of two specimens.

** See Figure 4. 22.

Table 4. 7 Strengths of concrete (Series 3)

Compressive strength (kg/cm^2)	Tensile strength (kg/cm^2)	Flexural strength (kg/cm^2)
285	29.7	43.9

Table 4. 8 Corrosion depth

Specimen	Type of model	Ratio of Ac/Aa	Corrosion depth according to pickling method* (mm)	Corrosion depth due to macro-cell**(mm)	Estimated corrosion depth calculated from current***(mm)
C - 30	Crack model	30	0.0766	0.0490	0.0303
C - 19		19	0.0851	0.0575	0.0305
H - 30	Half model	30	0.1994	0.1718	0.1349
H - 19		19	0.0879	0.0603	0.0323
S - 300	Sepa-rate model	300	0.8728	0.8452	0.6886
S - 100		100	0.2710	0.2434	0.1988
S - 30		30	0.1848	0.1572	0.1430
S - 10		10	0.1692	0.1416	0.0517
S - 0		0	0.0276	0.0000	0.0000

* Observed corrosion depth

** Observed corrosion depth due to macrocell

= Each corrosion depth according to pickling method

- Value of (S - 0)

*** Calculated using Faraday's law

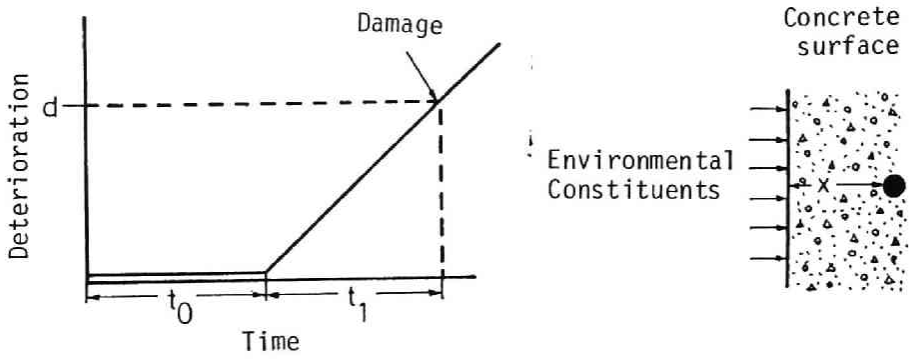

Fig. 4. 1--Time from exposure to significant deterioration for concrete due to steel corrosion

t_0 = time taken for constituents of environment to activate the steel at a particular location, a distance x from a surface.

t_1 = time thereafter for the critical constituents to cause significant deterioration (d) at that point x.

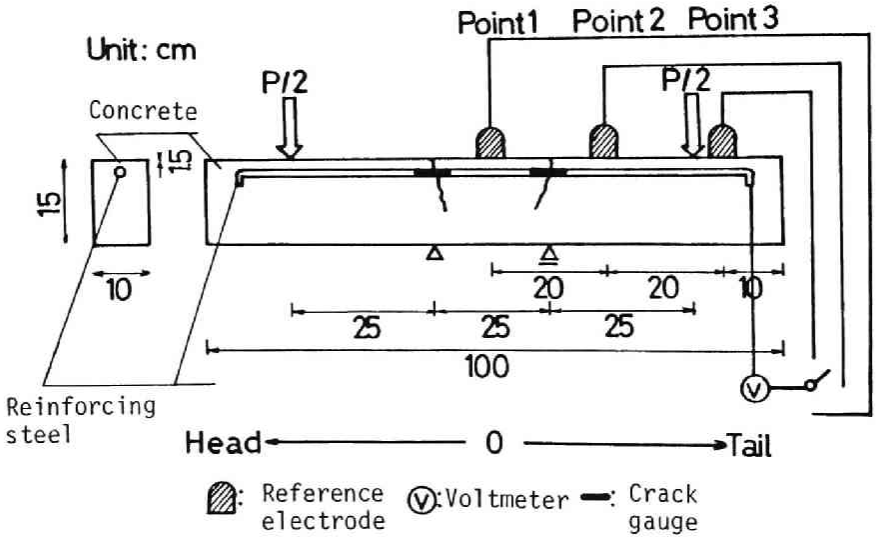

Fig. 4. 2--Specimen -Series 1-

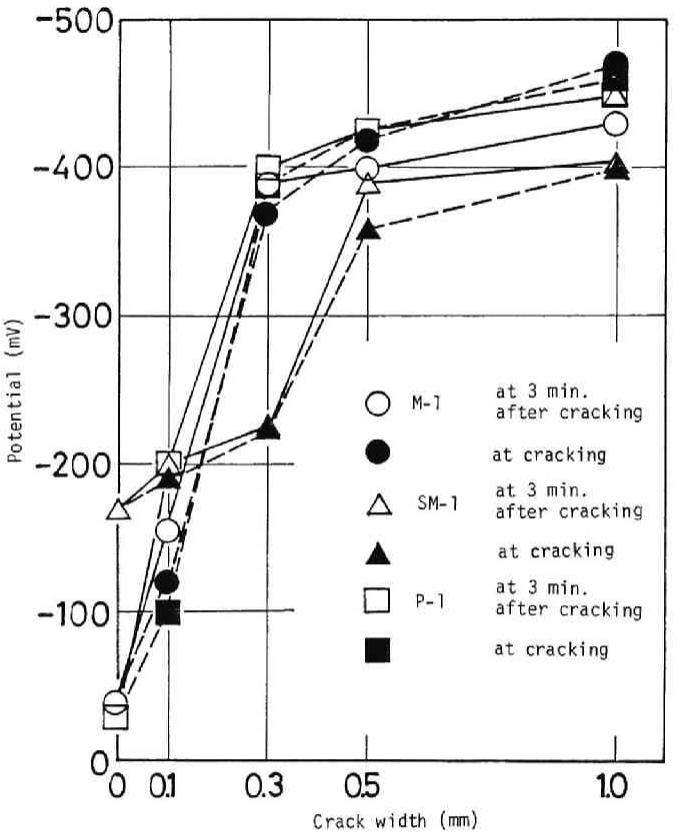

Fig. 4. 3--Half cell potentials during load

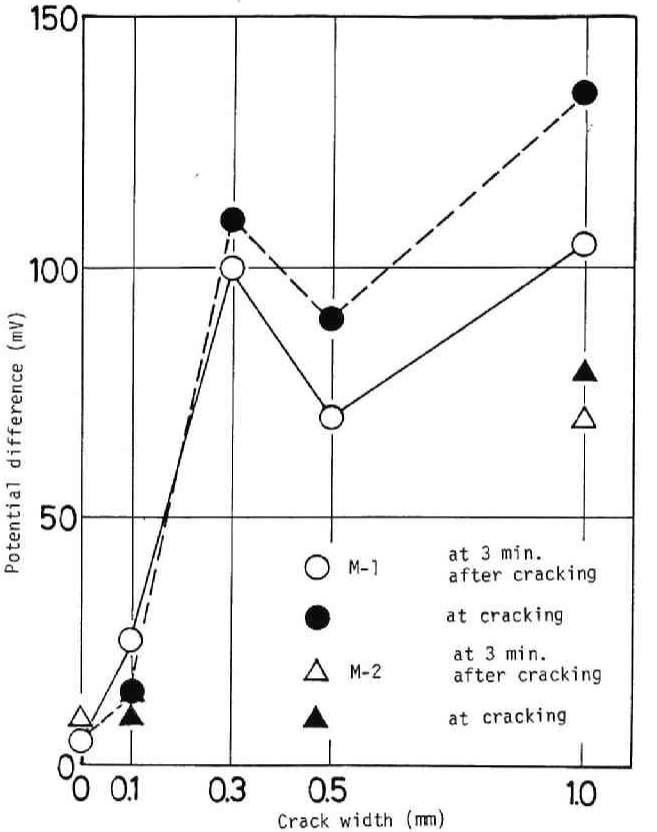

Fig. 4. 4--Relation between potential difference and crack width (M)

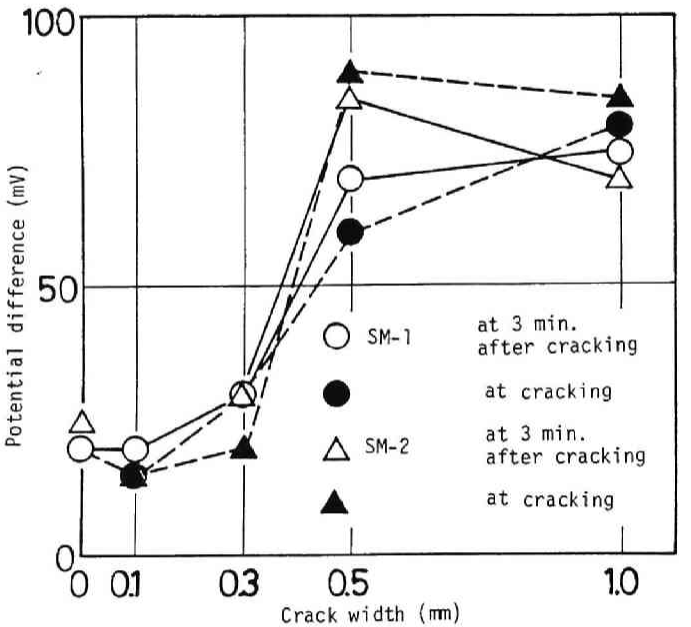

Fig. 4. 5--Relation between potential difference and crack width (SM)

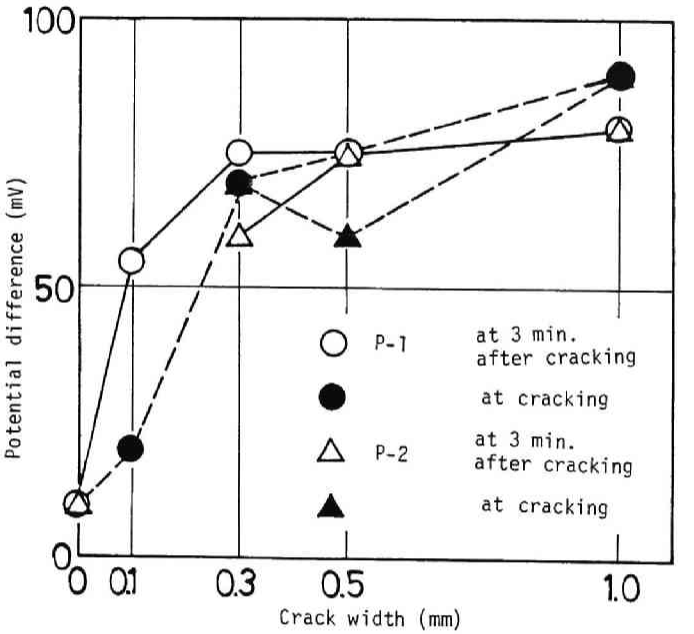

Fig. 4. 6--Relation between potential difference and crack width (P)

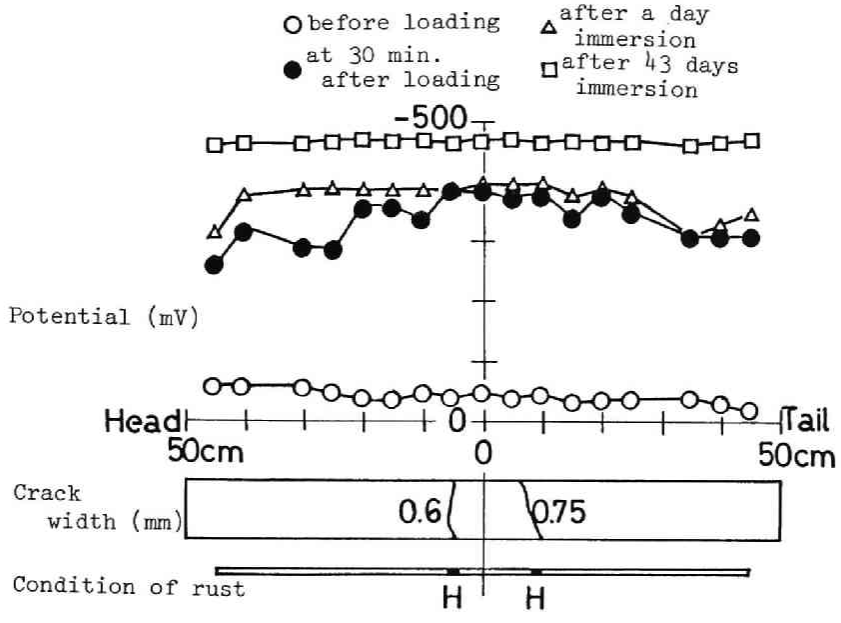

Fig. 4. 7--Relation between potential and cracks (M-1)

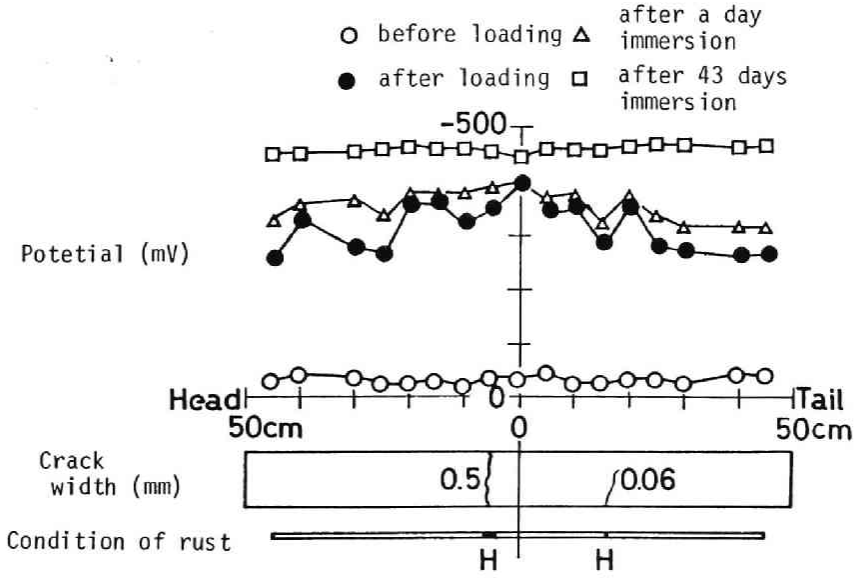

Fig. 4. 8--Relation between potential and cracks (M-2)

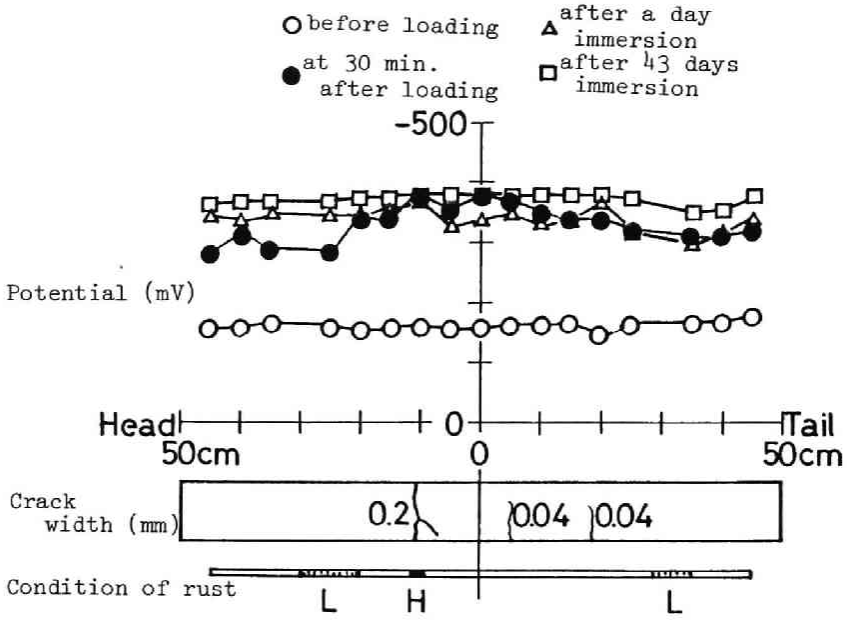

Fig. 4. 9--Relation between potential and cracks (SM-1)

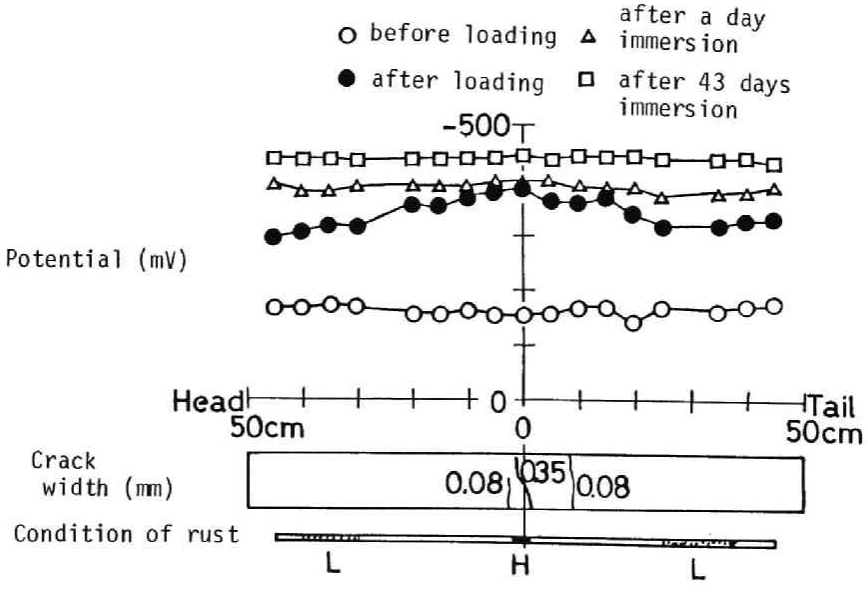

Fig. 4. 10--Relation between potential and cracks (SM-2)

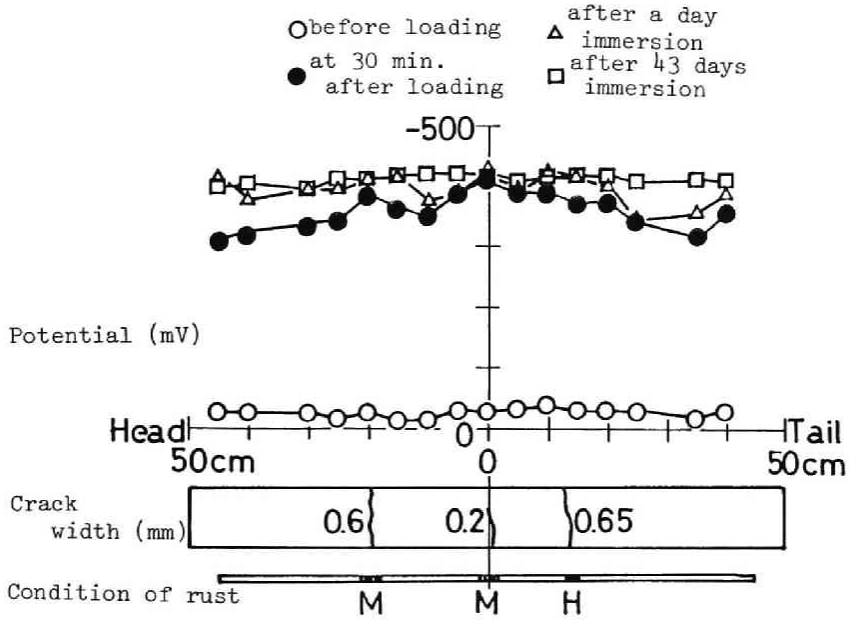

Fig. 4. 11--Relation between potential and cracks (P-1)

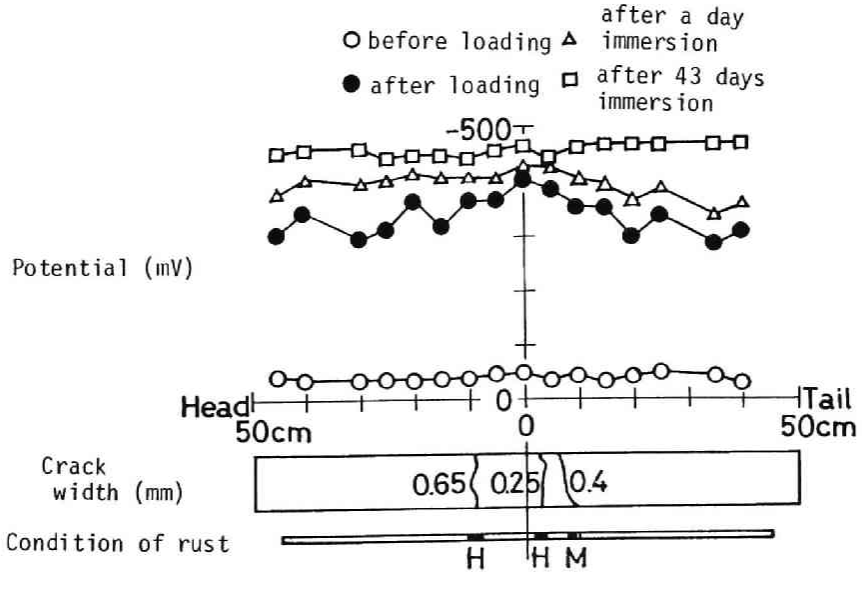

Fig. 4. 12--Relation between potential and cracks (P-2)

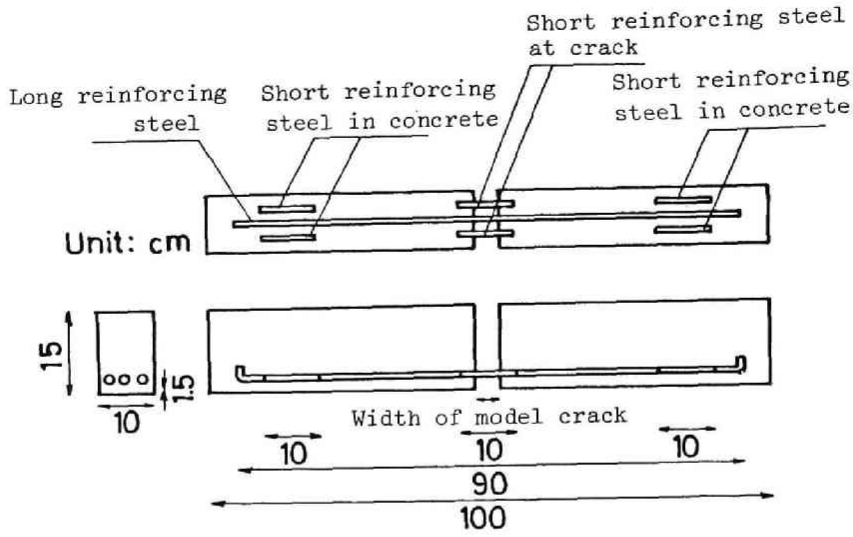

Fig. 4. 13--Specimen -Series 2-

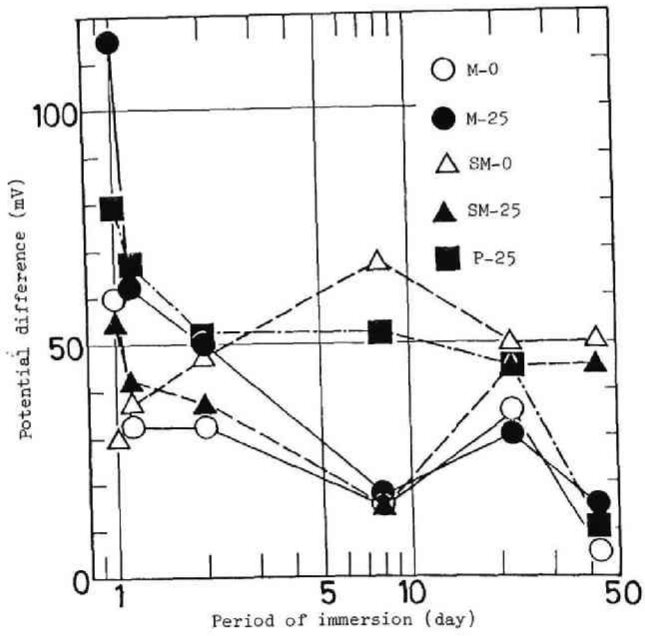

Fig. 4. 14--Relation between potential difference and period of immersion (1)

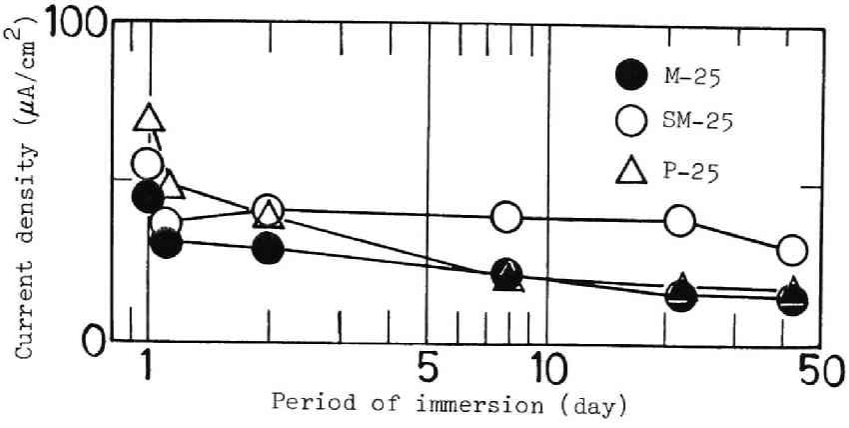

Fig. 4. 15--Relation between potential difference and period of immersion (2)

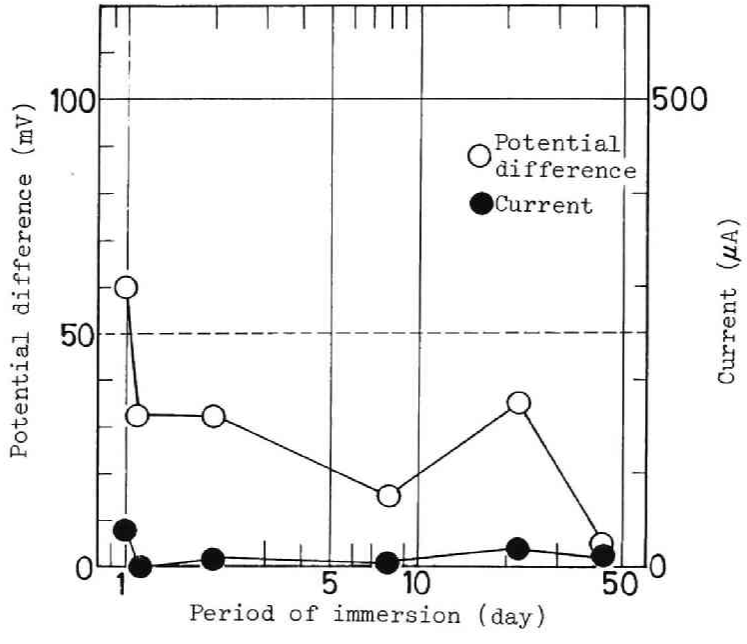

Fig. 4. 16--Potential difference and current (M-0)

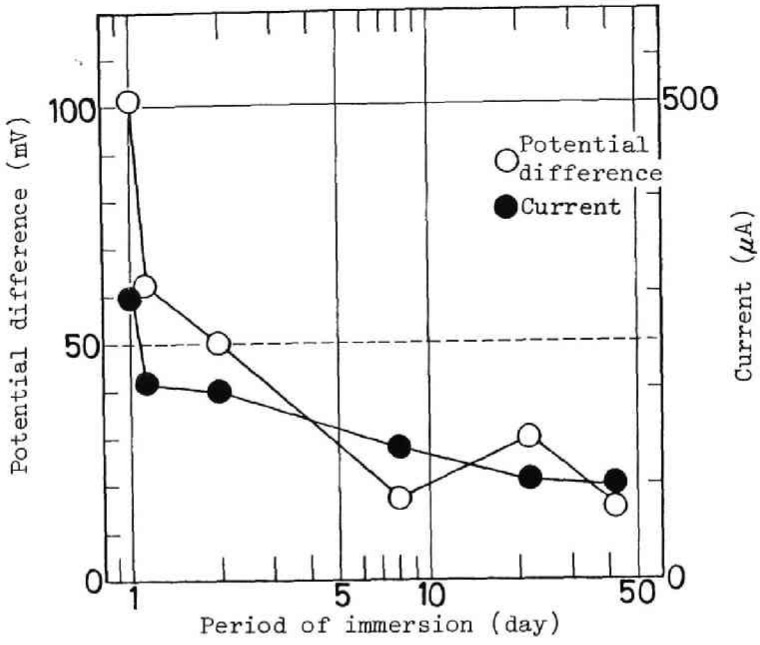

Fig. 4. 17--Potential difference and current (M-25)

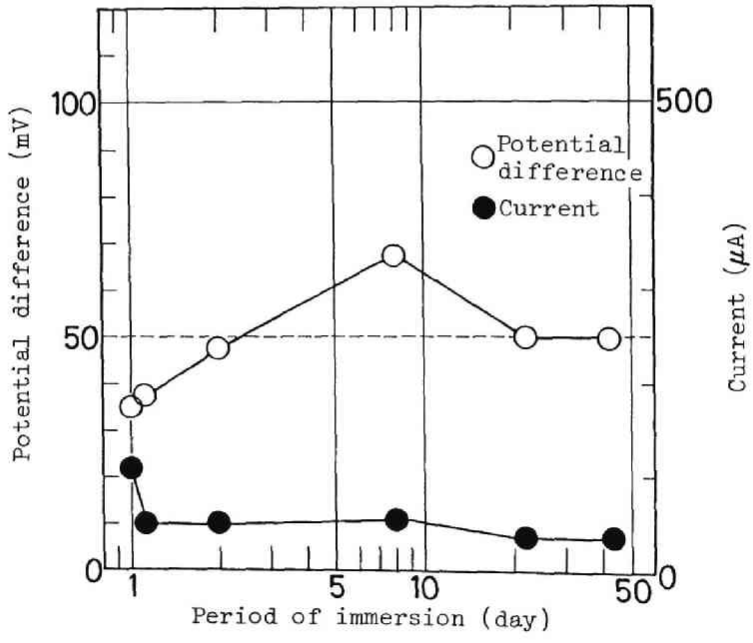

Fig. 4. 18--Potential difference and current (SM-0)

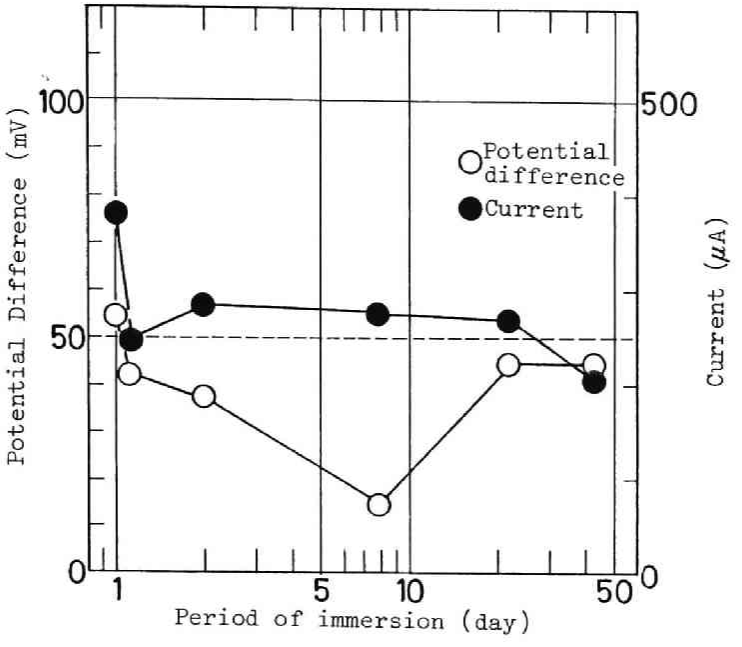

Fig. 4. 19--Potential difference and current (SM-25)

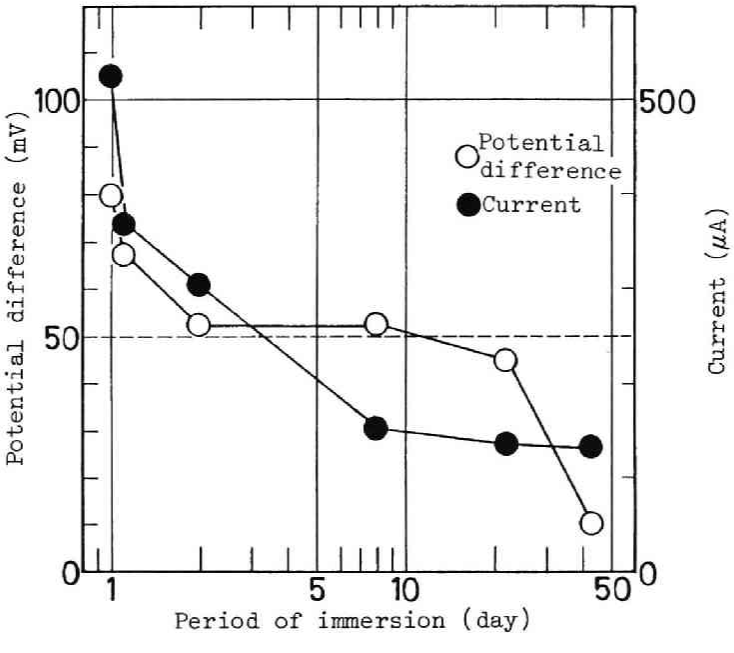

Fig. 4. 20--Potential difference and current (P-25)

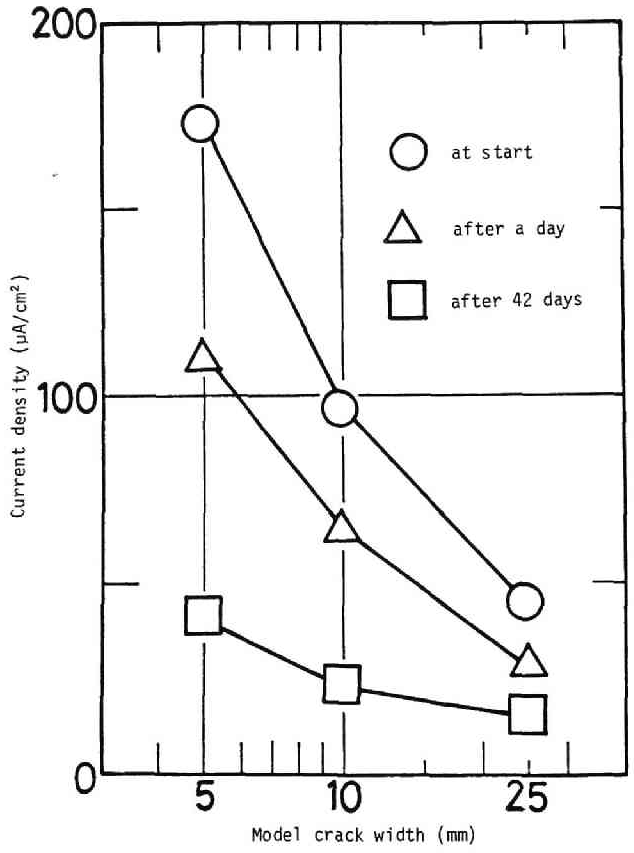

Fig. 4. 21--Relation between current density and model crack width

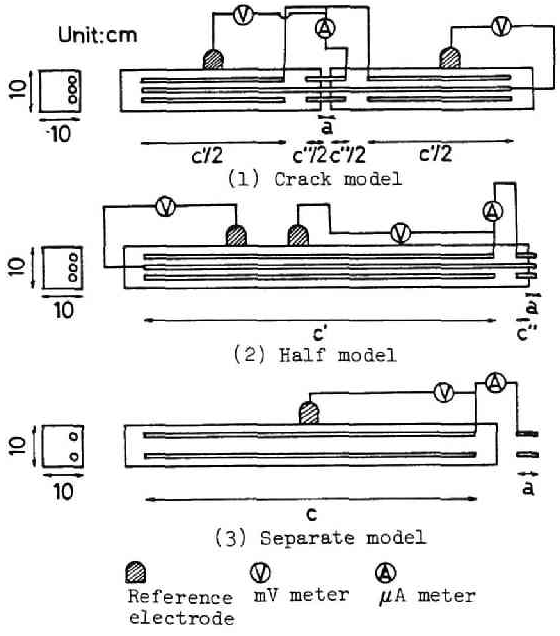

Fig. 4. 22--Specimen -Series 3-

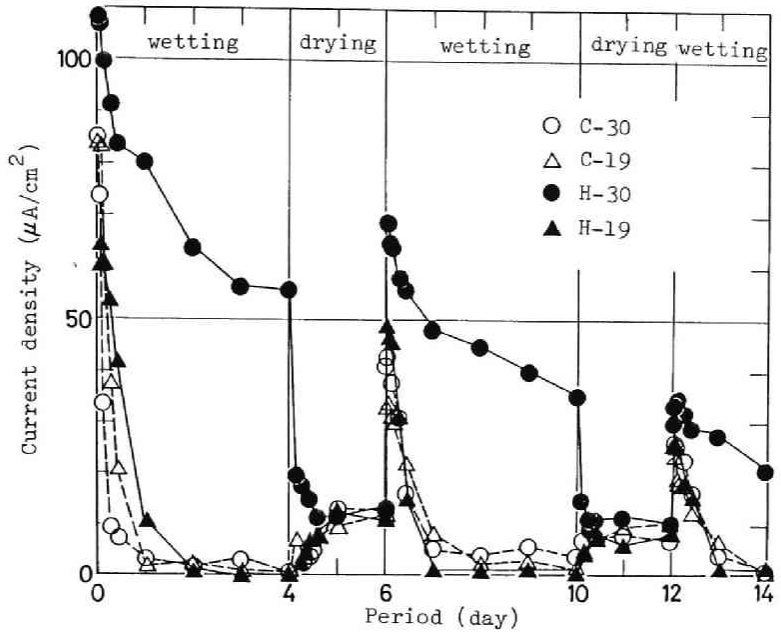

Fig. 4. 23--Relation between current density and period (Crack and half models)

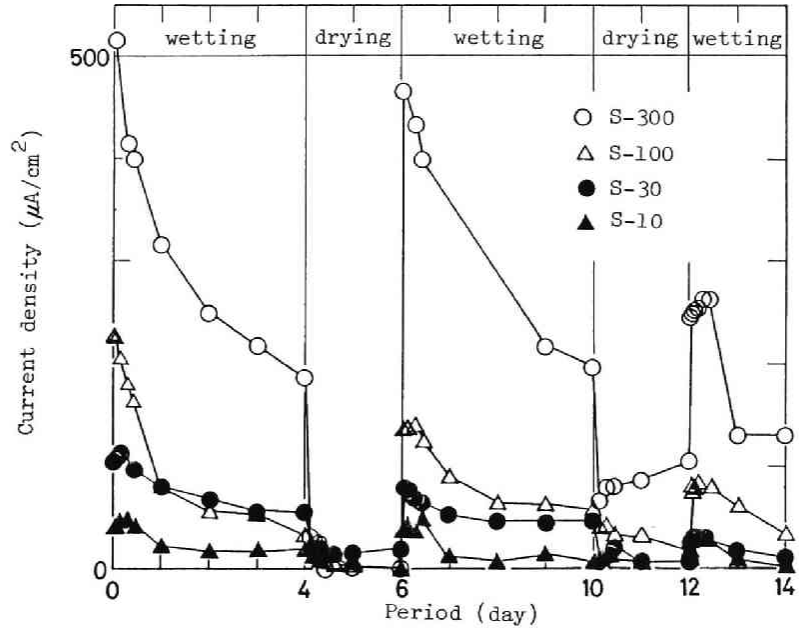

Fig. 4. 24--Relation between current density and period (Separate model)

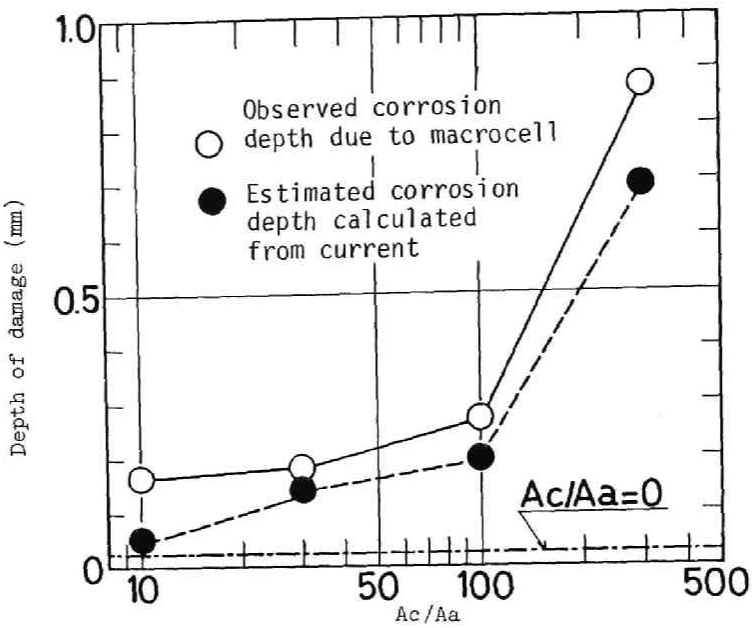

Fig. 4. 25--Calculation and observed depth of damage (Separate model)

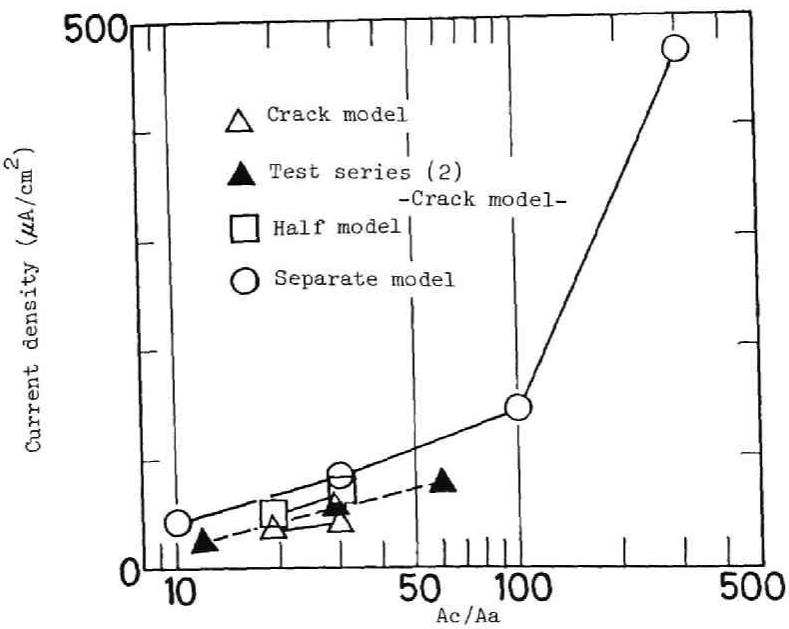

Fig. 4. 26--Relation between current density and ratio of Ac/Aa

5 MECHANISM OF CHLORIDE CORROSION OF REINFORCING STEEL IN CRACKED CORROSION

5.1 Introduction

Crack width induced in the model specimens in Chapter 4 was so wide that t_0 in Fig. 4.1 was almost equal to zero and macrocell corrosion proceeded. In the case of narrow crack width, however, it should be essentially discussed whether the corrosion reaction due to existence of cracks proceeds or not. And, macrocell corrosion current may be neglected in discussing the corrosion of reinforcing steel, when the electric resistance of cover concrete is very high.

The principal purpose of this chapter is to examine the influences of crack width and electric resistance of cover concrete on the corrosion mechanism of reinforcing steel.

5.2 Factors Influencing Reinforcement Corrosion in Cracked Concrete

According to many previous papers, the crack width of cover

concrete has little influence on the rate of reinforcement corrosion. It was concluded in Chapter 4 that the rate of crack corrosion depends upon not only the crack width but also the ratio of cathodic area to anodic area (Ac/Aa).

Schiessl (5.1) reported that there was a considerable increase in the percentage of active cracks with increase in width. But, the longer the duration of the exposure test, the smaller will be the influence of crack width and hence, viewed in terms of the design life of a structure, crack width will not have an influence on corrosion. As a result, Schiessl concluded that the apparent linear increase in degree of corrosion with crack width is a statistical illusion.

On the other hand, Beeby (5.2), referring to Shciessl's report, stated that the rate at which corrosion take place is likely to depend on two factors as follows; (i) Electric resistance of the path between the anode and cathode through the electrolyte occupying the pore structures of the surrounding concrete, and (ii) the ability of oxygen to reach the cathode. The conclusions in Chapter 4 confirmed the significance of latter factor.

However, the reports by Schiessl and Beeby cann't explain clearly the crack corrosion performance due to (i) the wide crack, in which a new steel surface is always exposed so that the corrosion products may be washed away, and (ii) the narrow, critical crack. Especially, in the latter case , it becomes an important problem to

be made clear whether the crack corrosion, highly influencing the mechanism of total corrosion, proceeds or not.

5.3 Test Programs

Tests were conducted on two series of model specimens. In Series 1, study was made on the critical crack width and mechanism of reinforcement corrosion. On the other hand, in Series 2, the influence of electric resistance of concrete on reinforcement corrosion was investigated.

5.4 Test Series 1

-Critical Crack Width and Mechanism of Corrosion-

5.4.1 Test Program

When the crack width is very small, crack corrosion will not proceed actively. The reasons are as follows; (i) Cracks and therefore the chloride don't reach the reinforcing steel. (ii) Even if cracks reach the reinforcing steel, a passive film due to high alkalinity covers the exposed surface of reinforcing steel. (iii) When chloride can penetrate through a porous concrete cover easily, all the area of reinforcing steel may be corroded. This series mainly deals with former two cases. In these two cases, crack width, mix proportion, quantity of chloride and thickness of

covering concrete influence the mechanism and the rate of crack corrosion. The test program is shown in Table 5.1.

5.4.2 Materials and Test Specimens

Materials--Ordinary Portland cement, Echi river sand for fine aggregate (Specific gravity = 2.61, F.M. = 3.00) and Kurama crushed gravel for coarse aggregate (Specific gravity = 2.67, Maximum size = 10 mm) were used in concrete mix. Deformed bars (D10, SD35) with mill scale were used for reinforcing steel.

Mix Proportion--The water cement ratios ranged from 0.40 to 0.70. A weight of mixing water of 196 kg/m^3 was used to obtain constant slump. Table 5.2 shows the mix proportions of concrete for Series 1.

Test Specimens--The details of specimens for Series 1 are shown in Fig. 5.1. The thickness of cover for reinforcing steel was 20 mm. Specimens No. 1 was tensioned to produce cracks for measuring half cell potential distribution. Specimen No. 2 had a preformed crack of 1 cm width in the middle portion. No. 3 was a model of macrocell corrosion to simulate the corrosion current at a crack. The sodium chloride solution (NaCl 3.13% sol.) was sprayed once a day on No. 1 and No. 2 specimens except on the steel bar protruding at both ends of No. 1. Specimen No. 3 was immersed in the sodium chloride soluion (NaCl 3.13% sol.) of about 25^{o}C.

One day after casted, all of the test specimens were stripped and stored in water of about 20°C for 4 weeks until the tests were started.

5.4.3 Test Procedures

Test setup are shown in Fig. 5.1. The half cell potentials were measured at spacing of about 5 cm along the reinforcing steel on the cover concrete surface, using Ag/AgCl reference electrode and voltmeter of input impeadance 10^{11} ohm. Currents between reinforcing steels were measured by means of the zero-shunt amperemeter. And, in this test, corrosion levels of reinforcing steel were defined as follows;

Level H : Red rust is mounted.

Level M : Between H and L.

Level L : Trace of rust.

5.4.4 Results and Discussions

As clearly shown in Fig. 5.2, potential distributions were found to be different among specimen types, which had the same water cement ratio. The potentials became less noble at the vicinity of exposed steel surface and wide cracks.

Without Cracks--Potential distributions of specimens having the same size as No. 1 but with no cracks are shown in Fig. 5.3. A high water cement ratio makes concrete permeable enough for chloride to

penetrate to reinforcing steel easily. And then chloride makes reinforcement depassivated. Thus the water cement ratio increased, the potential became less noble. The effect of the chloride in mixing water was not clear.

With Cracks--Typical potential distributions, crack width and the condition of corrosion after three months' spray are shown in Fig. 5.4. Where the potential became locally less noble, corrosion product was found. The tendency for the potential to become less noble at the location of a crack could be recognized clearly at early stage. When the crack width was larger than about 0.1 mm, this phenomenon due to the direct effect of the crack was generally found.

Thus, local potential difference (-ΔmV) given as this direct effect was calculated as shown in Fig. 5.5, and is illustrated in Figs. 5.6 - 5.9. The dashed lines on Figs. 5.6 - 5.9 mean the maximum potential differences between each 20 cm interval observed in the specimens with no cracks. When the water cement ratio was 0.40 or 0.50, the potential difference increased with increasing crack width. It is supposed that this direct effect is meaningful only when the potential difference is high compared with the maximum potential difference above mentioned. Thus it may be considered that critical crack width ranged between 0.1 and 0.2 mm. But as the water cement ratio increased, a corelation between crack width and the potential difference was less evident.

When the water cement ratio was low, the potential differences of preformed crack specimens were large. And the macrocell current density was large (Fig. 5.10), especially for water cement ratio of 0.40. Thus, water cement ratio affects both the macrocell corrosion rate at cracks, and the mechanism of corrosion. And, the chloride in mixing water made the macrocell current large.

Typical potential distributions, longitudinal cracks and rust conditions of steels having the same size as specimen No. 2, are shown in Figs. 5.11 - 5.16. Potentials became less noble and flatter with increase in the period of spraying chloride solution and with increase in the water cement ratio. After 18 months' spray, the influence of chloride on potential was recognized to be smaller in concrete of higher water cement ratio. High water cement ratio increases permeability of concrete, and permits chloride to penetrate easily to reinforcing steel. Thus, the influence of chloride in mixing water on potential is considered to be smaller in the concrete of higher water cement ratio. And, as the potentials became less noble, both corrosion and crack along the reinforcing steel due to corrosion became more obvious.

Though all potentials which decreased after 18 months to more negative value than -0.35 V vs $Cu/CuSO_4$ ($\fallingdotseq$ -0.24 V vs Ag/AgCl) ranged in the active region proposed in ASTM C876 (5.3), all of corrosion levels were not H. This may be explained by the fact that the concrete cover was thin and that small size of specimens were used.

When reinforcing steel was corroded wholly, the potential distribution was flat, and the potential value reached about -0.5 V vs Ag/AgCl. But, where reinforcing steel was corroded locally, the potential locally became less noble, too. These findings are useful to detect the corrosion by using the half cell potential method as described in Chapter 7.

5.5 Test Series 2

-Electric Resistance of Cover Concrete-

5.5.1 Test Program

Even though the potential difference between anode and cathode is kept constant, the macrocell current increases with decreasing electric resistance of cover concrete. And, the macrocell current may be negligible, when electric resistance is very high. The electric resistance of concrete is influenced by various factors, for instance, concrete mix proportion. In particular, environmental condition has a significant effect on it. In Series 2, the influence of concrete mix proportion and environmental conditions on electric resistance of concrete were investigated. The test program is shown in Table 5.3.

5.5.2 Preparatory Test

On the same concrete mixes as used in Series 1, the electric

resistance of concrete in drying process(in the air : 20±1°C, 90% R. H.) and in wetting process (immersed in NaCl 3.13% sol. : 20±1°C) were measured. The results of test are shown in Fig. 5.17 - 5.20. Until about three weeks' drying, the larger the water cement ratio, the smaller the resistance. After two months' drying, specimens were immersed in the sodium chloride solution. In this wetting period, a similar tendency was found, but resistance of every specimen was as small as about 1000 ohm.cm. Thus, in the submerged zone, high water cement ratio accelerates the rate of corrosion, but the influence may be small as far as the electric resistance is concerned. The effect of chloride in mixing water was not clearly recognized.

5.5.3 Materials and Test Specimens

Materials--High early strength Portland cement, Yasu river sand for fine aggregate (Specific gravity = 2.61, F.M. = 3.03) and Kurama crushed gravel for coarse aggregate (Specific gravity = 2.62, Maximum size = 10 mm) were used in concrete mix. Superplasticizer, synsetic rubber and silicone as antifoaming agent for polymer cement concrete (PCC) and solvent type urethane for polymer impregnated concrete (PIC) were also used. Polymer was impregnated by two times of brushing.

Mix Proportion--The water cement ratios ranged from 0.32 to 0.60. Design slump of concrete mix except for PCC was 6±2 cm. The mix proportions of concrete for Series 2 are shown in Table 5.4.

Test Specimens--In Fig. 5.21, is shown the details of test specimen used to calculate the specific electric resistance of concrete. The 10ϕx20 cm cylinders were prepared for compressive test. One day after casted, all of the test specimens were stripped and stored in the water of about 20°C for two weeks until the tests started.

5.5.4 Test Procedures

After cured, test specimens were dried in the air (20±1°C, 90% R.H.) to be weighed constant. Wetting and drying conditions were chosen as a typical environmental condition. The test specimens were subjected to cycles of wetting (immersed in tap water : 20±1°C) and drying (in the air : 20±1°C, 90% R.H.) in several conditions of cycles as listed in Table 5.3. The electric resistance and weight of concrete spscimen were measured. The specific electric resistance was calculated from the measured electric resistance. The water absorption of concrete was determined using as the base the weight of air dried specimen at the beginning of test.

5.5.5 Results and Discussions

Compressive strengths of concrete are shown in Table 5.4.

Figs. 5.22 - 5.26 show the time dependence nature of specific electric resistance of concrete. Specimens 0.32, 0.40 and PCC had high specific electric resistance, and their resistances didn't

decrease in any conditions except for continuous immersion in water. On the other hand, the specific electric resistance of specimen 0.60 decreased with time in all conditions except in air dry, in which it was as low as that of specimen 0.40 in water. From these observations, the electric resistance of concrete having high water cement ratio may be considered to be less than that of concrete having low water cement ratio, even when exposed to any conditions.

Fig. 5.27 shows the specific electric resistance measured when weight of concrete at the end of drying and wetting periods reached each constant value. The specific electric resistance was clearly recognized to decrease with increasing wetting period. The resistance of specimen PCC showed the highest value. And, that of plain concrete increased with decrease in the water cement ratio because of reduction in permeability of concrete. The impregnating polymer used in this test series had little influence on the electric resistance.

The relation between specific electric resistance and water absorption in steady state is shown typically in Fig. 5.28. In the same conrete mix, the specific electric resistance decreased approximately linearly with increasing water absorption. And, the electric resistance was also found to be highly influenced by water content of concrete.

5.6 Conclusions

In this chapter, two series of tests were carried out on various types of specimens, and the critical crack width and electric resistance of concrete were discussed. The conclusions in this chapter are summarized as follows;

(1) According to the experimental method measuring the local potential difference (- mV) used here, from the view point of reinforcement corrosion, the critical crack width is between 0.1 and 0.2 mm.

(2) Water cement ratio influences significantly both the macrocell corrosion rate at cracks and mechanism of corrosion.

(3) As water cement ratio of concrete increases, the half cell potential of reinforcing steel becomes less noble, and the electric resistance of concrete cover becomes lower due to low permeability, resulting in accelerating the corrosion of reinforcing steel.

(4) Environmental conditions, such as wetting and drying repetitions also influence considerably the electric resistance of concrete, due to penetration of water and chloride into concrete.

5.7 References

(5.1) Schiessl, P., "Zusammenhang zwishen Rissbreite und Korrosionsabtragung an der Bewehrung", Betonwerk+Fertigteil Technik, 41 Jahrgang, Heft 12, S. 594-598, Dec. 1975

(5.2) Beeby, A. W., "Corrosion of reinforcing steel in concrete and

its relation to cracking", The Structural Engineer, Vol. 56A, No. 3, pp. 77-81, March 1978

(5.3) ASTM C876, "Half Cell Potentials of Reinforcing Steel in Concrete", 1977

(5.4) Okada, K. and Miyagawa, T., "Influence of water cement ratio on chloride corrosion of reinforcing steel in cracked concrete", Proc. of CAJ, Vol. 33, pp. 494-497, Dec. 1979

(5.5) Okada, K. and Miyagawa, T., "Chloride corrosion of reinforcing steel in cracked concrete", ACI SP-65, pp. 237-254, Aug. 1980

(5.6) Okada, K., Kobayashi, K., Miyagawa, T. and Eguchi, I., "Deterioration techniques for chloride corrosion of reinforcing steel", Trans. of JCI, Vol. 2, pp. 77-84, Dec. 1980

(5.7) Okada, K, Miyagawa, T. and Kiuchi, Y., "Electric resistance and oxygen penetration of concrete", Annual Meeting of JSCE, Vol. 38-5, pp. 265-266, Sept. 1983

Table 5. 1 Test Program for Series 1

Factor	Level
W/C	0.40, 0.50, 0.60, 0.70
Chloride in mixing water (NaCl, %)	0, 3.13
Maximum crack width (mm)	0.2-0.3, 0.1-0.2, 0

Table 5. 2 Mix proportion of concrete for Series 1

Specimen*	Slump (cm)	Water cement ratio	Absolute fine aggregate ratio (%)	Unit weight (kg/m^3)			
				Water	Cement	Sand	Gravel
0.40	4±2	0.40	50	196	490	820	839
0.50		0.50		196	392	861	881
0.60		0.60		196	327	888	908
0.70		0.70		196	280	907	928

*) When sodium chloride solution (NaCl 3.13%) is used, specimen is expressed such as 0.40-Cl etc.

Table 5. 3 Test Program for Series 2

Factor		Level
Concrete mix	W/C	0.32, 0.40, 0.60
	Polymer	Polymer impregnation Polymer cement concrete)W/C=0.40
Environmental condition*		0/24, 4/20, 8/16, 24/0

*(Wetting hour/Drying hour)

Table 5. 4 Mix proportion of concrete for Series 2

Specimen	Slump (cm)	Water cement ratio	Absolute fine aggregate ratio(%)	Unit weight (kg/m^3)				
				Water	Cement	Sand	Gravel	Admixture
0.32	6±2	0.32	50	174	580	812	815	Super plasticizer:5.8
0.40		0.40	50	198	495	816	819	—
0.60		0.60	50	198	330	883	887	—
PIC*		0.40	50	198	495	816	819	—
PCC	20±2	0.40	40	198	495	693	696	Polymer: 50 Anti former Agent: 0.55

* impregnated by two times of brushing

** Sulphonated melamine formaldehyde condensate

Table 5. 5 Compressive strength of concrete

Specimen	W/C	Compressive strength (kg/cm^2)
0.32	0.32	741
0.40	0.40	572
0.60	0.60	383
PCC	0.40	480

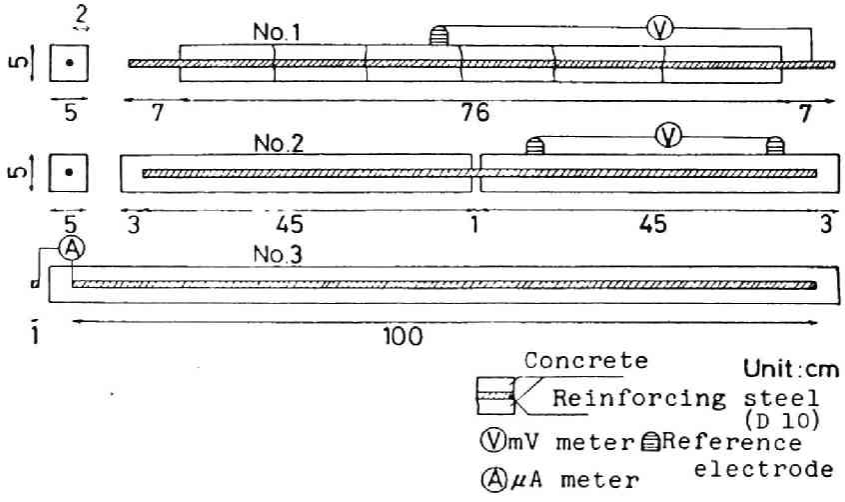

Fig. 5. 1--Specimens and measurement methods

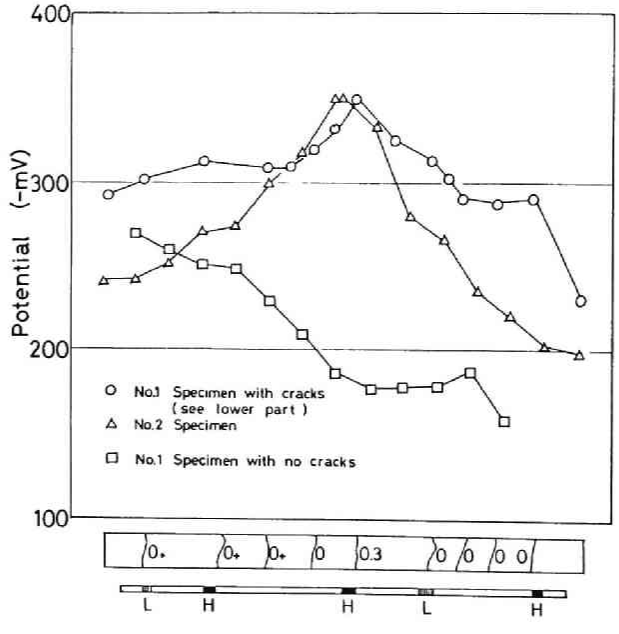

Fig. 5. 2--Typical potential distributions (w/c=0.50, after 3 months' spray)

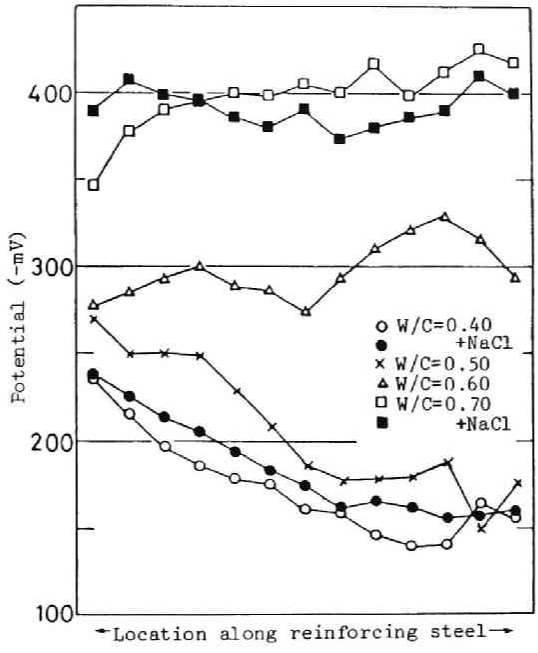

Fig. 5. 3--Influence of water cement ratio on potential (Type No. 1 specimens with no cracks after 3 months' spray)

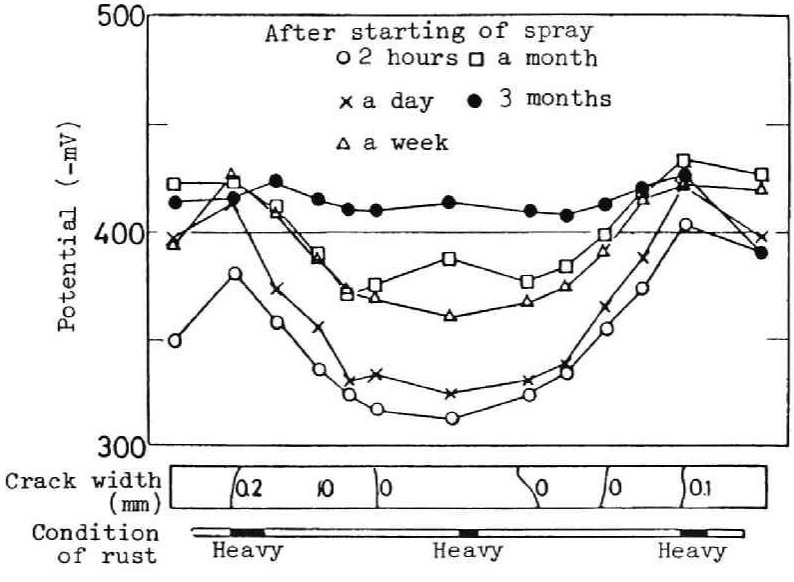

Fig. 5. 4--Example of potential distribution (Type No. 1 specimen, w/c=0.70)

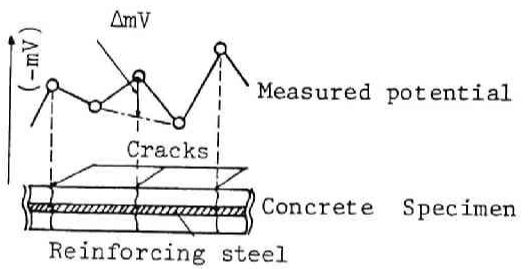

Fig. 5. 5--Calculation of potential difference

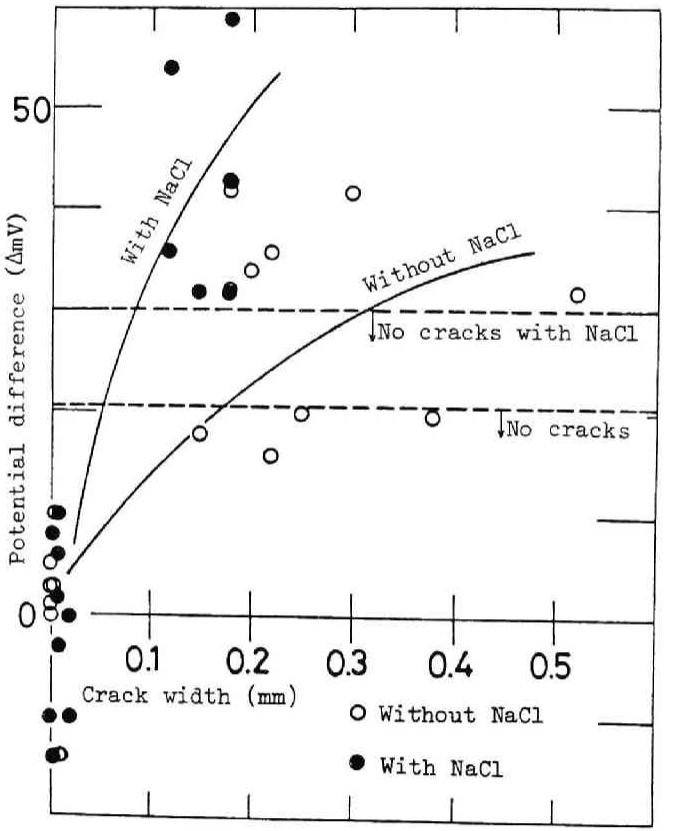

Fig. 5. 6--Relation between crack width and potetial difference (w/c=0.40)

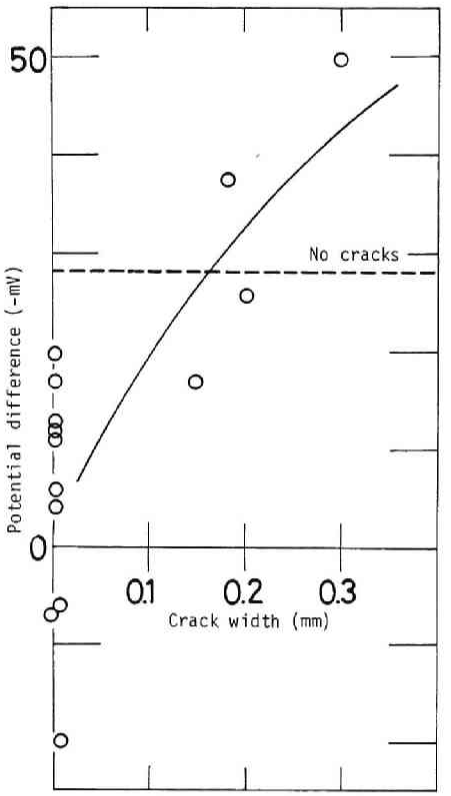

Fig. 5. 7--Relation between crack width and potential difference (w/c=0.50)

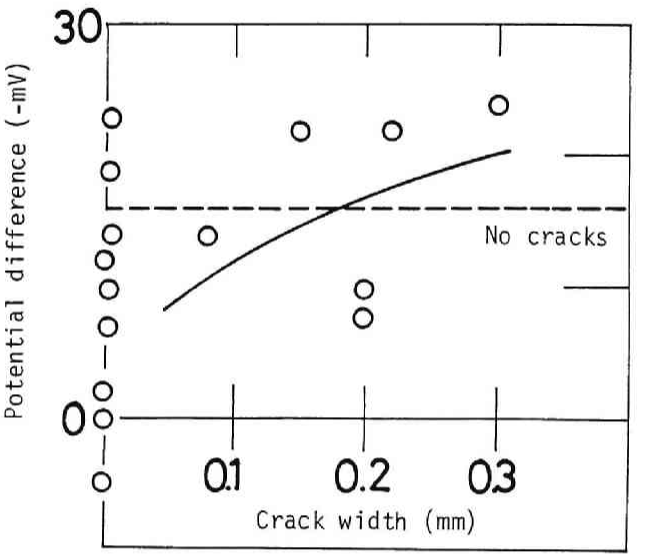

Fig. 5. 8--Relation between crack width and potential difference (w/c=0.60)

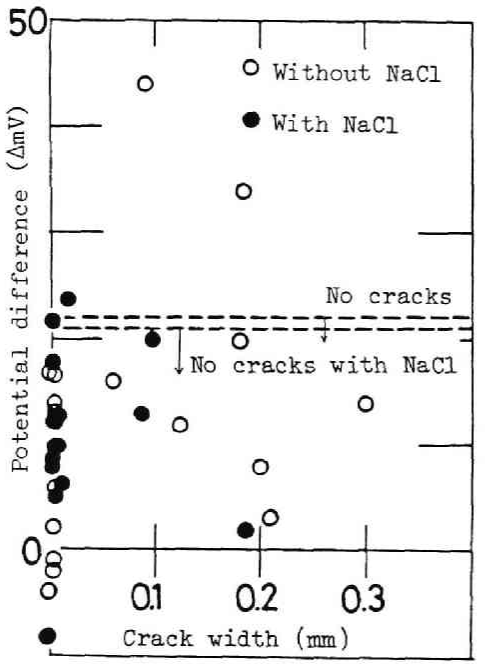

Fig. 5. 9--Relation between crack width and potential difference (w/c=0.70)

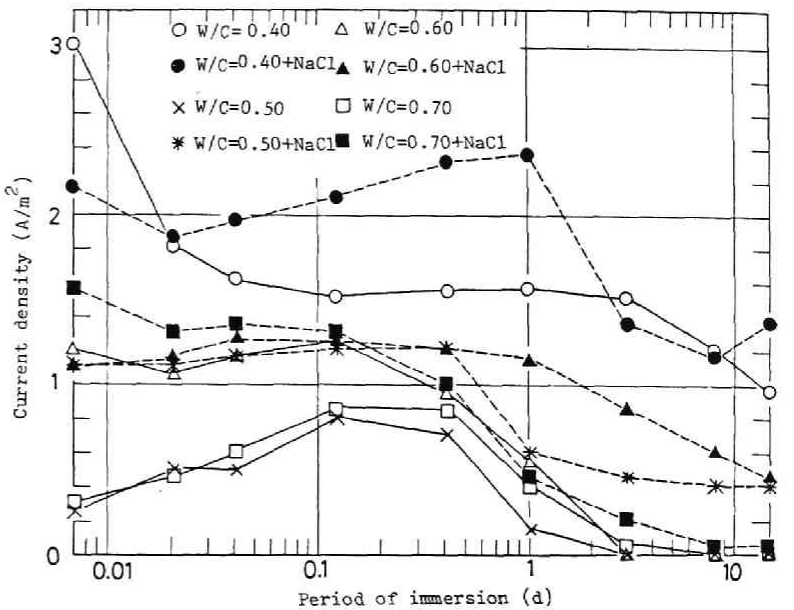

Fig. 5. 10--Influence of water cement ratio on current density

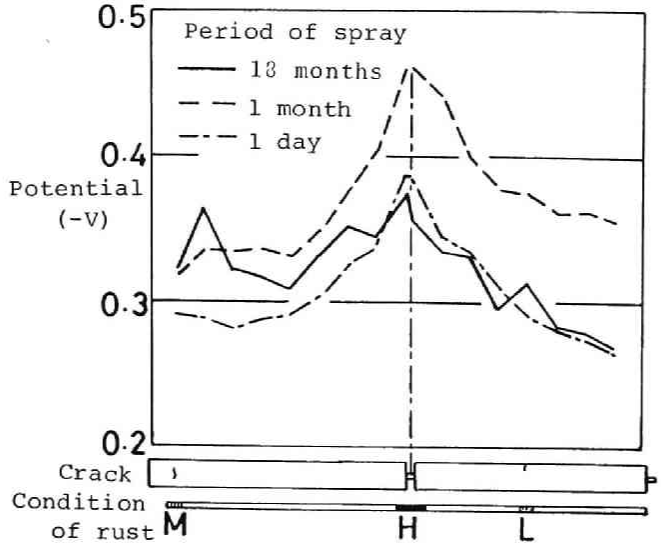

Fig. 5. 11--Potential distribution, crack and condition of rust (w/c=0.40)

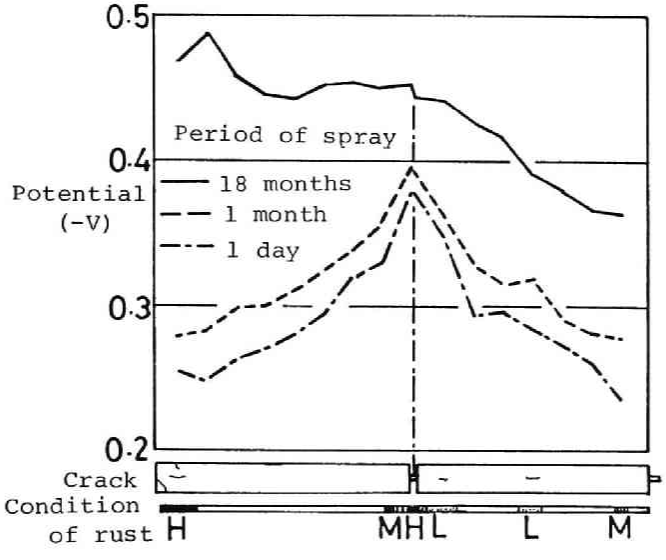

Fig. 5. 12--Potential distribution, crack and condition of rust (w/c=0.40+NaCl)

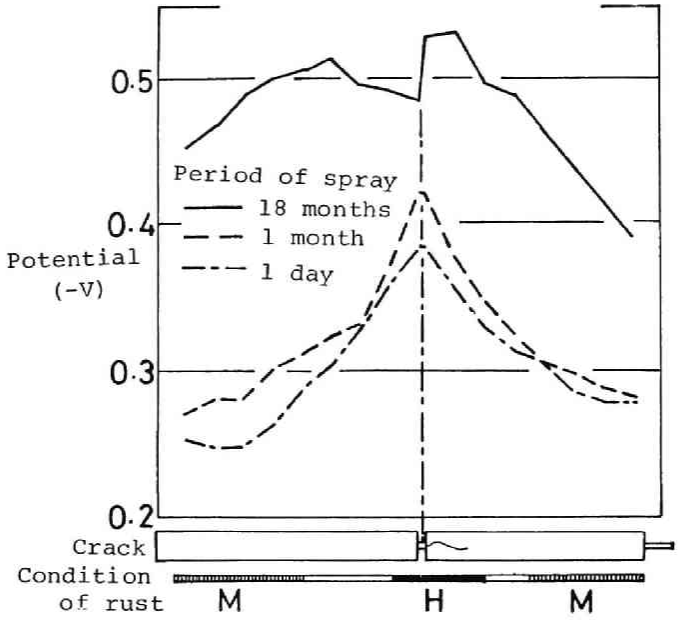

Fig. 5. 13--Potential distribution, crack and condition of rust (w/c=0.50)

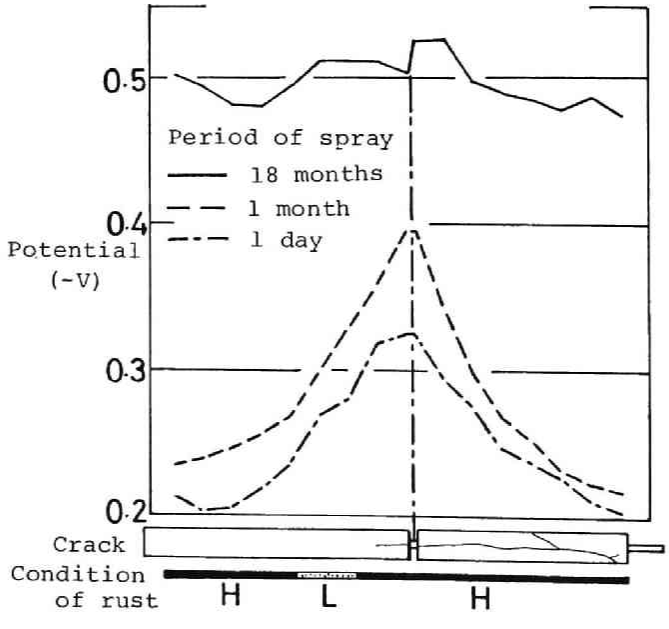

Fig. 5. 14--Potential distribution, crack and condition of rust (w/c=0.60)

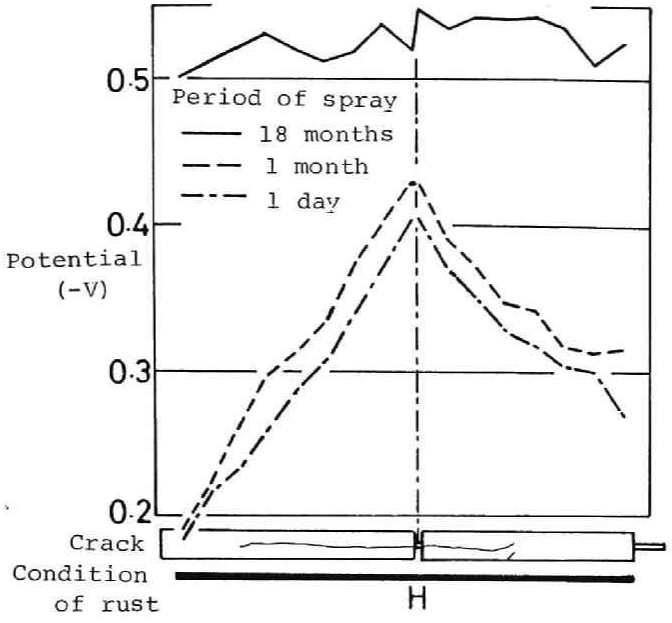

Fig. 5. 15--Potential distribution, crack and condition of rust (w/c=0.70)

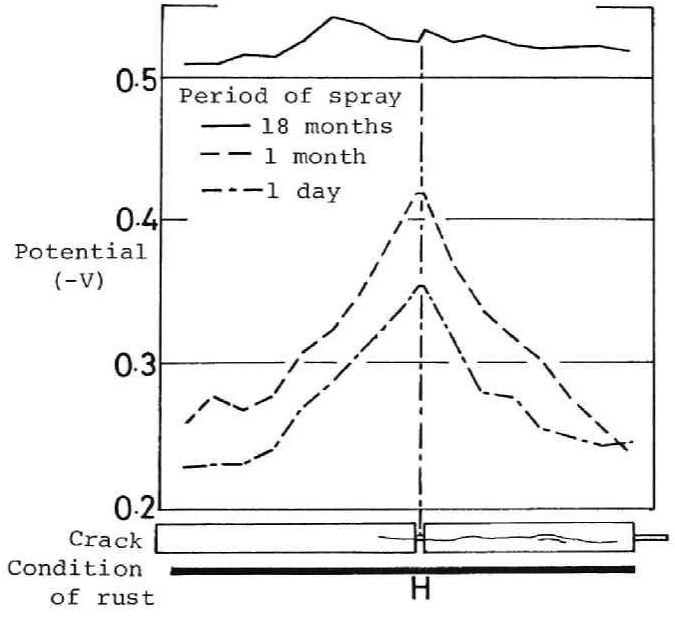

Fig. 5. 16--Potential distribution, crack and condition of rust (w/c=0/70+NaCl)

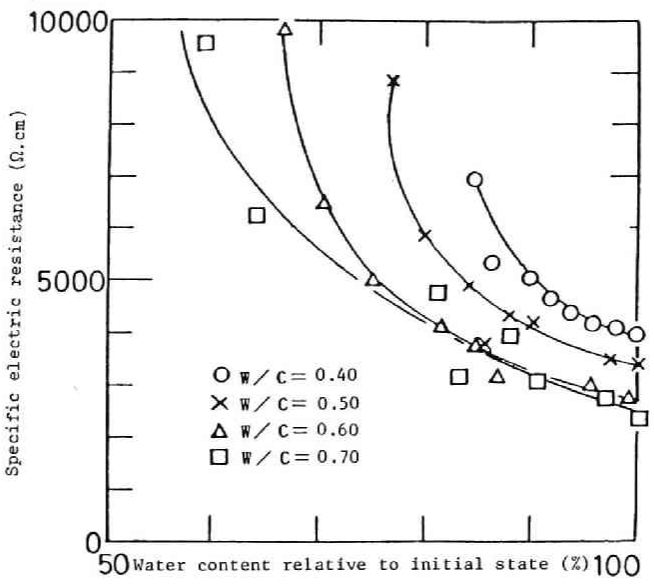

Fig. 5. 17--Influence of water cement ratio on specific electric resistance of concrete -1- (drying period, with no chloride in mixing water)

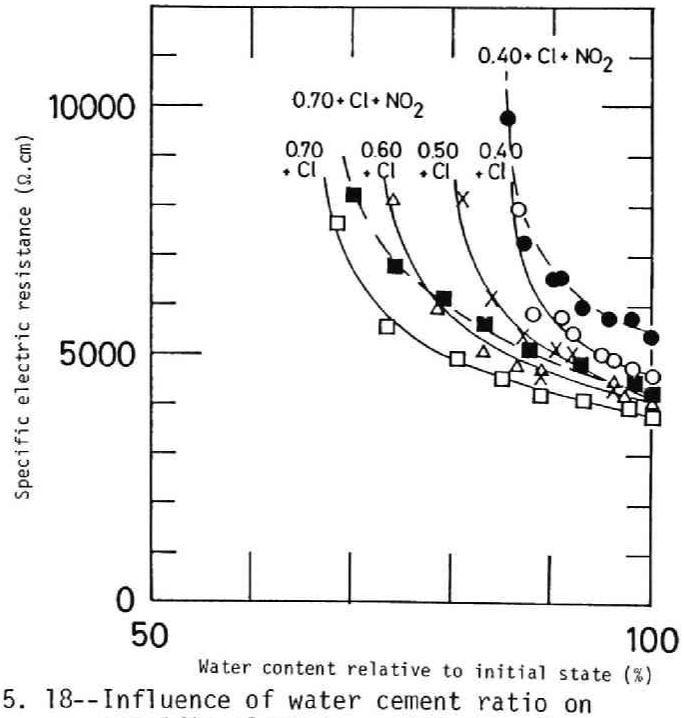

Fig. 5. 18--Influence of water cement ratio on specific electric resistance of concrete -2- (drying period, with chloride in mixing water)

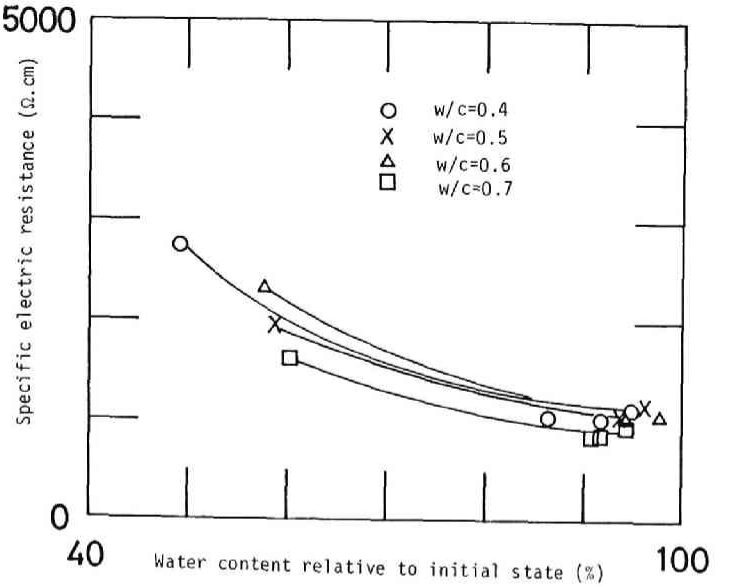

Fig. 5. 19--Influence of water cement ratio on specific electric resistance of concrete -3- (wetting period, with no chloride in mixing water)

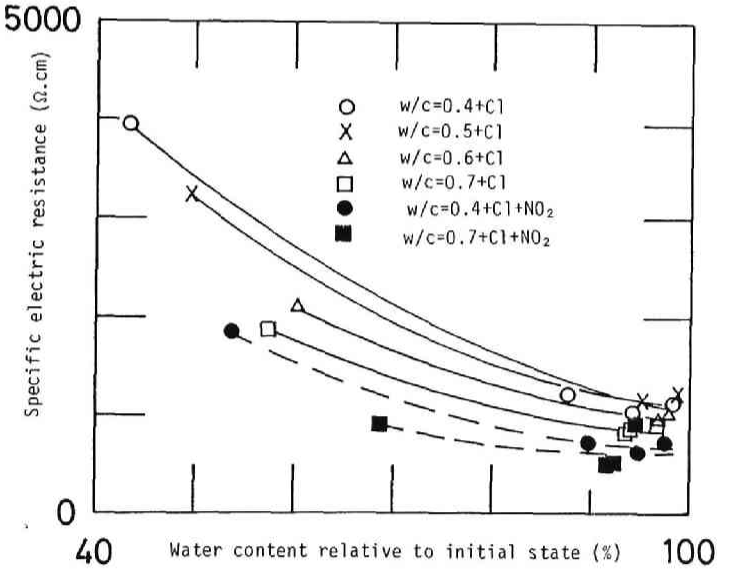

Fig. 5. 20--Influence of water cement ratio on specific electric resistance of concrete -4- (wetting period, with chloride in mixing water)

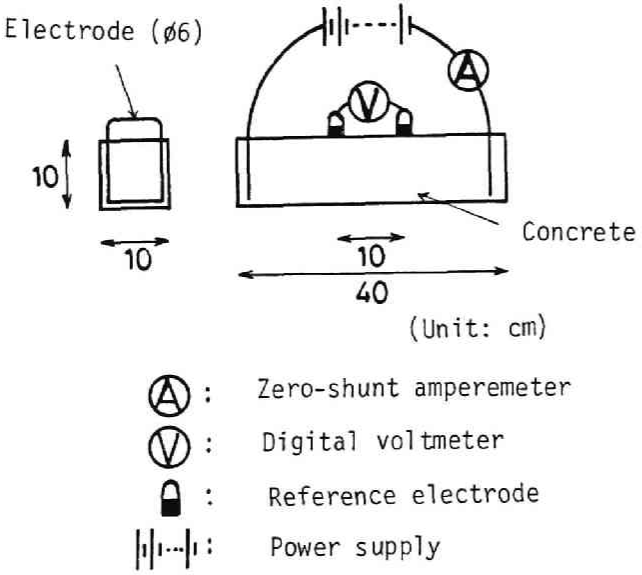

Fig. 5. 21--Specimen and measurement method

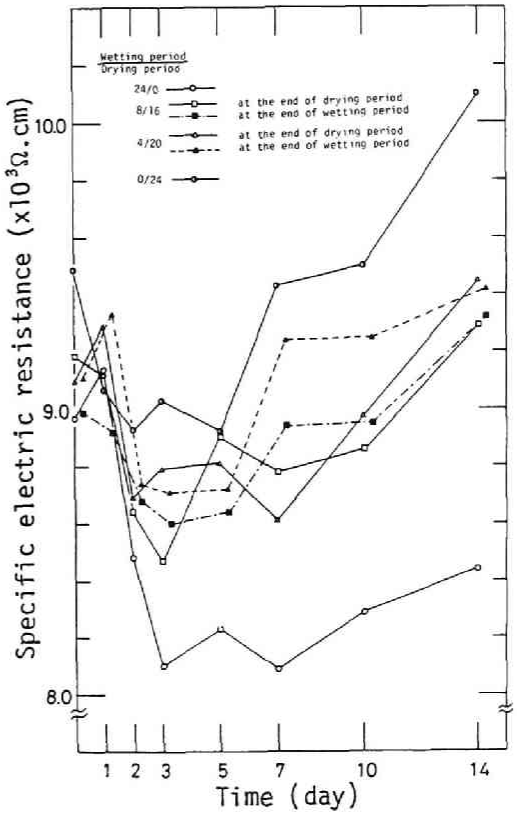

Fig. 5. 22--Specific electric resistance of concrete (Specimen 0.32)

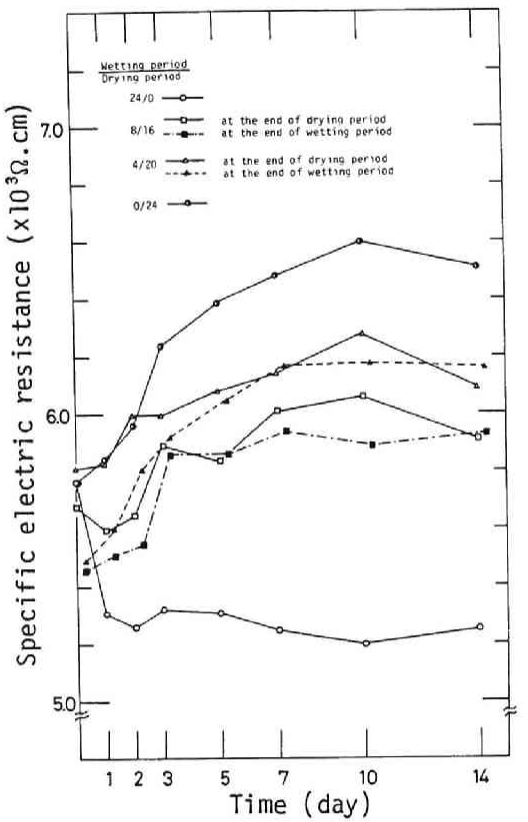

Fig. 5. 23--Specific electric resistance of concrete (Specimen 0.40)

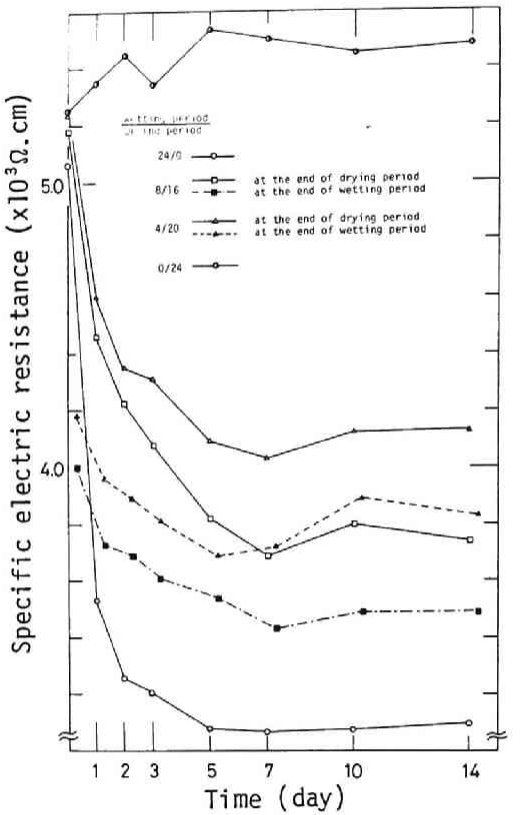

Fig. 5. 24--Specific electric resistance of concrete (Specimen 0.60)

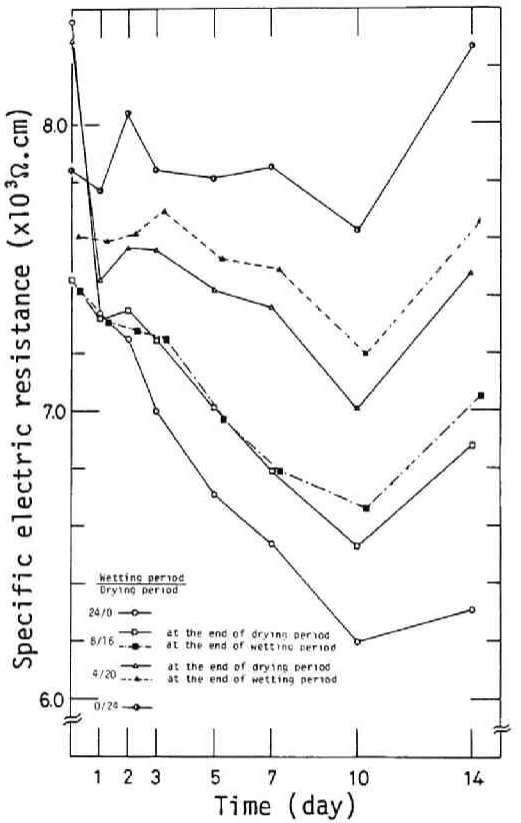

Fig. 5. 25--Specific electric resistance of concrete (PIC)

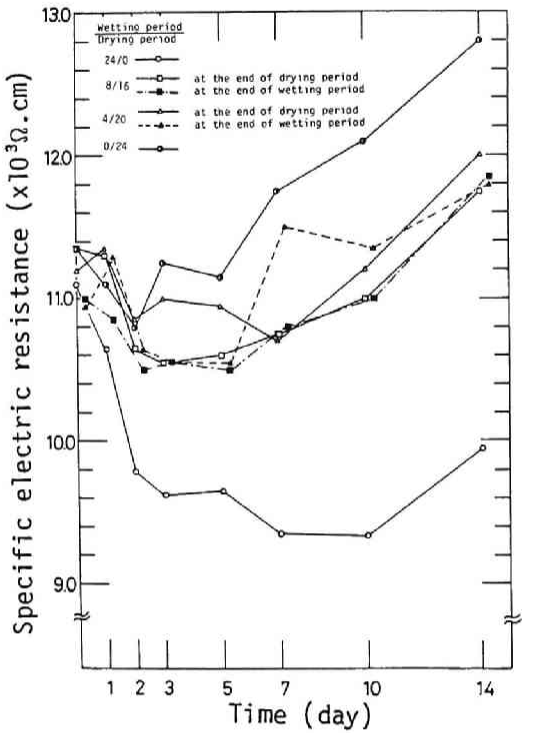

Fig. 5. 26--Specific electric resistance of concrete (PCC)

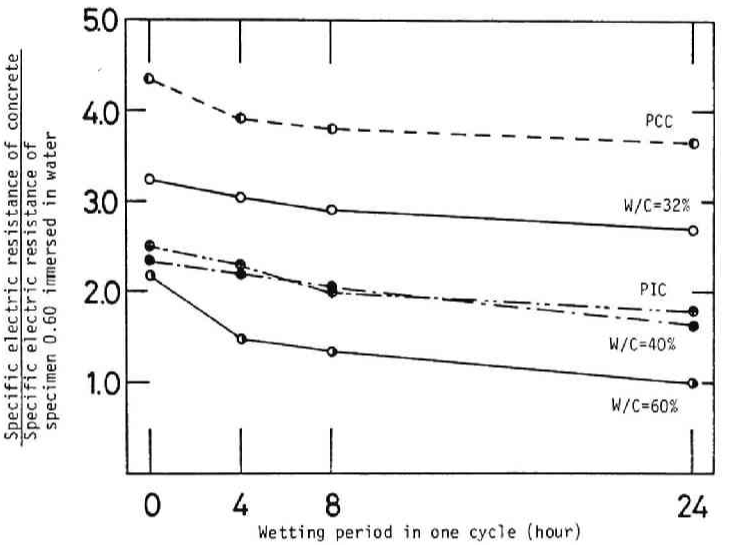

Fig. 5. 27--Relation between specific electric resistance and wetting period in one cycle

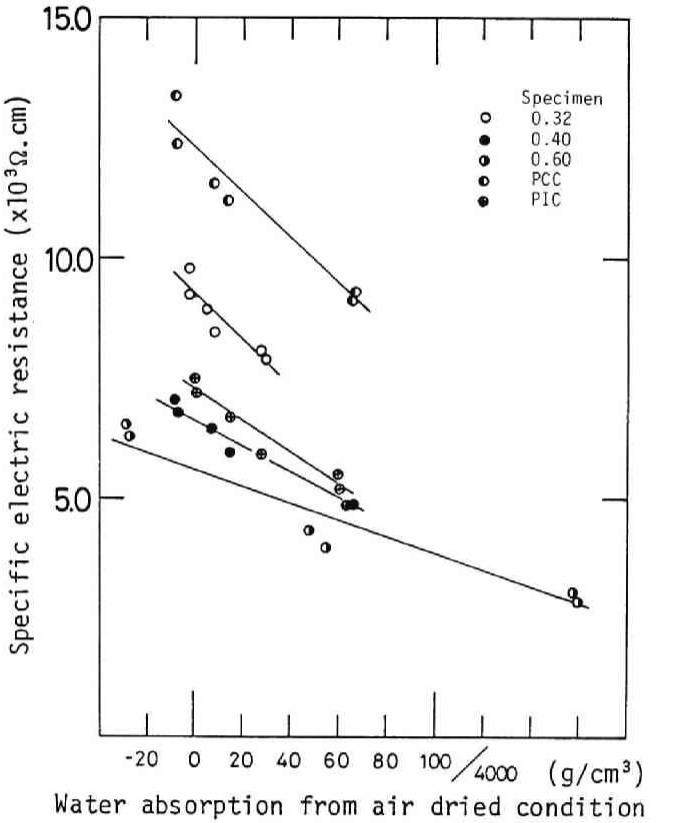

Fig. 5. 28--Relation between specific electric resistance and water absorption from air dried condition

6 INFLUENCES OF COVER CONCRETE ON CHLORIDE CORROSION OF REINFORCING STEEL

6.1 Introduction

As the cracks of reinforced concrete structures can often be a trigger of reinforcement corrosion, the crack corrosion was discussed in detail in Chapters 4 and 5. And, it is made clear that the water cement ratio does influence both the corrosion rate and mechanism of corrosion. Concrete of high water cement ratio, therefore, has no significant critical crack width relating to reinforcement corrosion, and then concrete having high electric resistance gives small corrosion current according to Ohm's law. This implies explicitly that the offshore concrete structures of low water cement ratio generally can be permitted to have rather narrower critical crack width in service condition.

In the concrete structures without cracks or with cracks narrower than the so-called critical crack width, the time t_0 represnted in Fig. 4.1 has a positive finite value, depending upon the environmental conditions, concrete quality and cover thickness.

The most reliable corrosion protection method is to increase the clear cover with good concrete of low water cement ratio. In marine environment, however, the time needed for chloride to penetrate from concrete surface to reinforcing steel is much shorter than the service life required for the reinforced concrete structures (6.1). Therefore, it is essentially important to analyse both the penetration process of water and chloride, and the corrosion properties after chloride penetration to reinforcement.

In this chapter, the influences of, particularly, the water cement ratio of concrete on both the permeability for water and oxygen, and the corrosion protection were discussed.

6.2 Penetration of Water and Oxygen into Concrete

The water permeability of concrete has been experimentally determined by using either in-put method or out-put method under the high pressure water. On the other hand, it is widely known that the corrosion rate of reinforcing steel shows the maximum value in the splash zone. Thus, water penetration due to absorption through capillary in concrete should be estimated in the reinforcement corrosion.

Chloride may penetrate into concrete by diffusion from the outside of cover concrete. A distinction, however, has to be made between the direct diffusion of chloride ions and the conveyance of

chloride ions in conjunction with diffusion of water. The actual chloride diffusion may be considered to depend mainly upon water penetration.

The diffusion of air in concrete is maybe in proportion to that of water (6.2). As the rate of reinforcement corrosion is primarily controlled by concentration polarization caused by diffusion of dissolved oxygen through the concrete cover, the diffusion rate of dissolved oxygen plays an important role.

6.3 Test Programs

Test programs consisted of two series. In Series 1, the influence of cover concrete on chloride corrosion protection performance was examined. And, the penetration of water and oxygen, being related to corrosion process, was studied in Series 2.

6.4 Test Series 1
-Influence of Cover Concrete-

6.4.1 Test Program

Influences of cover concrete on chloride corrosion process are characterized by two items as follows: (i) penetration of water and chloride to reinforcing steel in the period t_0, as already shown in

Fig. 4.1, and (ii) corrosion rate in the period t_1. Test program is shown in Table 6.1, in which the absorption and porosity tests correspond to the above item (i), while the accelerated corrosion and polarization tests on chloride contaminated concrete to (ii).

6.4.2 Materials and Test Specimens

Materials--Ordinary Portland cement, Yasu river sand for fine aggregate (Specific gravity = 2.60, F.M. = 2.87) and Kurama crushed gravel for coarse aggregate (Specific gravity = 2.64, Maximum size = 10 mm) were used in concrete mix. Four kinds of polished round bars (ø6, 13 and 25, SGD4) were used for reinforcing steel. And, partially, solvent type urethane for polymer impregnated concrete (PIC) was also used. Polymer was impregnated by two times of brushing.

Mix Proportion--Two levels of water cement ratio - 0.40 as good quality concrete and 0.60 as ordinary one - were used. A weight of mixing water of 196 kg/m^3 was used to obtain constant slump. Table 6.2 shows the mix proportions of concrete for Series 1. On the other hand, wet-screened mortar was used for the porosity tests.

Test Specimens--The details of specimens for the absorption and porosity tests are schematically shown in Fig. 6.1, and those for the accelerated corrosion and polarization tests in Fig. 6.2. One day after casted, all of the test specimens were stripped and stored in water of about 20°C for four weeks until those tests were

started.

6.4.3 Test procedures

Absorption; The absorption of artificial sea water by capillarity was estimated by measuring the height of capillary rise around the reinforcing steel after the immersion period of one month, according to RILEM Tentative Recommendations No. 11.2 (6.3).

Porosity; The pore volume in the specimen shown in Fig. 6.1 made of wet-screened mortar from concrete was measured using the mercury penetration method.

Accelerated corrosion; The accelerated corrosion test under raised temperature (60°C) and high humidity (90% R.H.) was conducted for 6 weeks.

Polarization; The potentiostatic polarization test between -1.0 and +1.0 V vs Ag/AgCl was also made, in which the potential scanning rate was 5 mV/h.

6.4.4 Results and Discussions

Absorption by Capillarity--In Figs. 6.3 and 6.4 are shown the average heights of capillary rise on the cutting plane between the reinforcing steel surface and the steel radius distance from steel surface.

In the plain concrete, the capillary rise in specimen with horizontal steel was found to be larger than that with vertical steel. And, specimens having W/C of 0.40 showed a little higher capillary rise than those of W/C of 0.60. In the specimens with vertical reinforcement, the clear cover scarcely affected the capillary rise, while in the specimens with horizontal reinforcement the maximum height of capillary rise attained when the thickness of cover used was minimum in this test. The weight of water absorbed by capillarity in concrete specimen having W/C of 0.60 was up to about 1.5 times as much as that in concrete of W/C of 0.40. This means that the former concrete had much more capillary voids attributing to water absorption.

The capillary rise of PIC was much lower than that of plain concrete.

Porosity of Mortar--Figs. 6.5 - 6.8 show the pore diameter distribution measured on the wet-screened mortar. That of specimen with horizontal steel was found to have two peaks at about 7.5×10^{-6} m and 0.075×10^{-6} m.

Table 6.3 shows the pore volume distribution, each corresponding to large diameter of $2.4\text{-}75 \times 10^{-6}$ m and small one of less than 2.4×10^{-6} m. Total pore volume of specimen having W/C of 0.60 with horizontal steel was considerably larger than W/C of 0.40. And, total pore volume of mortar having W/C of 0.60 with horizontal steel was larger than that with vertical one. The volume occupied

by large pores also showed the same tendency.

Most of large pores, which may induce the serious reinforcement corrosion, could be found at the lower part of reinforcing steel in the specimen of lower W/C of 0.40, while in the specimen of higher W/C of 0.60, large pores were distributed uniformly over the reinforcement surface. Thus, it is considered that the corrosion occurred locally at the lower part of reinforcing steel in the former concrete, especially, at an early stage, while the corrosion reaction proceeds at both of the upper and lower parts of steel in the latter one. And it is considered that the reinforcement corrosion in concrete may shown quite the same tendency in this test by using mortar specimens.

Accelerated Corrosion Test under Raised Temperature--The relation between total corroded area and thickness of cover are shown in Figs. 6.9 and 6.10. And, in Figs. 6.11 and 6.12 are shown the relations between total corroded area and diameter of reinforcing steel. Total corroded area decreased with increasing thickness of cover in any cases except for W/C of 0.40 and cover thickness of 13 mm. The influence of reinforcing steel diameter on total corroded area, however, was not clear.

The increased thickness of cover reduces the water, chloride and oxygen permeability, resulting in an effective corrosion protection. On the other hand, the increased diameter of reinforcing steel constrains the volume change due to plastic or

drying shrinkage of concrete and then increases the interface area between concrete and steel, resulting in an adverse affect on the corrosion process.

In the durability design of reinforced concrete structures, therefore, both of the thickness of cover (c) and the diameter of reinforcing steel (ϕ) should be considered together in combined form as expressed by c/ϕ in Figs. 6.14 - 6.17. For reinforcement located within the range of c/ϕ of 2 - 4, the total corroded area decreased with increasing c/ϕ. The corroded area fronting on the cover surface (see Fig. 6.13) decreased with increasing c/ϕ, although scarcely affected by c/ϕ in the specimen having W/C of 0.60 and horizontal steel. And, the corroded area fronting on the interior (see Fig. 6.13) increased with c/ϕ in the specimen having W/C of 0.60 and horizontal steel, while quite contrary tendency in any other specimens. Influence of c/ϕ on (Corroded area fronting on the cover surface / corroded area) was not clear in the specimen with vertical steel. When a reinforcing steel was embedded horizontally in the specimen having W/C of 0.40, most of corrosion products were found at the lower part of steel. And, in the case of W/C of 0.60 and horizontal reinforcement, the ratio decreased with an increase in c/ϕ. This may be due to bleeding of concrete, showing quite the same tendency as found in the porosity tests.

Polarization Test--Figs. 6.18 and 6.19 show the typical polarization diagram with compensation for concrete resistance. And, the influence of c/ϕ on corrosion rate index defined as the

reciprocal of apparent polarization resistance is shown in Fig. 6.20. Because of insufficient available data about polarization of reinforcing steel embedded in concrete, it is difficult to explain accurately the meanings of these diagrams. However, it is indicated in Fig. 6.20 that the ratio, c/ϕ, had not a distinct influence on corrosion rate index. The corrosion rate index of specimen immersed in artificial sea water for 8 days was twice as much as that of corresponding specimen of the same quality. This implies that the environmental condition should be taken into account as a major influencing factors, when analyzing the result of polarization test.

6.5 Test Series 2

-Permeability for Water and Oxygen-

6.5.1 Test Program

Two series of tests on permeability were conducted in Series 2. The water permeability of concrete was assessed by measurement of water absorption by capillarity. And then, the oxygen permeability of cover concrete was rated using the electrochemical measurement proposed by Gjørv (6.4). Test program for Series 2 is listed in Table 6.4.

6.5.2 Materials and Test Specimens

Materials--High early strength Portland cement, Yasu river sand

for fine aggregate (Specific gravity = 2.61, F.M. = 3.03) and Kurama crushed gravel for coarse aggregate (Specific gravity = 2.62, Maximum size = 10 mm) were used in concrete mix. Moreover, superplasticizer, synthetic rubber latex and silicone as antifoaming agent for polymer cement concrete (PCC), and solvent type urethane for polymer impregnated concrete (PIC) were used. Polymer was impregnated by two times of brushing.

Mix Proportion--The water cement ratio ranged from 0.32 to 0.60, and design slump was 6±2 cm except for PCC. The mix proportions of concrete are shown in Table 6.5.

Test Specimens--The specimen for water absorption test was 15ø x 30 cm cylinder as shown in Fig. 6.21. And, that for oxygen permeability test is shown in Fig. 6.22. 10ø x 20 cm cylinders were also prepared for compressive test. One day after casted, all of the test specimens were stripped and stored in water of about 20°C for two weeks.

6.5.3 Test Procedures

Absorption of Water by Capillarity--After cured, all of the test specimens were dried in air of about 20°C and 80% R.H. to be weighed constant. As shown in Fig. 6.20, the height of capillary rise was measured according to RILEM Tentative Recommendation No. 11.2 (6.3). Immediately after the height of capillary rise became constant, the specimen, except for PIC, was dried in the oven of

about 120°C to be weighed constant and measurement restarted.

Permeability for Oxygen--After cured, the wet model specimens were placed in the container as shown in Fig. 6.23, while the 80% R. H. model specimens in the room of about 20°C and 80% R.H. (Fig. 6.24). After the weight of each specimen became constant, the steel sheet embedded in concrete was polarized cathodically at the potential where reduction of oxygen was the only possible cathodic reaction to occur. There was a difinite relationship between the amount of oxygen at the electrode surface and the current which could be measured.

6.5.4 Results and Discussions

Strengths of concrete are shown in Table 6.6.

Absorption of Water by Capillarity--The water absorptions by capillarity are shown in Figs. 6.25 and 6.26, and the height of capillary rises in Figs. 6.27 and 6.28. The water absorption increased with elapsed time. The water absorption of air dried concrete was small in comparison with that of oven dried one. On the contrary, the height of capillary rise of air dried concrete was higher than that of oven dried one. These results may be due to that the oven dried process deteriorated the micro structures of concrete. The height of capillary rise increased with time and reached each constant vaue after duration of 72 hours. The height of capillary rise of PIC could not be measured due to its colour.

In Figs. 6.29 and 6.30 are shown the water absorption by capillarity and the height of capillary rise after duration of 72 hours, respectively. Both of them increased with increasing water cement ratio, especially, when W/C > 0.40. Although PCC showed the minimum values, the effects of polymer impregnation was not so clear.

The relations between height of capillary rise and water absorption are shown in Figs. 6.31 and 6.32. Although the water absorption increased with increasing height of capillary rise, the latter rather decreased after a long duration. This may be caused by change of water or moisture distribution in concrete.

Permeability to Oxygen--Fig. 6.33 shows the typical cathodic polarization of steel in concrete. Limiting current for reduction of oxygen could be measured at about -860 mV vs Ag/AgCl, being almost equal to -800 mV reported by Gjørv et al. (6.4).

Typical time dependence of electric current, being observed after steel sheet embedded in concrete was polarized to -860 mV vs Ag/AgCl, are shown in Figs. 6.34 - 6.38. It is generally recognized in these diagrams that the current decreased with elapsed time

On the other hand, Table 6.7 indicates the flux values of oxygen calculated from the electric current after being almost constant. Influences of both of the cover thikness and water cement ratio on the flux value were not clearly found. The 80% R.H. model

and PIC had higher values of oxygen flux. Thus, because of large flux of oxygen, it is considered that the oxygen diffusion was not always controlled by the passive layer (6.5) of reinforcing steel when concrete was dried.

6.6 Conclusions

In this chapter, two series of tests were carried out to make clear the influences of cover concrete on chloride corrosion of reinforcing steel, and the penetration of water and oxygen into concrete was discussed. The conclusions in this chapter are summarized as follows;

(1) All factors of water cement ratio of concrete, thickness of cover and arrangement of reinforcing steel (vertical or horizontal) have influences on the absorption of chloride solution by concrete, the pore diameter distribution in the cover concrete and finally on mechanism of chloride corrosion.

(2) The diameter of reinforcing steel (ϕ) and the thickness of cover (c) should be considered together in combined form such as c/ϕ ratio to assure effective corrosion protection by concrete.

(3) When analyzing the results of polarization test, the influence of environmental condition, such as wetting condition of concrete, must be taken into account.

(4) Both the water absorption by capillarity and the height of capillary rise increase with increasing water cement ratio, especially when W/C > 0.40.

(5) The environmental conditions, such as wetting condition of concrete, have a major influence on the flux of oxygen to cathode surface of reinforcing steel due to water content of concrete.

6.7 References

(6.1) Ohtsuki, N., Mori, Y. and Seki, H., "Some consideration for the chloride content of the concrete in marine environment", Proc. of JSCE, No. 332, pp. 107-118, Apr. 1983

(6.2) Kasai, Y. and Matsui, I., "On the air permeability of mortar", Cement & Concrete, No. 436, pp. 8-15, June 1983

(6.3) RILEM Recommendation CPC 11.2, "Absorption of water by capillarity", June 1977

(6.4) Gjørv, O. E., Vennesland, Ø. and El-Busaidy, A. H. S., "Diffusion of dissolved oxygen through concrete", Corrosion/76, Paper No. 17, pp. 1-13, March 1976

(6.5) Kobayashi T., "Corrosion and corrosion protection of steel in concrete", Recommendations for Prevention against Deterioration of Offshore Concrete Structures, pp. 39-46, Feb. 1983

(6.6) Kobayashi, K., Miyagawa, T., Honda, S. and Tomiyama, H., "Influences of cover concrete on corrosion mechanism of reinforcing steel", Proc. of CAJ, Vol. 36, pp. 497-501, Dec. 1982

(6.7) Okada, K., Miyagawa, T. and Kiuchi, Y., "Electric resistance and oxygen penetration of concrete", Annual Meeting of JSCE, Vol. 38-5, pp265-266, Sept. 1983

Table 6. 1 Test program

Test item	Factor				
	W/C	Diameter of reinforcing steel (ø :mm)	Thickness of cover (C:mm)	Arrangement of reinforcing steel*	Mixing water
Absorption	0.40,0.60	13	13,26,52	V,H	Tap water
Porosity	0.40,0.60	13	26	V,H	Tap water
Accelrated corrosion	0.40,0.60	6,13,25	13,26,52	V,H	Artificial sea water
Polarization	0.40,0.60	6,13,25	13,26,52	V,H	Artificial sea water

* V:Vertical, H:Horizontal

Table 6. 2 Mix proportion of concrete for Series 1

Specimen	Slump (cm)	Water cement ratio	Absolute fine aggregate ratio(%)	Unit weight(kg/m³)			
				Water	Cement	Sand	Gravel
0.40	5±1	0.40	50	196	490	818	830
0.60		0.60	50	196	327	885	899

Table 6. 3 Pore volume distribution (cc/g)

W/C	Arrangement of reinforcing steel*	Upper part or lower part	Total pore volume	Small pore ~2.4μm	Large pore 2.4 ~ 75μm	Large pore H/V	Large pore L/U	Large pore 0.60/0.40
0.40	H	L	0.0598	0.0439	0.0159	1.31	1.39	—
		U	0.0673	0.0559	0.0114	0.94		—
	V		0.0816	0.0695	0.0121	—	—	—
0.60	H	L	0.0922	0.0661	0.0261	1.43	1.07	1.64
		U	0.0874	0.0631	0.0243	1.34		2.13
	V	—	0.0793	0.0611	0.0182	—	—	1.50

* H:horizontal, V:vertical
L:lower part, U:upper part

Table 6. 4 Test Program for Series 2

Factor	Level	
Concrete mix	W/C	0.32, 0.40, 0.60
	Polymer	Polymer impregnation, Polymer cement concrete) W/C=0.40
Thickness of cover(mm)	20, 50	

Table 6. 5 Mix proportion of concrete for Series 2

Specimen	Slump (cm)	Water cement ratio	Absolute fine aggregate ratio(%)	Unit weight (kg/m^3)				
				water	Cement	Sand	Gravel	Admixture
0.32	6±2	0.32	50	174	580	812	815	Super ** plasticizer : 5.8
0.40		0.40	50	198	495	816	819	—
0.60		0.60	50	198	330	883	887	—
PIC*		0.40	50	198	495	816	819	—
PCC	20±2	0.40	40	198	495	693	696	Polymer:50 Antiforming agent:0.55

* after dried in the air to be weighed constant and impregnated by two times of brushing

** Sulphonated melamine formaldehyde condensate

Table 6. 6 Compressive strength of concrete

Specimen	W/C	Compressive strength (kg/cm^2)
0.32	0.32	741
0.40	0.40	572
0.60	0.60	383
PCC	0.40	480

Table 6. 7 Flux values of oxygen

Concrete mix (W/C)	Thickness of cover (mm)	Flux ($\times 10^{-14}$mol $O_2/cm^2 \cdot sec$)
0.32	20	11.3
	50	12.6
0.40	20	7.0
	50	10.0
	50*	436
0.60	20	5.2
	50	8.3
PIC	20	53.7
	50	105
PCC	20	6.8
	50	7.9

* 80%R.H.

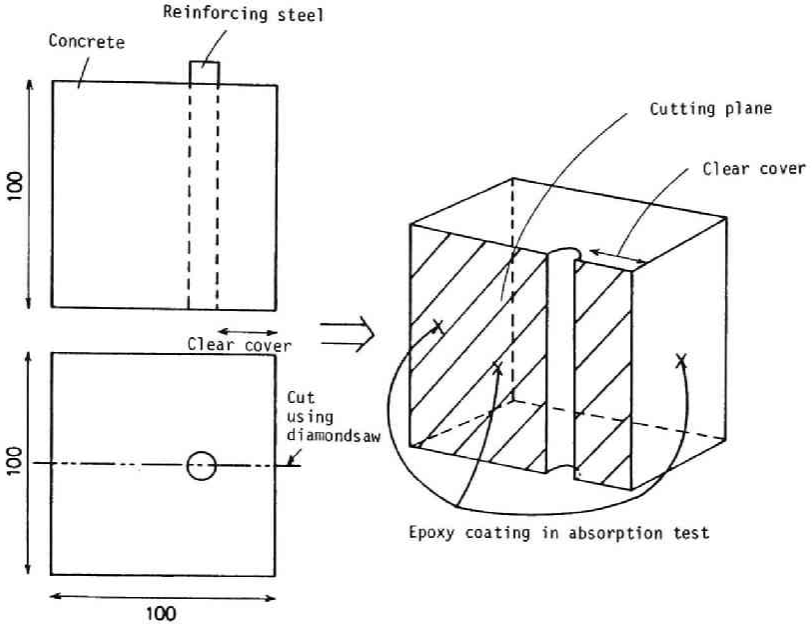

Fig. 6. 1--Specimens for absorption test and porosity test

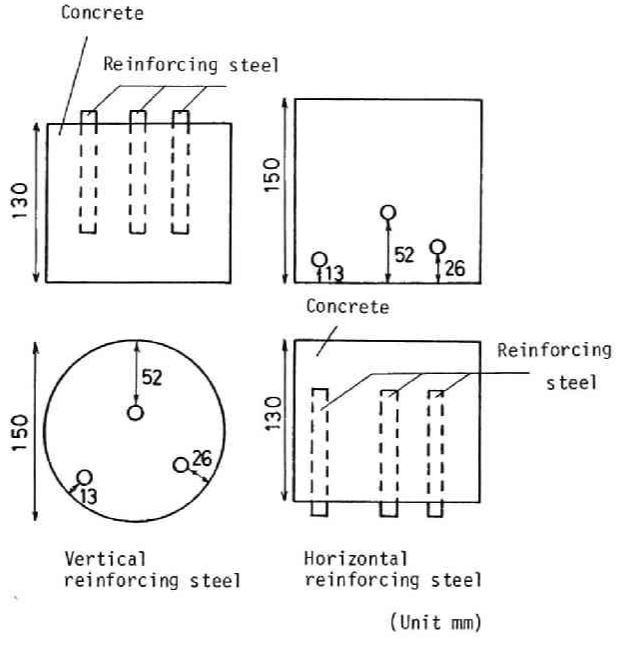

Fig. 6. 2--Specimens for accelerated corrosion test and polarization test

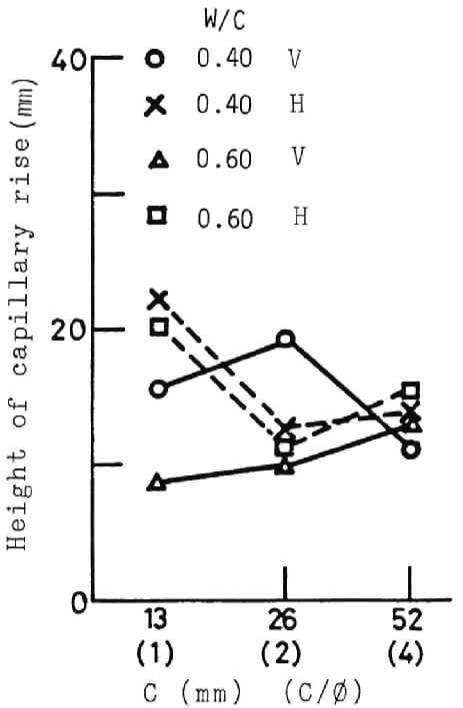

Fig. 6. 3--Average height of capillary rise (Plain concrete)

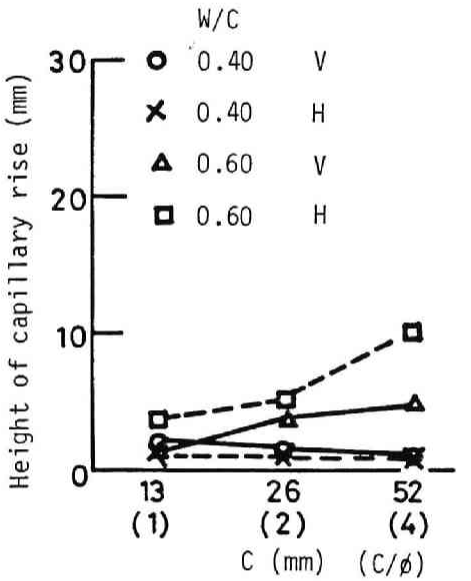

Fig. 6. 4--Average height of capillary rise (PIC)

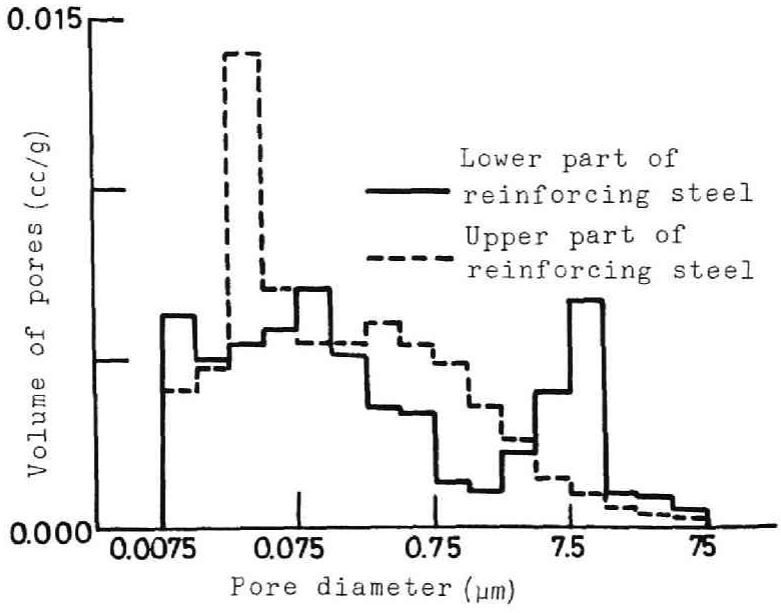

Fig. 6. 5--Pore diameter distribution of mortar (w/c=0.40, Horizontal reinforcing steel)

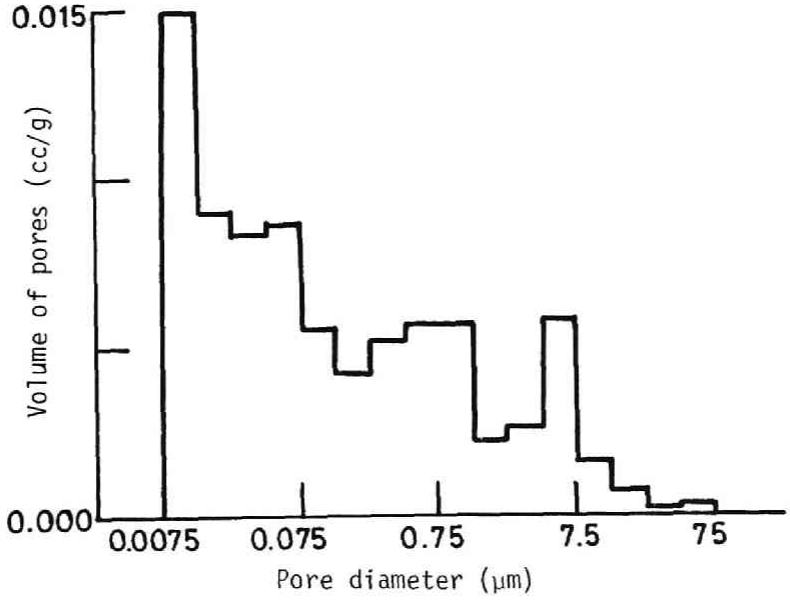

Fig. 6. 6--Pore diameter distribution of mortar (w/c=0.40, Vertical reinforcing steel)

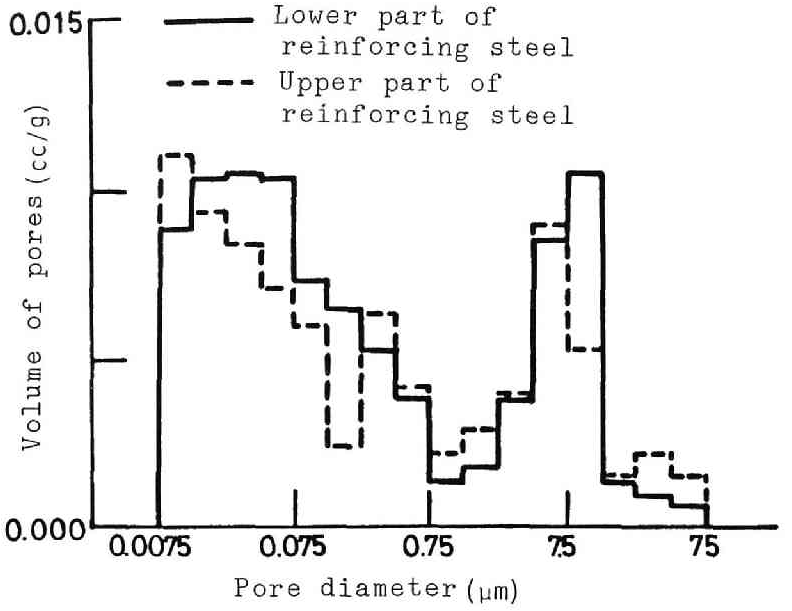

Fig. 6. 7--Pore diameter distribution of mortar (w/c=0.60, Horizontal reinforcing steel)

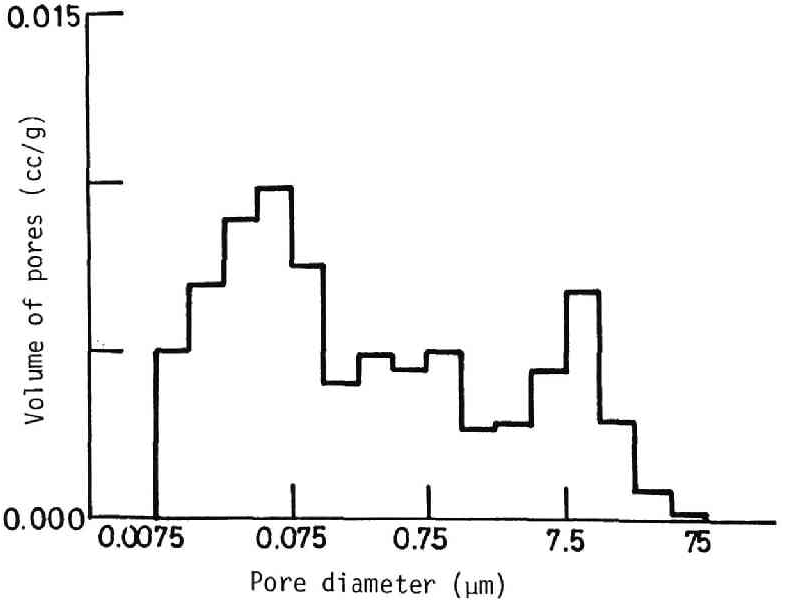

Fig. 6. 8--Pore diameter distribution of mortar (w/c=0.60, Vertical reinforcing steel)

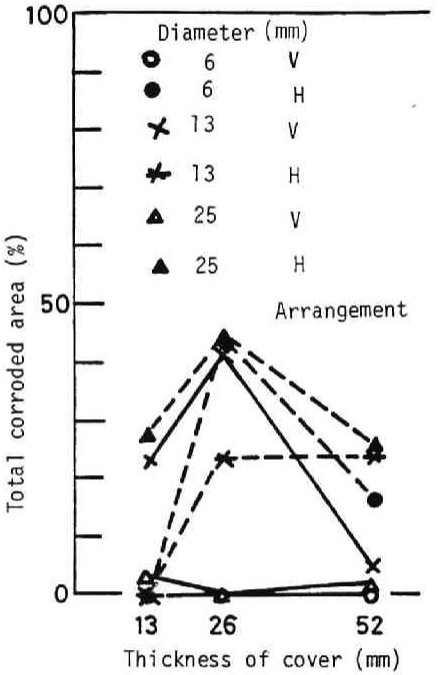

Fig. 6. 9--Relation between total corroded area and thickness of cover (w/c=0.40)

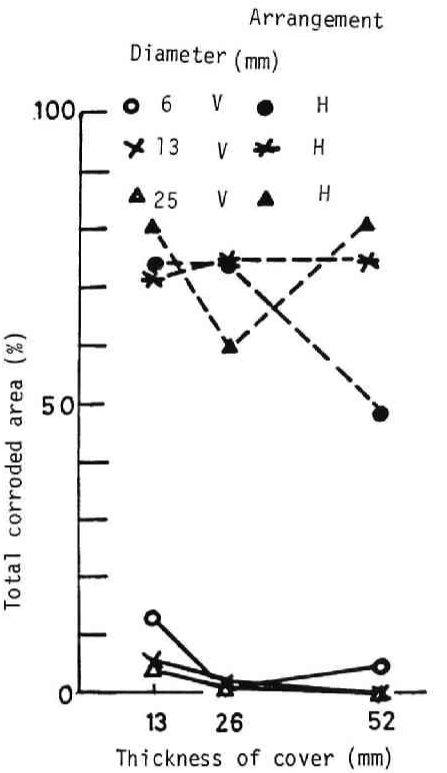

Fig. 6. 10--Relation between total corroded area and thickness of cover (w/c=0.60)

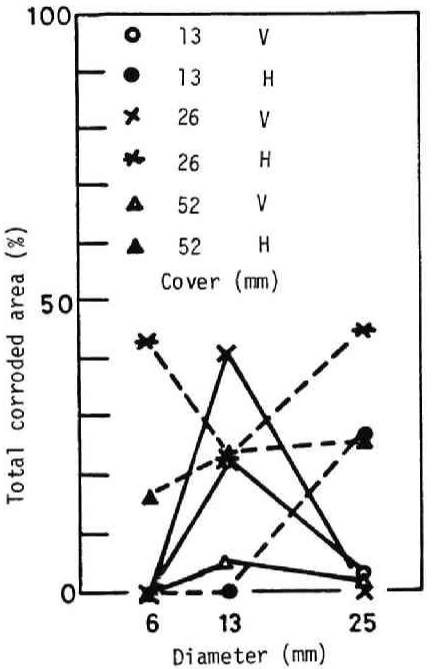

Fig. 6. 11--Relation between total corroded area and diameter of reinforcing steel (w/c=0.40)

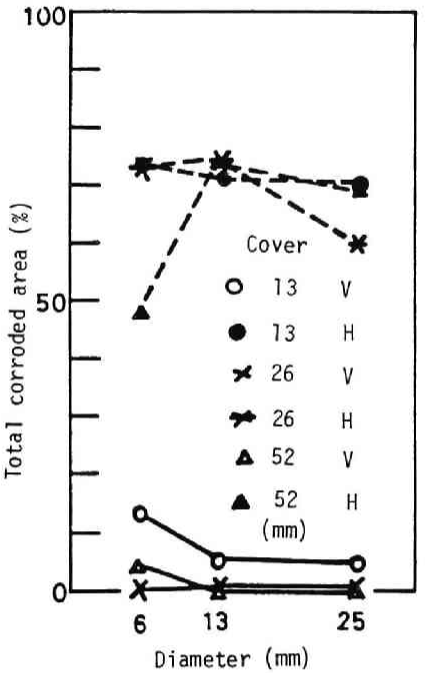

Fig. 6. 12--Relation between total corroded area and diameter of reinforcing steel (w/c=0.60)

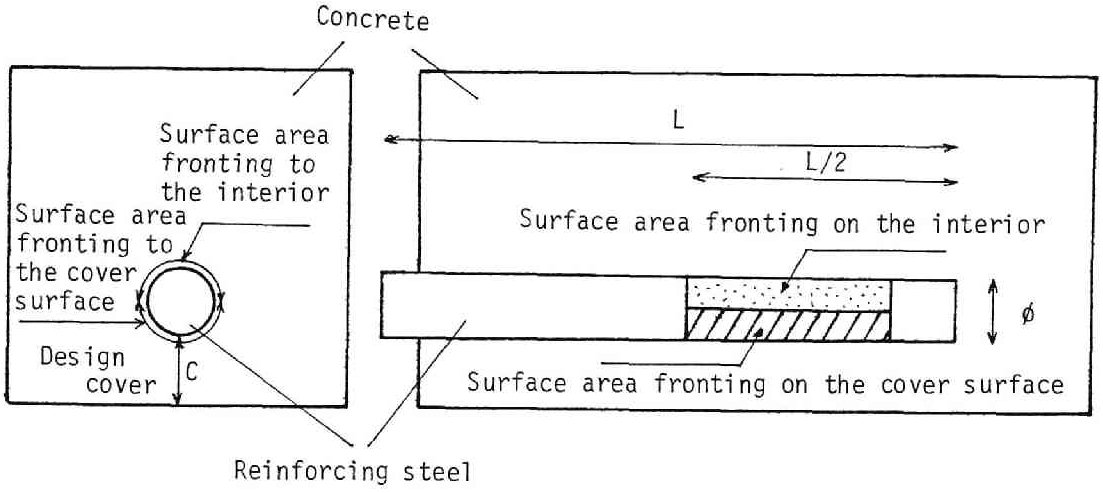

Fig. 6. 13--Schematic view of steel surface with design cover

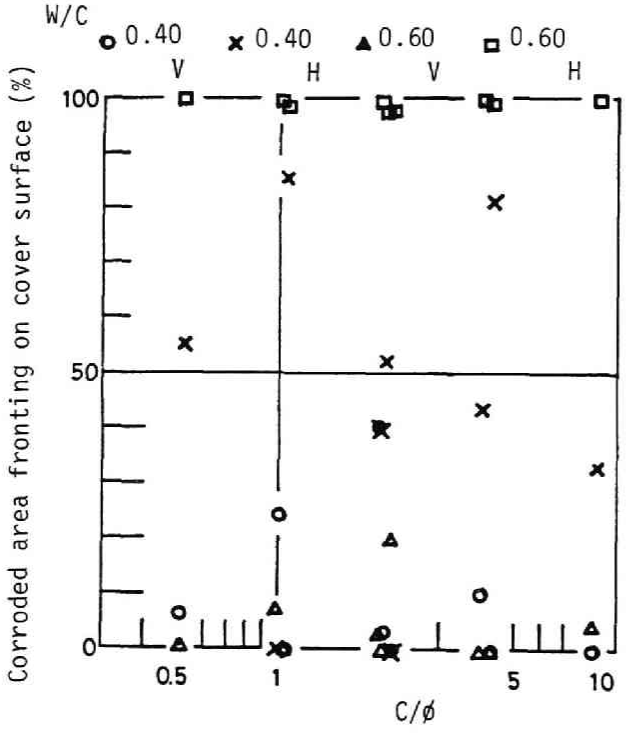

Fig. 6. 14--Influence of C/ø on corroded area fronting on cover surface

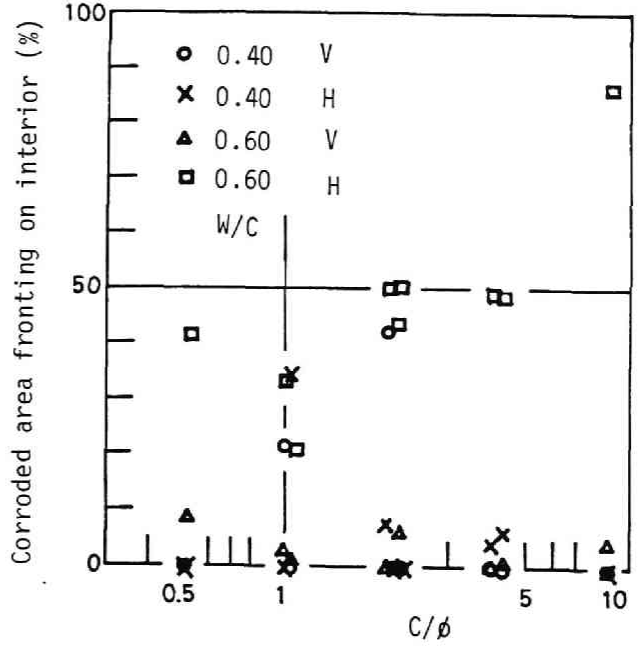

Fig. 6. 15--Influence of C/ø on corroded area fronting on interor

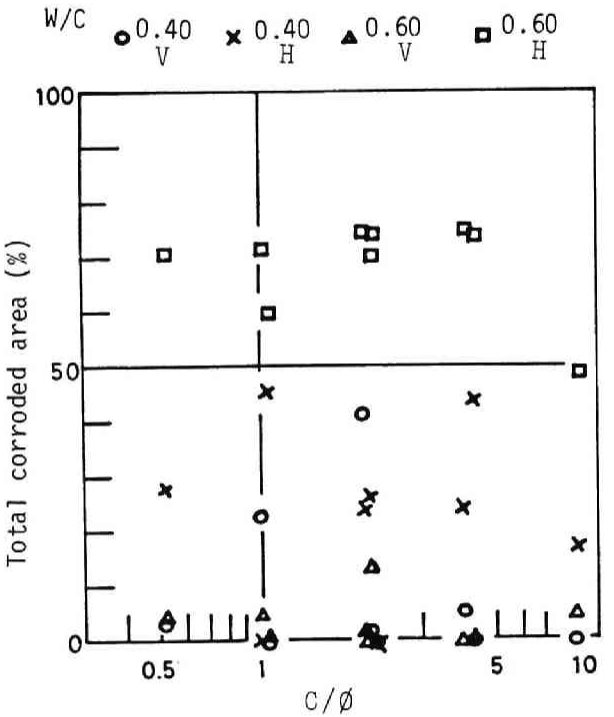

Fig. 6. 16--Influence of C/ø on total corroded area

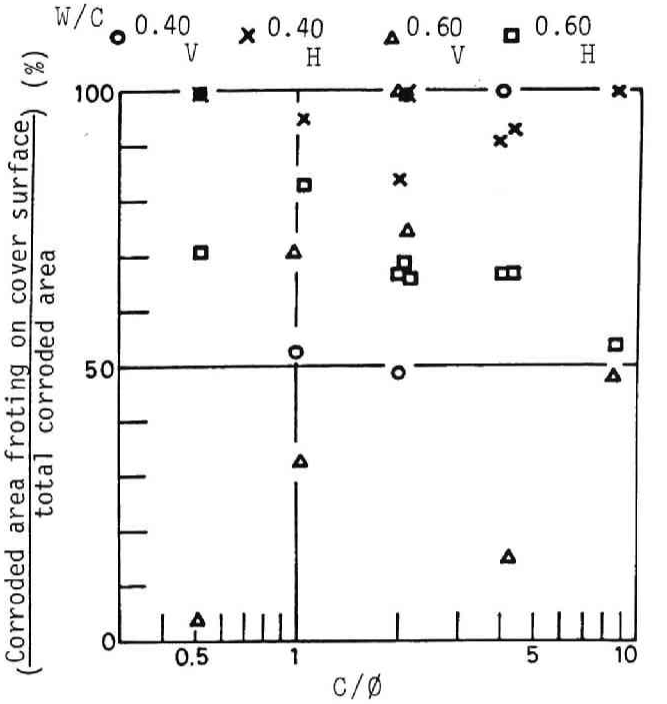

Fig. 6. 17--Influence of C/ø on (corroded area fronting on cover surface / total corroded area)

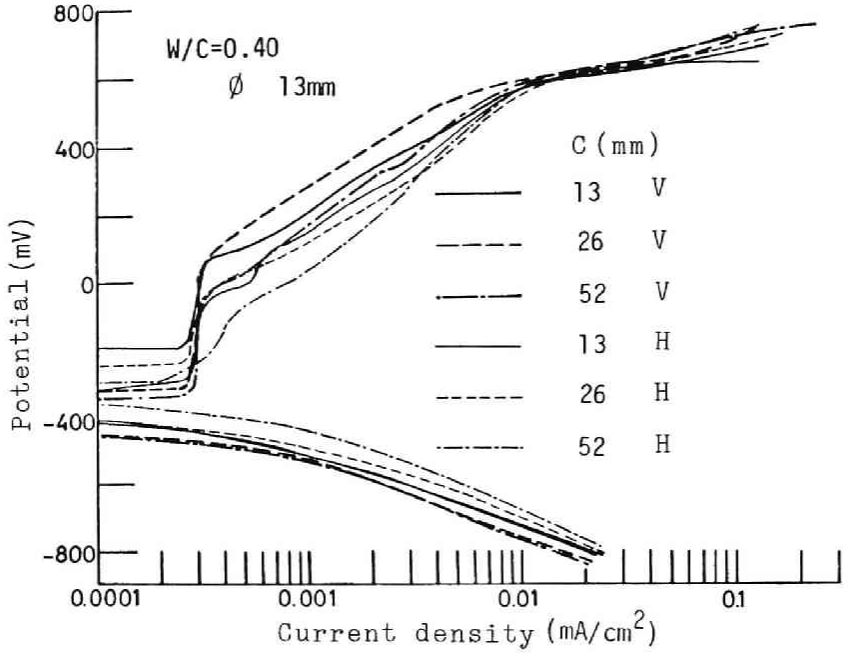

Fig. 6. 18--Potentiostatic polarization diagram (w/c=0.40)

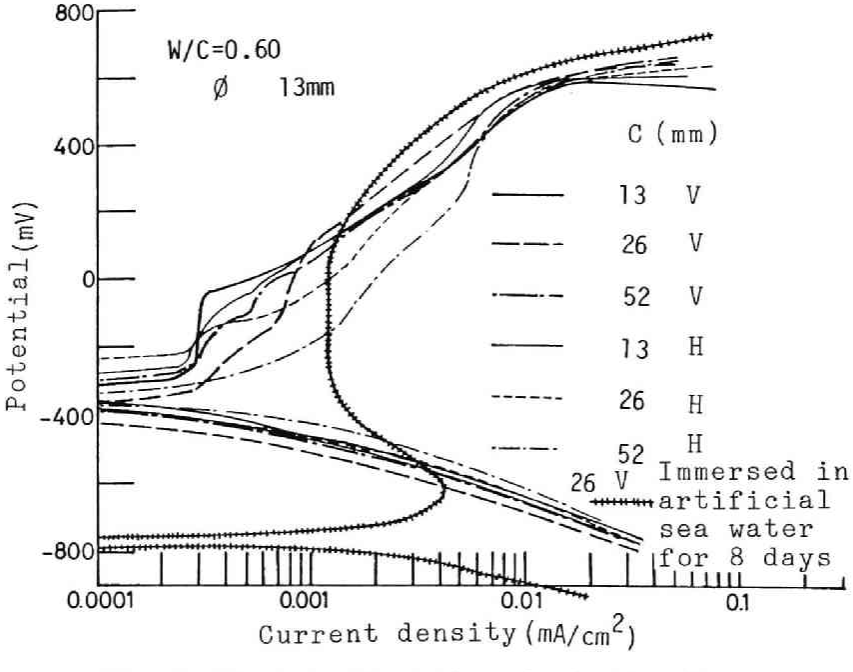

Fig. 6. 19--Potentioatatic polarization diagram (w/c=0.60)

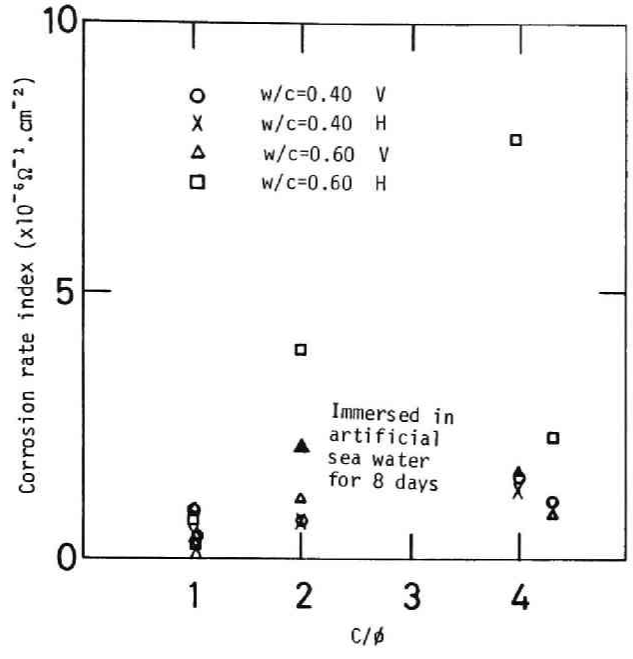

Fig. 6. 20--Influence of C/ø on corrosion rate index

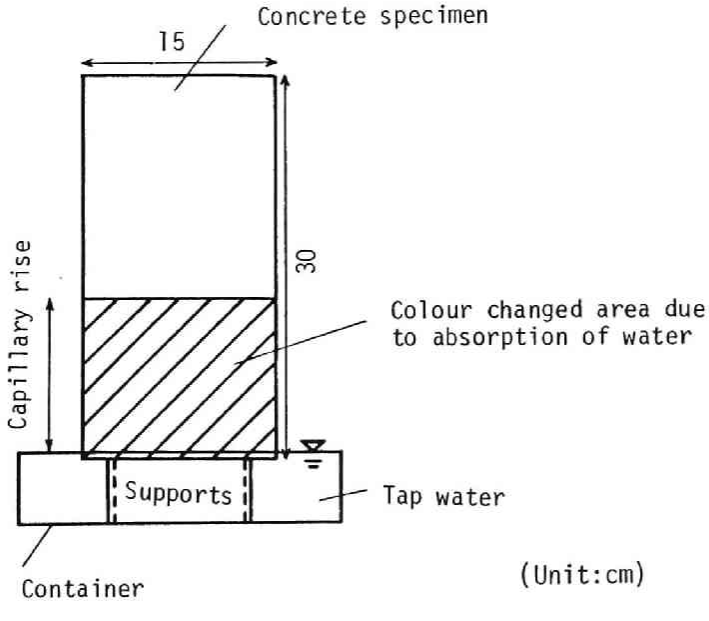

Fig. 6. 21--Test specimen for capillary rise test

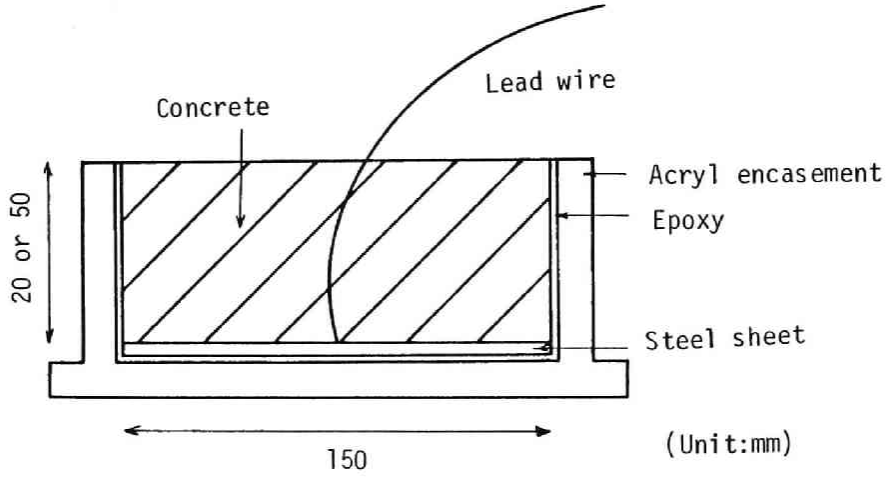

Fig. 6. 22--Test specimen for oxygen permeability test

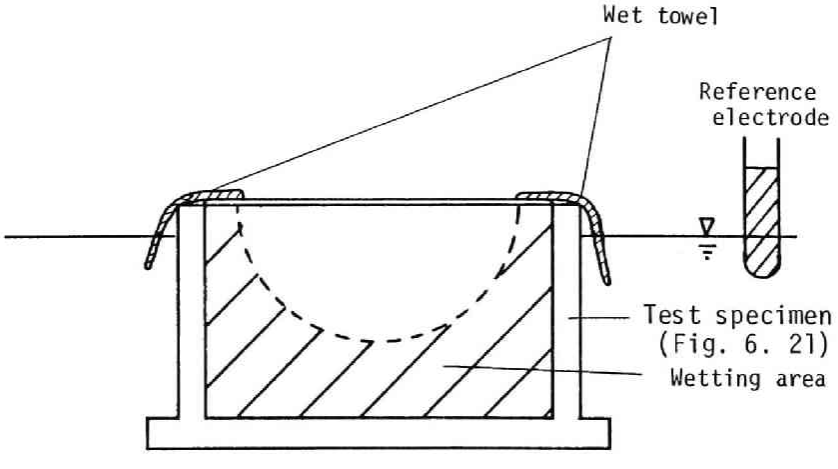

Fig. 6. 23--Schematic view of wet model

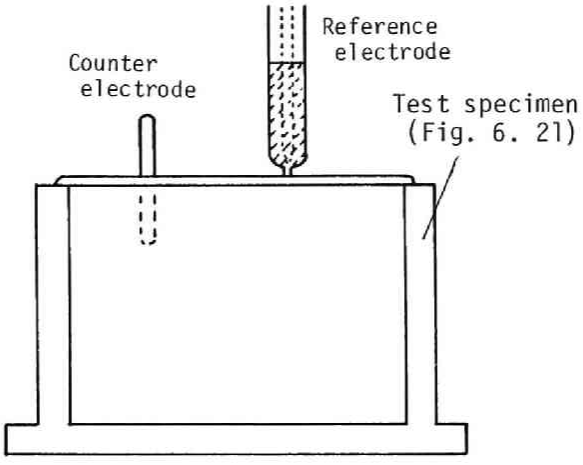

Fig. 6. 24--Schematic view of 80%R.H. model

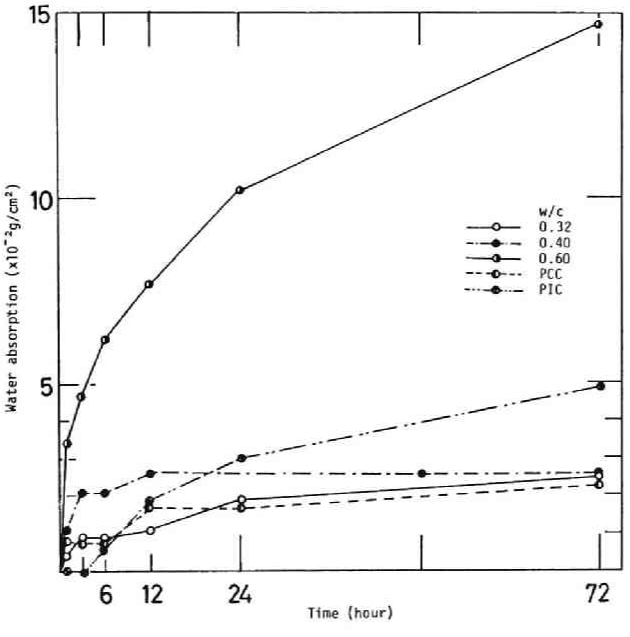

Fig. 6. 25--Water absorption by capillary
(air dried condition)

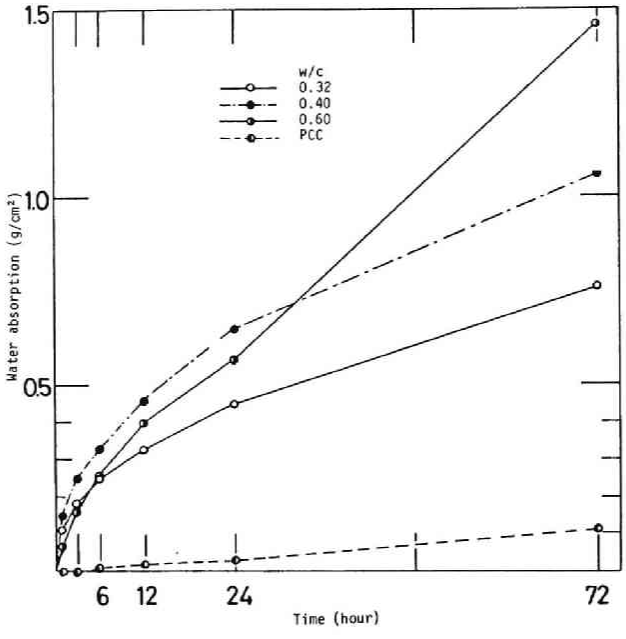

Fig. 6. 26--Water absorption by capillary (oven dried condition)

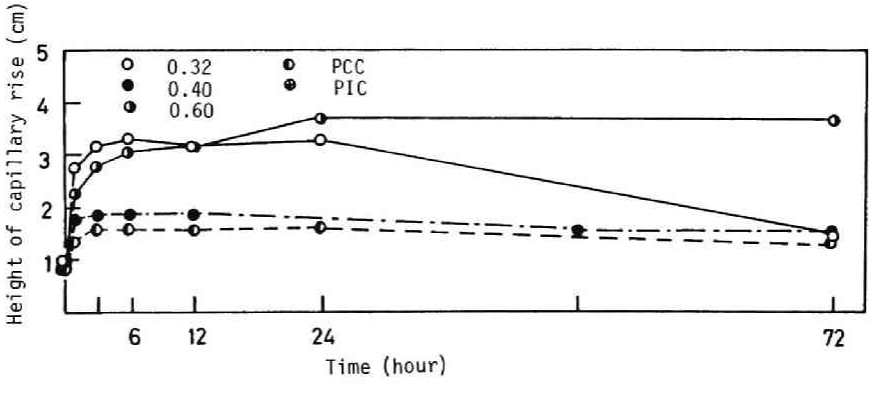

Fig. 6. 27--Height of capillary rise (air dried condition)

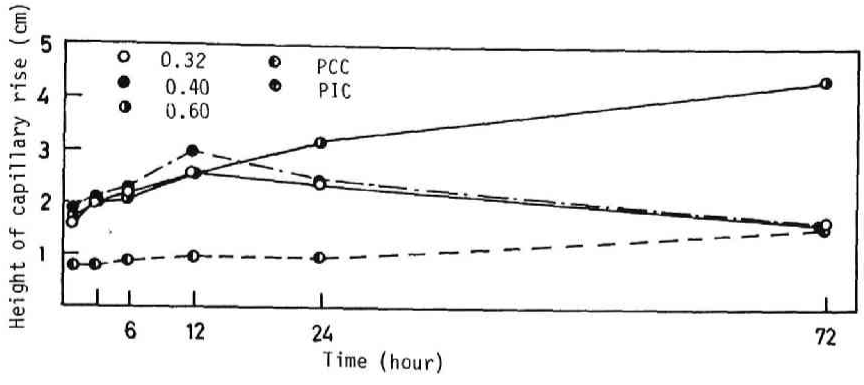

Fig. 6. 28--Height of capillary rise
(oven dried condition)

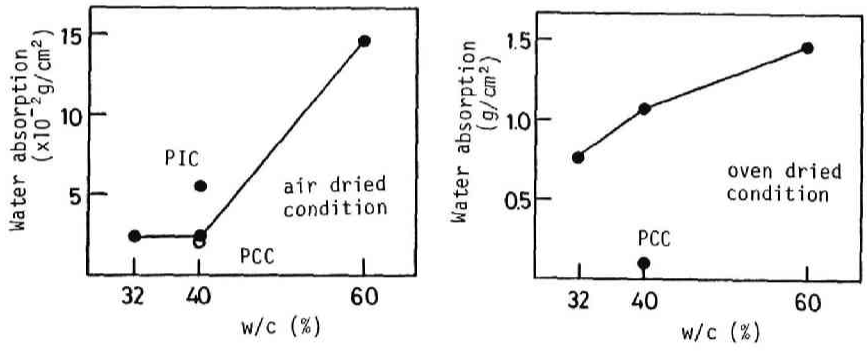

Fig. 6. 29--Relation between water absorption
and water cement ratio

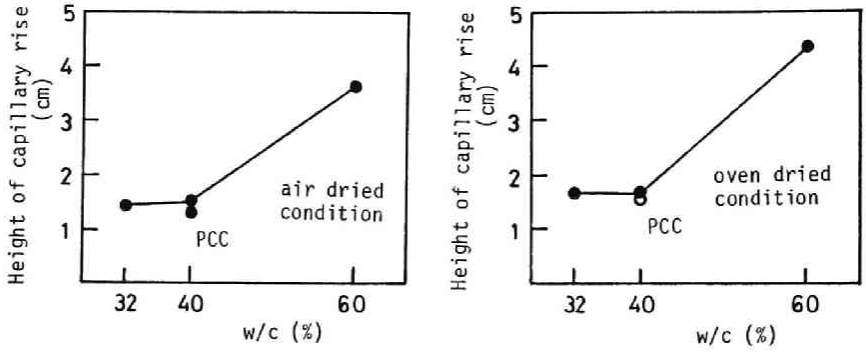

Fig. 6. 30--Relation between capillary rise and water cement ratio

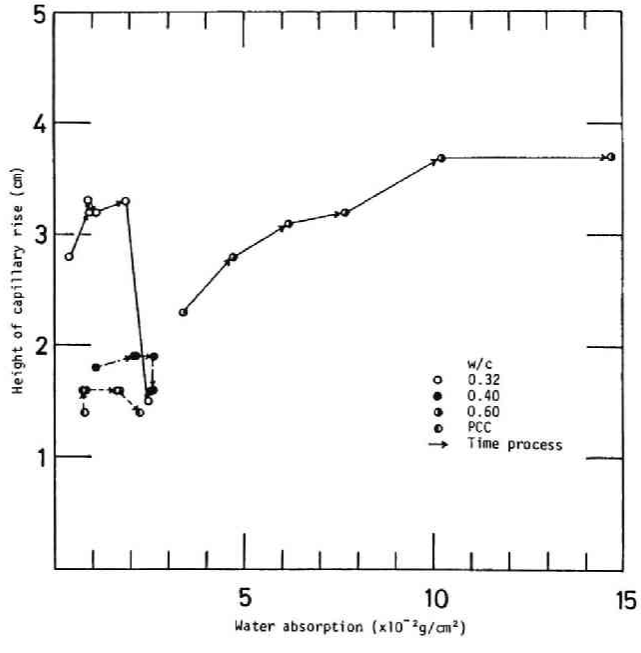

Fig. 6. 31--Relation between water absorption and capillary rise (air dried condition)

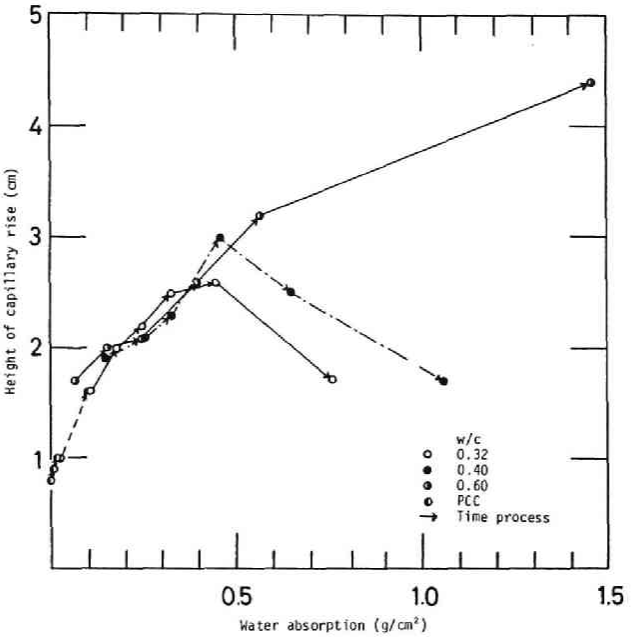

Fig. 6. 32--Relation between water absorption and capillary rise (oven dried condition)

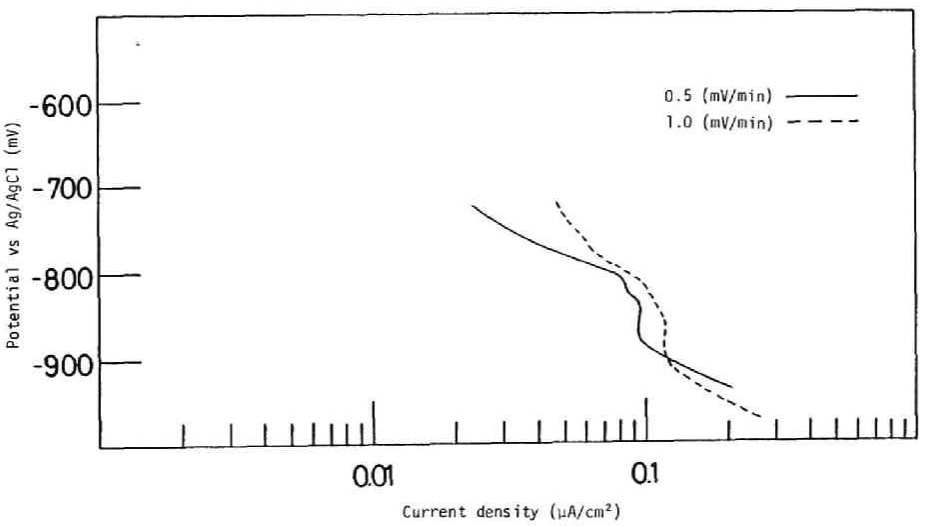

Fig. 6. 33--Typical cathdic polarization

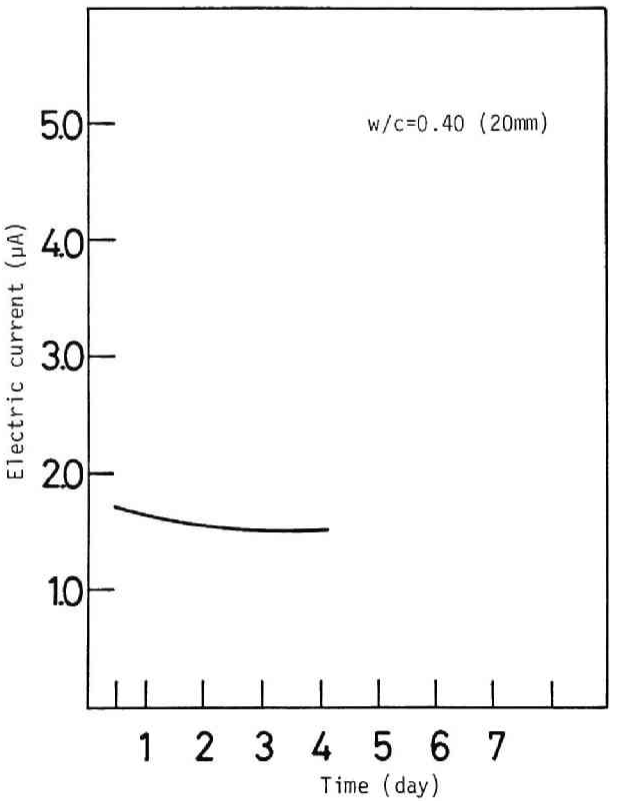

Fig. 6. 34--Typical time dependence of electric current (1)

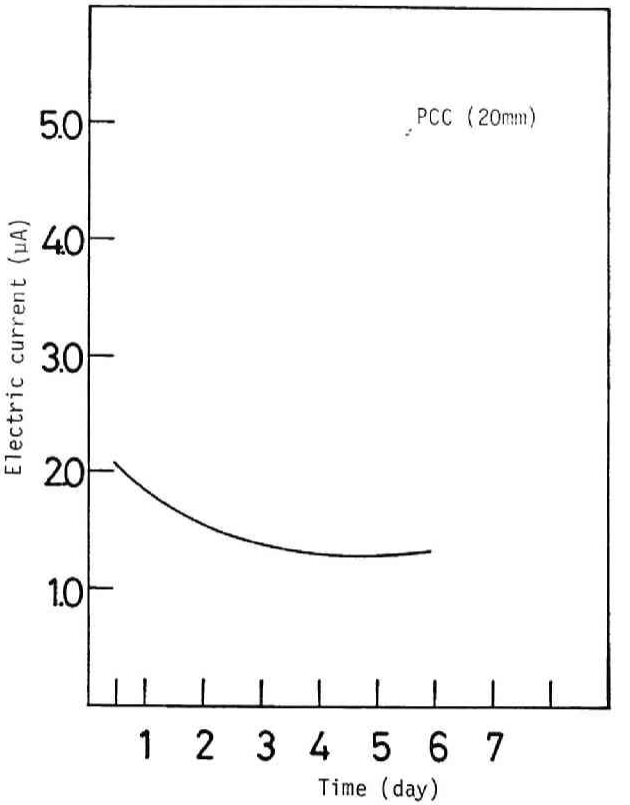

Fig. 6. 35--Typical time dependence of electric current (2)

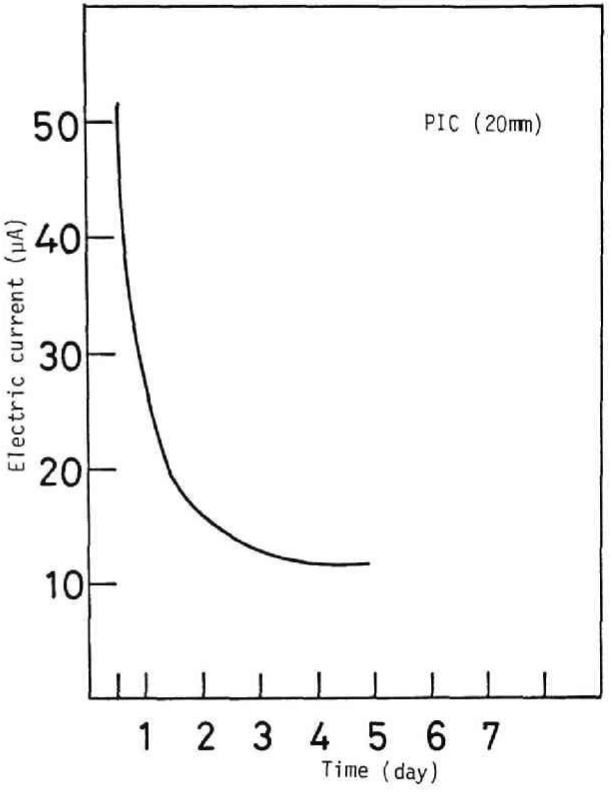

Fig. 6. 36--Typical time dependence of electric current (3)

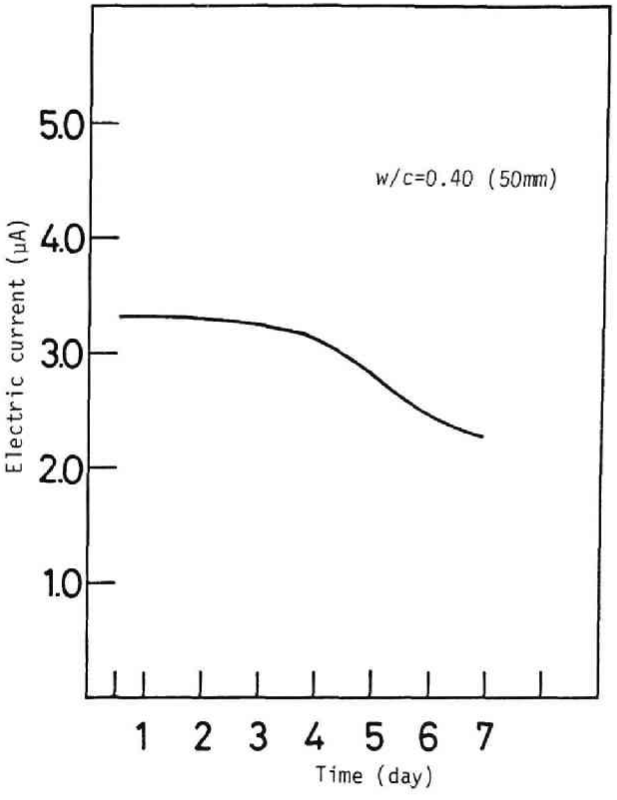

Fig. 6. 37--Typical time dependence of electric current (4)

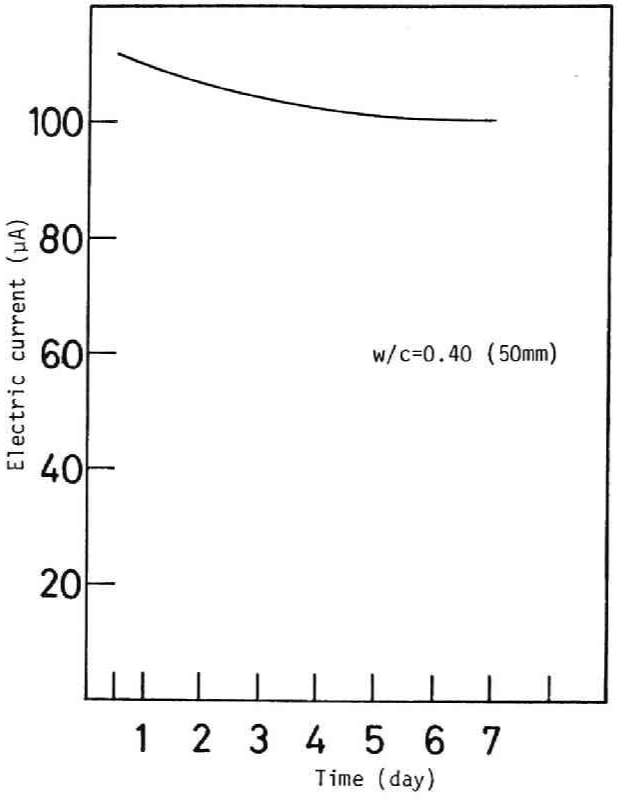

Fig. 6. 38--Typical time dependence of electric current -80%R.H.-

7 CORROSION MONITORING METHOD FOR CONCRETE STRUCTURES

7.1 Introduction

The progress of corrosion reaction cann't easily be detected until longitudinal cracks or rust stains occur on the concrete surface. The repair of concrete structures damaged by corrosion of reinforcement should be carried out as early as possible after corrosion is started (7.1). It is therefore important, for maintenance purpose to develop monitoring techniques for determining corrosion characteristics of reinforced concrete.

In Chapters 3 - 6, various types of non-destructive testing methods were used to determine the corrosion properties of reinforcing steel embedded in concrete specimen. However, there remain some problems in applying the measuring methods to field tests. On the other hand, the half cell potential method can be more easily applied to field tests, as it needs no special equipments and no difficult procedures, though the relations between obtained values and actual corrosion condition are not clear.

The purpose of this chapter is to examine the time dependence of potentials of reinforcing steel and applicability of half cell potential method to field tests.

7.2 Corrosion Detection Technique

The most reliable method for detecting corrosion of reinforcing steel is to measure directly the corroded area and the weight loss due to corrosion. This destructive method, however, needs much time and labour. And, as a non-destructive technique, the electrochemical measurement may be worth-while more investigations.

Bazǎnt (7.2) presented the electrochemical corrosion model of reinforcing steel, which is characterized by parameters such as (1) diffusion of oxygen and chloride ions through the concrete cover, (2) production, diffusion and mass sinks of corrosion products, (3) cathodic and anodic electric potentials according to Nernst equation and their polarizations, (4) flow of electric current through the electrolyte in pores of concrete, and so on. Parameter (3) implies the existence of corrosion reaction, and (4) does the rate of corrosion reaction.

Tuutti (7.3) suggested that measuring the potential levels and differences of reinforcing steel was useful for detecting steel corrosion which could be calculated by using Ohm's law when the electric resistance of concrete was known.

Several corrosion monitoring methods, such as the electrical resistance probe method (7.4) and the measurement of electric resistance of cover concrete (7.5) are used, but the half cell potential method and the polarization resistance method are considered most reliable.

7.2.1 Half Cell Potential Method

As the corrosion of reinforcing steel in concrete results from electrochemical process, the electrical half cell potential technique may be used advantageously to assess the corrosion potential of reinforcement. According to ASTM C876 (7.6), the measured potential E by the laboratory test results of reinforced concrete specimens has the following significance.

1) -0.20 V vs CSE (-0.09 V vs Ag/AgCl) $< E$

   If the potential < -0.20 V, there is greater than 90% probability that no corrosion is occurring in that area at that time.

2) -0.20 V $\geq E \geq -0.35$ V vs CSE

   Corrosion activity of the reinforcing steel in that area is uncertain.

3) $E < -0.35$ V vs CSE (-0.24 V vs Ag/AgCl)

   There is greater than 90% probability of corrosion in the measured area at the time of measurement.

It should be noted that applicability of this method is limited by electrical cicuitry. The concrete surface that has dried to the extent to be dielectric or is covered with water will not provide an acceptable electrical circuit. This method requires no special

probe in concrete for monitoring, and therefore increasingly adopted in the field. But, the corrosion rate must be estimated by using potential distribution.

7.2.2 Polarization Resistance Method

The cathodic reaction of corrosion process of steel in concrete is most probably governed by the diffusion of oxygen. And in this case, near the corrosion potential, the relation between polarization and impressed currents can be expressed by the following equation.

$$Icorr = (Ba/2.3)(i/E) = K/Rp$$

Where, Icorr = corrosion current

Ba = anodic Tafel slope

i = impressed current

E = polarization

K = constant

Rp = E/i = polarization resistance

This equation is derived with the following assumptions; (1) Only one electrode reaction occurs on the steel surface. (2) The electrode has an uniform surface. And, (3) the electrolyte doesn't move. These assumptions, however, are probably not valid in the practical case of corrosion of reinforcing steel. It is, therefore, desirable to obtain the constant coefficient K by using other appropriate techniques, for instance, the weight loss method.

Applying this method to existing structures may require a large

amount of electric current to polarize the reinforcing steel, and accurate control of polarization will be very difficult. Thus, the comparable small steel bar specimen for monitoring, which has the same quality as reinforcement used, must be embedded as close as possible to the reinforcement. But, the macro cell corrosion rate cann't be estimated by simply using this method.

7.3 Test Program

The water cement ratio (W/C) and the cracks of cover concrete influence both the mechanism and rate of steel corrosion. Since the anode and cathode exist apart in a macrocell, the relatively large specimens should be used to measure half cell potentials. The specimens were sprayed with sodium chloride solution (NaCl 3.13% sol.) once a day, and the half cell potentials and longitudinal crack extensions due to corrosion were measured. Six types of specimens, as shown in Fig. 7.1, were prepared, and these were divided into three types as follows.

1) Specimens without cracks, made of concrete having W/C of 0.40 or 0.60 (Type 0.40, Type 0.60)

2) Specimens with transverse cracks above 0.3 mm width, made of concrete having W/C of 0.40 or 0.60 (Type 0.40-crack, Type 0.60-crack)

3) Specimens without cracks, but hybrid type composed of two kinds of concrete having W/C of 0.40 and 0.60 (Type 0.40-0.60-0.40, Type 0.60-0.40-0.60)

7.4 Materials and Test Specimens

7.4.1 Materials

Ordinary Portland cement, Yasu river sand for fine aggregate (Specific gravity = 2.59, F.M. = 2.75) and Kurama crushed gravel for coarse aggregate (Specific gravity = 2.63, Maximum size = 10 mm) were used in concrete mix. And, deformed reinforcing steels (D10, SD35) with mill scale were also used.

7.4.2 Mix Proportion

The water cement ratio were chosen as 0.40 and 0.60, each representing typical good and poor quality of concrete, respectively. A weight of mixing water of 196 kg/m^3 was used to obtain constant slump of concrete. Table 7.1 shows the mix proportions of concrete tested.

7.4.3 Test Specimens

The test specimens are shown in Fig. 7.1. The cover thickness of reinforcing steel was 20 mm throughout the tests. One day after casted, all of the test specimens were stripped and covered with wet burlaps for four weeks.

7.5 Test Procedures

After cured, all of the specimens were dried in the air for 6 months. And, one day before the test started, the third pointed loading was applied for introducing the flexural cracks due to bending moment.

The half cell potentials were measured on the cover concrete along the reinforcing steel at spacings of 10 cm, using Ag/AgCl reference electrode and the voltmeter of input impeadance 10^{11} ohm.

7.6 Results and Discussions

Typical potential distributions, development of transverse and longitudinal cracks are shown in Figs. 7.2 - 7.7. Spacings and potential differences between the center of anode and cathode, and conditions of corrosion according to ASTM C876 (7.6) are indicated in Tables 7.2 and 7.3.

Measured potentials of specimens type 0.40 and 0.40-crack were less noble until 3 months' spray duration. However, the potentials after 8 months' became more noble, showing the specimens in the passive range according to ASTM C876. On the contrary, the potentials of specimens type 0.60 and 0.60-crack were similar after a long period of spray, showing the specimens in the active region after 8 months'. The potential differences in the specimens of type

0.60 were larger than those of type 0.40.

Near the location of cracks, the potential tended to become less noble at early ages. The potential differences in specimens of type 0.40-crack was larger than those of 0.60-crack. After 8 months' spray, the potential of specimens type 0.40-crack was in the uncertain zone, while that of type 0.60-crack existed in the active region. The spacing between the center of anode and cathode in specimens type 0.60-crack was shorter than in specimens of type 0.40-crack, and the corrosion in the former occurred not only near the cracks but also all over the reinforcement.

In specimens type 0.40-0.60-0.40 and 0.60-0.40-0.60, measured potentials became less noble for that having W/C of 0.60. Longitudinal cracks of cover concrete occurred at the location showing steep potential gradient near the negative peak potential.

The average spacings between the center of anode and cathode ranged from 35 to 95 mm. These values were almost equal to those given by Browne et al. (7.7).

7.7 Field Test

7.7.1 Bridge Deck Slab

Test Program--Tested area was 10x10 m which was a part of

bridge deck slab as shown in Table 7.4. In winter season, deicing salt, $CaCl_2$, was poured during the service life. Test items are also listed in Table 7.4. Potentials were measured using $Cu/CuSO_4$ reference electrode (CSE). The strength of slab concrete was estimated by Schmidt hammer test. These readings were taken at the spacing of 1 m both in the longitudinal and transverse directions of the slab.

Results and Discussions--When water was poured upon the dry concrete surface to measure potentials, potentials became less noble but not active. Thus, measurement of potentials is desired to be made after the water content of concrete becomes large enough and the stable state is reached.

Every electric resistance between reinforcing steels was almost zero. This means that all reinforcing steels in this deck slab weae electrically connected each other.

Distributions of estimated strengths of deck slab concrete and measured potentials of reinforcing steel are as shown in Figs. 7.8 and 7.9. The strength of slab concrete ranged 350 - 450 kg/cm^2, and therefore, the water cement ratio was considered to be relatively low. All of the potentials of reinforcing steels were more noble than -0.2 V vs CSE, that is, in a passive region. This means that reinforcing steel in the deck slab was not corroded because the water cement ratio of slab concrete was low.

7.7.2 Pier of Bridge

Test Program--The bridge pier which was constructed 10 years ago near Osaka Bay in Japan, was chosen for the field tests. Half cell potentials were measured along the tie reinforcement having concrete cover of 20-30 mm. The concrete cover was partially removed to inspect the surface condition of steel.

Results and Discussions--Although the values of measured potentials were slightly affected due to change in the water content of concrete, the shape and gradient of potential distributions didn't change. Typical examples of potential distributions and surface conditions of reinforcing steel, when cover concrete was removed, are shown in Figs. 7.10 and 7.11. Corrosion products were found at locations where the potential became locally less noble. These locations occurred at the same spots where the longitudinal cracks were found in the laboratory test. And, the critical potential was about -250 mV vs CSE.

7.8 Numerical Analysis of Macrocell Corrosion Rate

The numerical analysis was conducted by assuming that the critical potential E_t corresponded to the average of the potentials at the center of anode and cathode as illustrated in Fig. 7.12. Electric potential function can be considered to satisfy the Laplace equation, and thus each potential distribution on the concrete

surface shows similar shape, whatever potential function is adopted, if the ratio among factors such as potential difference, electric resistance, length, etc. are kept constant. Therefore the following limitted conditions were treated in the numerical analysis; the spacing between the center of anode and cathode = 50 cm, potential difference = 300 mV, anode length = 10 cm, cover thickness = 20 cm, and specific resistance of anode and cathode area = 2500 and 4000 ohm.cm (7.8). And, the macrocell corrosion rate was expressed by the electric current from steel surface into concrete cover.

It is shown in Fig. 7.13 that the distribution of macrocell corrosion current changes due to potential distributions. When applying the step function as potential distribution function on the steel surface, large electric current occurs at the location of steep potential gradient. This location coincides with the location where the longitudinal cracks occurred in the laboratory test. And, in the field test, the potential distribution was like a step function showing a large macrocell current. The value 100×10^{-6} A/cm^2 corresponds to a corrosion rate of 0.1 mm/year.

As the ratio of anode area to total area increases, the average electric current decreases (Fig. 7.14). And, the relation between the electric current and the ratio CR/AR is shown in Fig. 7.15. With an increasing cover thickness from 20 mm to 100 mm, potential differences on the concrete surface decrease as shown in Fig. 7.16.

7.9 Conclusions

In this chapter, corrosion monitoring method of reinforcing steel based on the half cell potential method was investigated. The laboratory test and two field tests were carried out together with the numerical analysis. The conclusions in this chapter are summarized as follows;

(1) The half cell potential method can be effectively used to assess the progress of reinforcing steel corrosion to a relative extent.

(2) The water content of concrete is a major factor influencing the measured half cell potential.

(3) The numerical model analysis proposed in this chapter can estimate considerably well the macrocell corrosion rate.

7.10 References

(7.1) Okada, K., Kobayashi, K., Miyagawa, T., Kutomi, O. and Noi, T., "Corrosion protection of reinforcing steel by using epoxy resin", Proc. of CAJ, Vol. 37, pp. 491-494, Dec. 1983

(7.2) Bažan, Z. P., "Physical model for steel corrosion in concrete sea structures", Jour. of SD, ASCE, Vol. 105, pp. 1137-1166, June 1979

(7.3) Tuutti, K., Private communication, SCCRI, Stockholm, 1979

(7.4) Gjørv, O. E., "Steel corrosion in reinforced and prestressed concrte structures", Nordisk Betong, Vol. 2, No. 4, pp. 147-151, Apr. 1982

(7.5) TRB, "Evaluating existing bridge decks", NCHRP SHP57, pp. 8-20, 1979

(7.6) ASTM C876, "Half Cell Potentials of Reinforcing Steel in Concrete", 1977

(7.7) Browne, R. D. and Domone, P. L. J., " The long-term performance of concrete in the marine environment", Off-Shore Structures, ICE, pp. 49-60, 1974

(7.8) Okada, K. and Miyagawa, T., "Chloride corrosion of reinforcing steel in crcked concrete", ACI SP-65, pp. 237-254, Aug. 1980

(7.9) Miyagawa, T. and Katawaki K., "Testing methods for chloride corrosion of reinforcing steel", Concrete Journal, Vol. 19, No. 3, pp. 48-54, March 1981

(7.10) Okada, K., Kobayashi, K., Miyagawa, T. and Eguchi, I., "Detection Techniques for chloride corrosion of reinforcing steel", Trans. of JCI, Vol. 2, pp. 77-84, Dec. 1980

(7.11) Okada, K., Kobayashi, K. and Miyagawa, T., "Corrosion monitoring method of reinforcing steel in off-shore concrete structures", ACI SP-82, pp. 703-720, Oct. 1984

Table 7. 1 Mix proportion of concrete

Specimem	Slump (cm)	Water cement ratio	Absolute fine aggregate ratio (%)	Unit weitht (kg/m³)			
				Water	Cement	Sand	Gravel
0.40	6±2	0.40	50	196	490	818	830
0.60		0.60	50	196	327	885	899

Table 7. 2 Potential distribution after 3 months' spray

Specimen	Spacing between anode and cathode (cm)	Potential diffrence between anode and cathode (mV)	Condition of corrosion
0.40	—	(35)	Passive region
0.60	50~80(65)	50~60(55)	Uncertaine zone
0.40-crack	30~140(85)	135~170(150)	Partially active
0.60-crack	40~90(60)	120~180(150)	Entirely active
0.40-0.60 0.40	—	(25)	Passive regin
0.60-0.40 -0.60	30~90(65)	60~95(75)	Almost entirely active

( ):Average value

Table 7. 3 Potential distribution after 8 months' spray

Specimen	Spacing between anode and cathode (cm)	Potential difference between anode and cathode (mV)	Condition of corrosion
0.40	—	(35)	Passive region
0.60	40~180(75)	25~85(50)	Entirely active, longitudinal cracks
0.40-crack	30~100(50)	25~100(53)	Uncertaine zone
0.60-crack	20~60(35)	25~145(75)*	Entirely active, longtudinal cracks
0.40-0.60-0.40	80~100(90)	115~185(155)	Partially active, longitudinal carcks
0.60-0.40-0.60	30~100(95)	95~150(120)	Almost entirely active, longitudinal cracks

( ):Average value * Many small ups and downs

Table 7. 4 Test deck

Item	
Construction	1963
Service life	1964-1978
Test Schedule	10-14/8/1979
Design strength of concrete	350kg/cm^2
Test	Strength by Schmidt hammer, Potential of reinforcing steel, Electric resistance between reinforcing steels

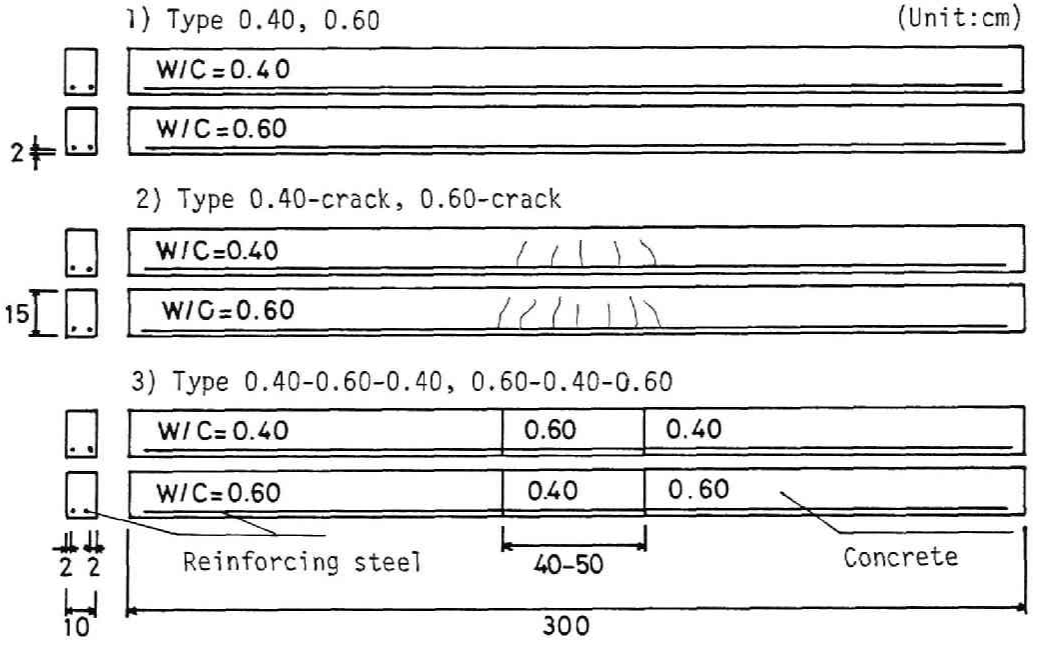

Fig. 7. 1--Types of specimens for laboratory test

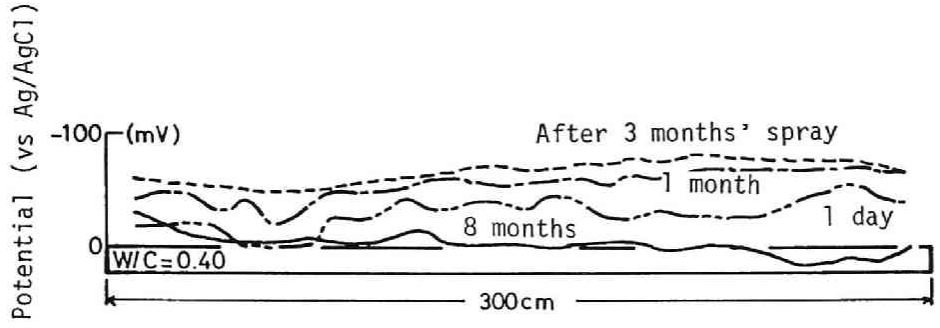

Fig. 7. 2--Potential distribution (Type 0.40 specimen)

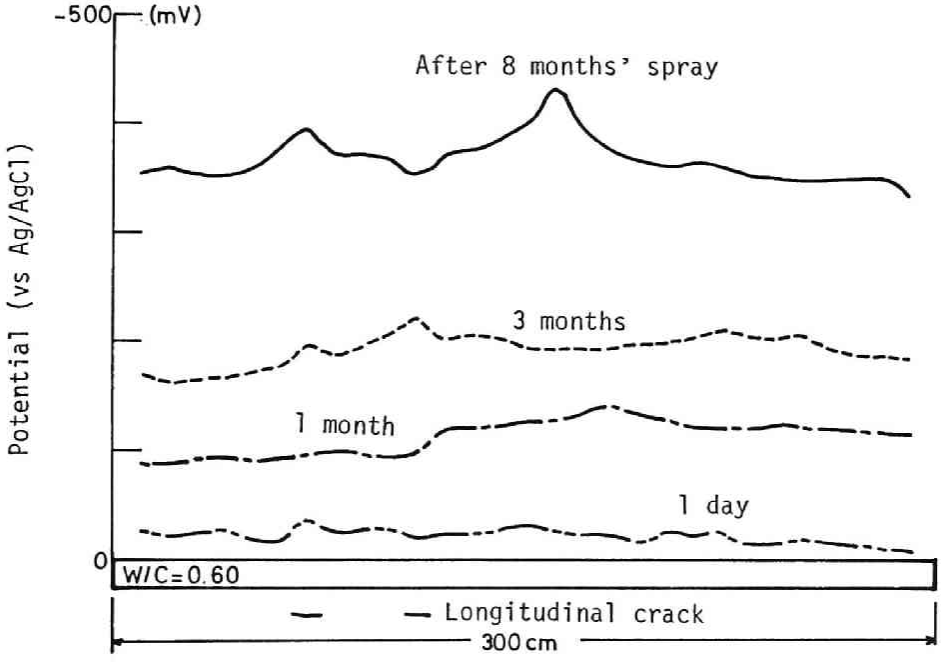

Fig. 7. 3--Potential distribution (Type 0.60 specimen)

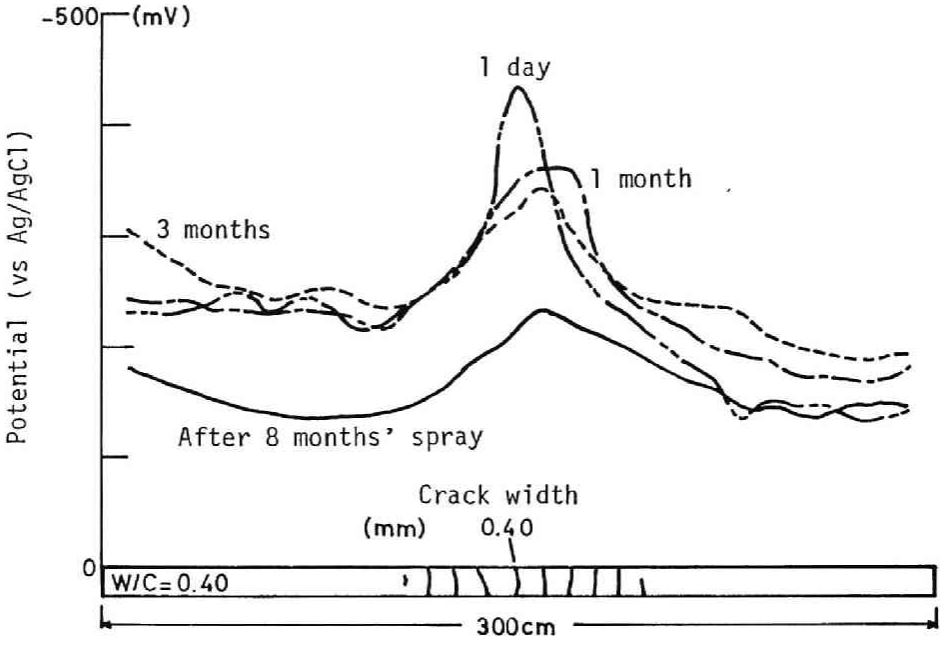

Fig. 7. 4--Potential distribution (Type 0.40-crack specimen)

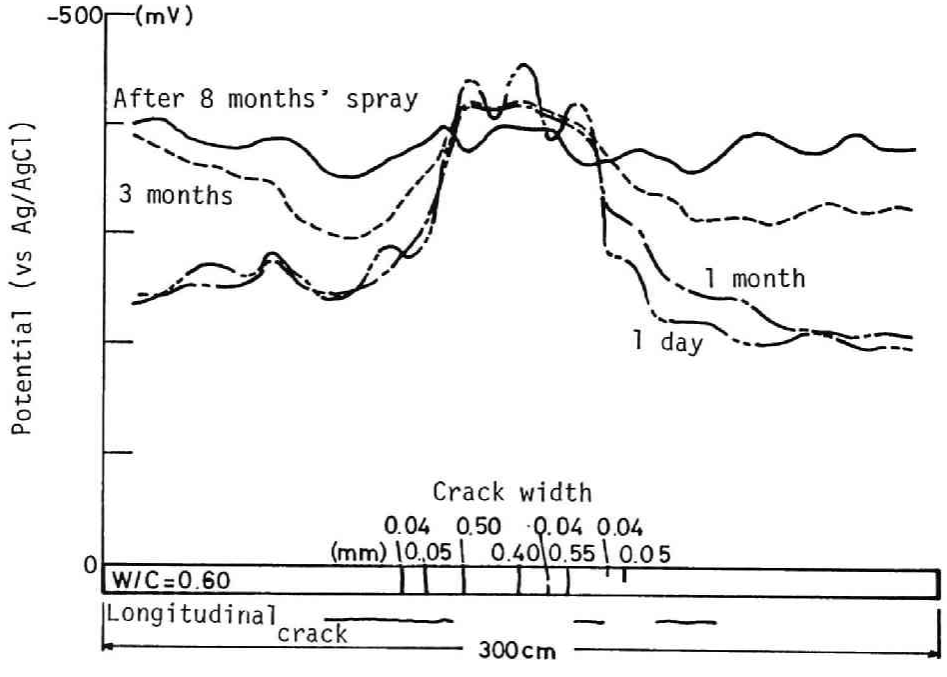

Fig. 7. 5--Potential distribution (Type 0.60-crack specimen)

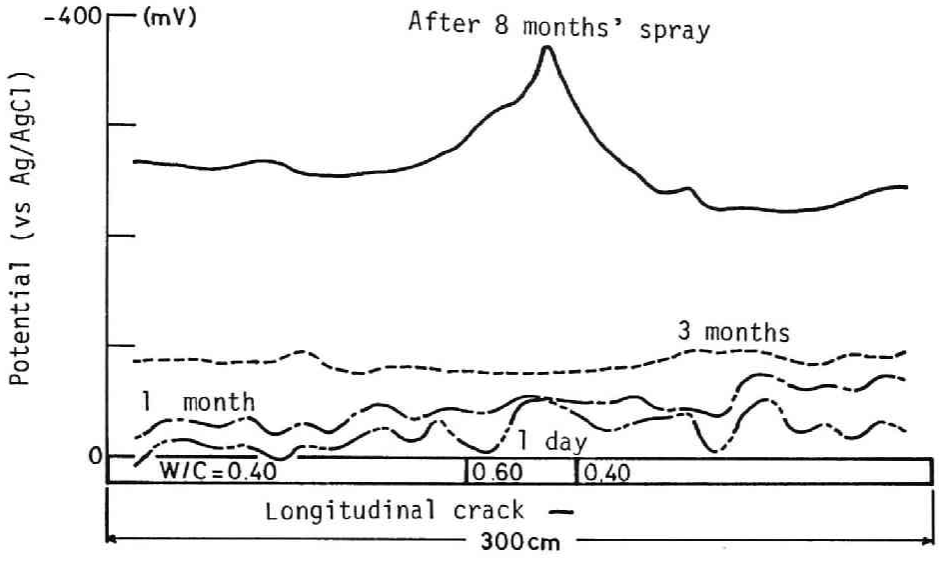

Fig. 7. 6--Potential distribution (Type 0.40-0.60-0.40 specimen)

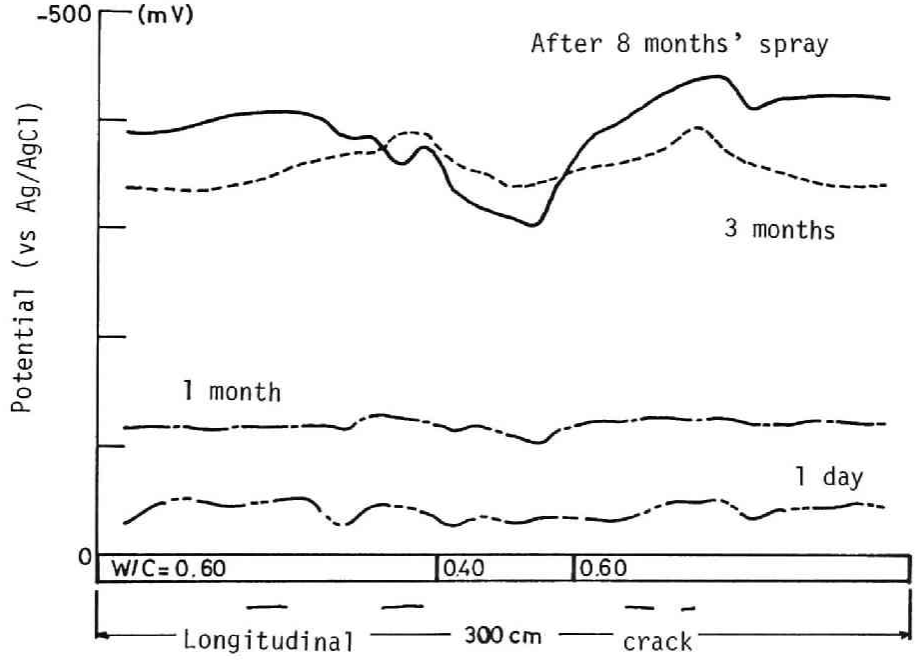

Fig. 7. 7--Potential distribution (Type 0.60-0.40-0.60 specimen)

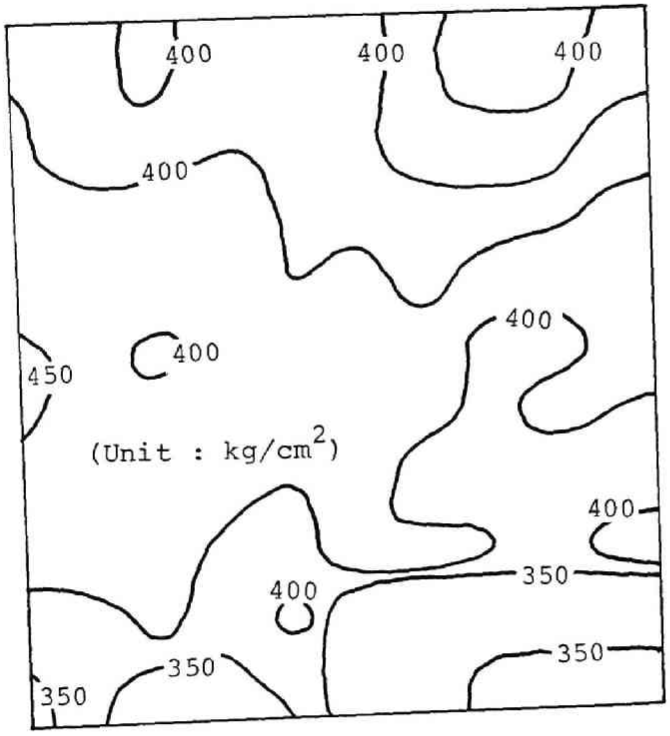

Fig. 7. 8--Equi-strength contour map using Schmidt hammer

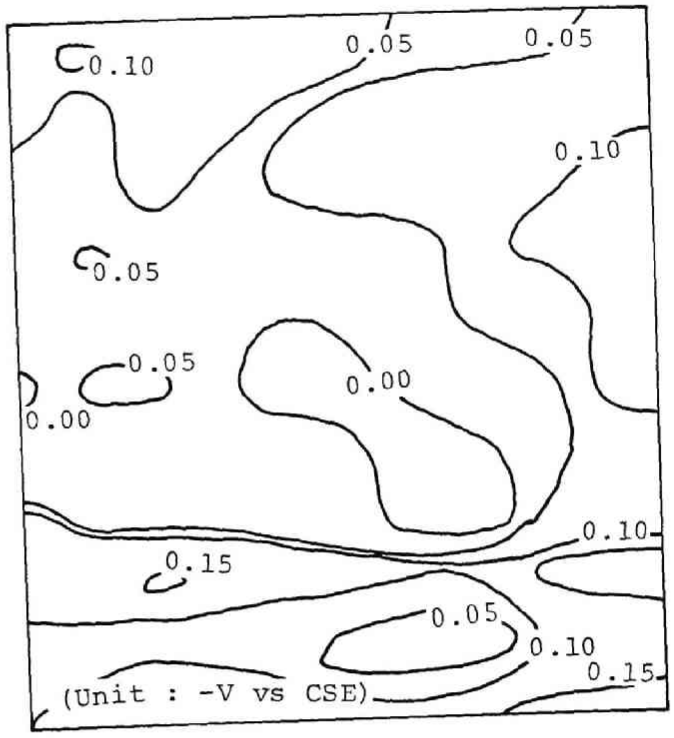

Fig. 7. 9--Equi-potential contour map

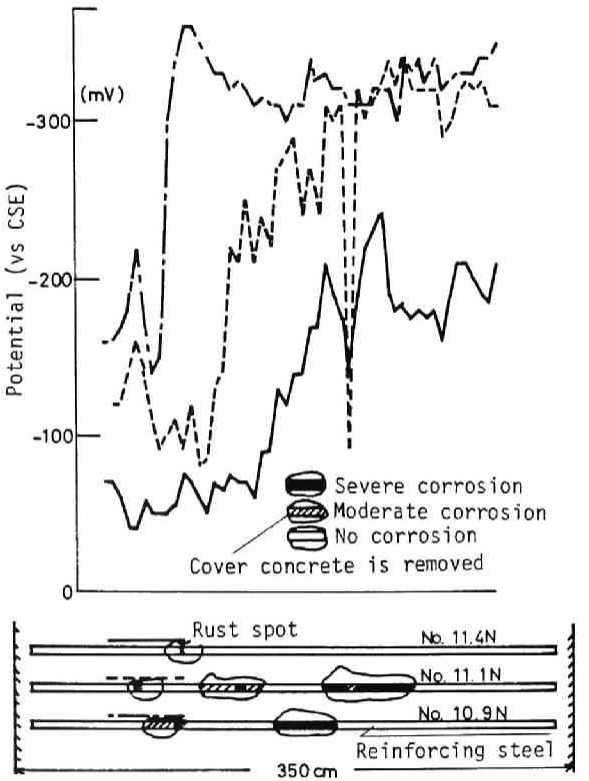

Fig. 7. 10--Typical potential distributions of field structure (1)

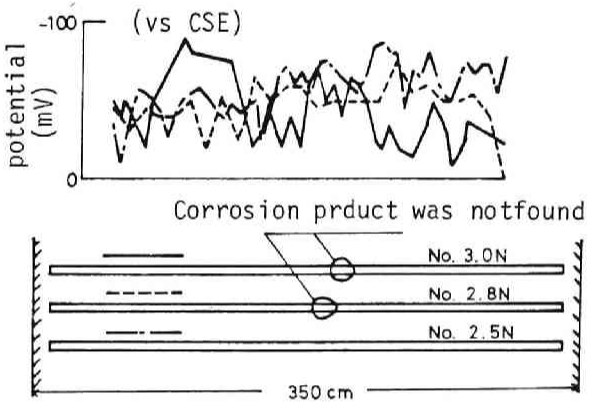

Fig. 7. 11--Typical potential distributions of field structure (2)

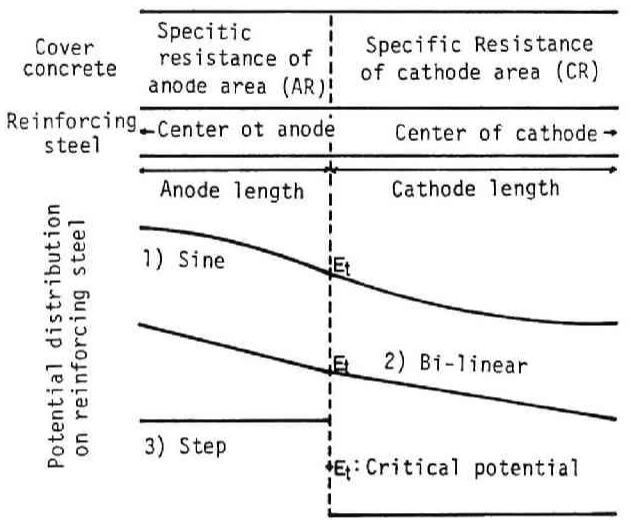

Fig. 7. 12--Assumption for numerical analysis

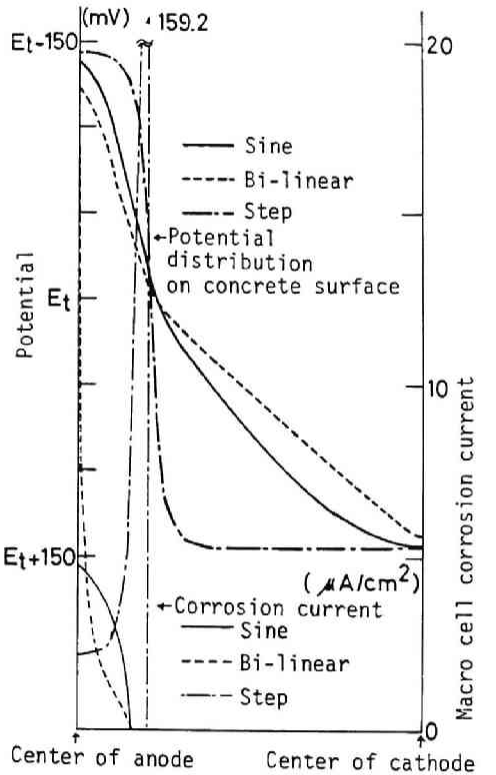

Fig. 7. 13--Potential distribution on concrete surtace and macro cell corrosion current density of reinforcing steel

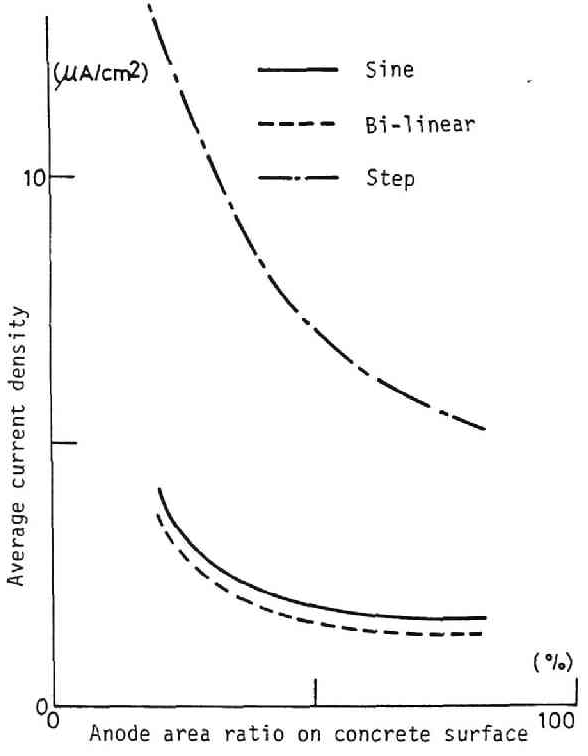

Fig. 7. 14--Relation between anode area ratio on concrete surface and average current density

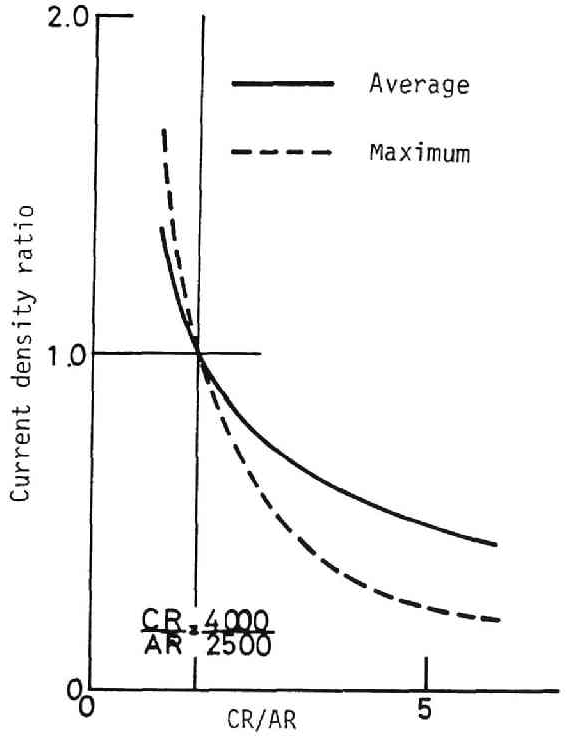

Fig. 7. 15--Influence of CR/AR on current density

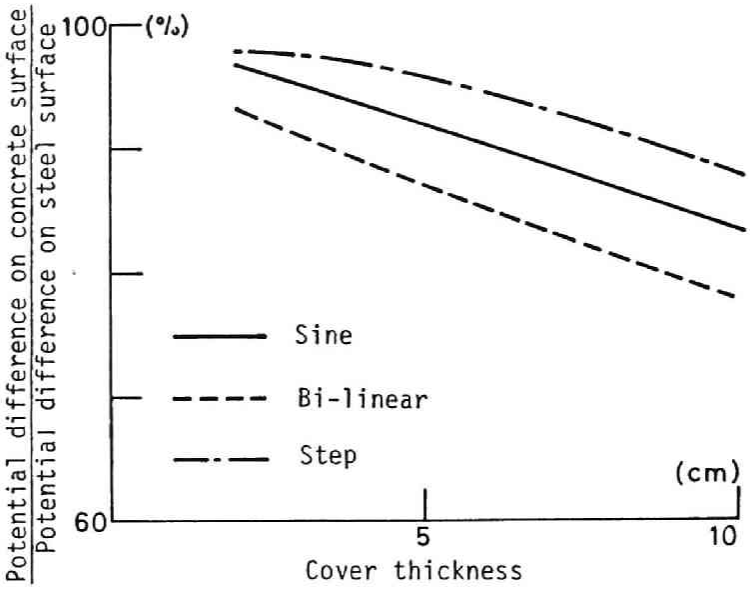

Fig. 7. 16--Influence of cover thickness on potential difference

8 CONCLUSION

This work aimed at a systematical approach for chloride corrosion problems of reinforcing steel embedded in concrete. Main objectives of this thesis were to investigate the mechanism and rate of reinforcement corrosion in both the cracked and uncracked concretes, and then to propose the corrosion monitoring technique based on the half cell potential method.

The conclusions obtained in each chapter were already described in detail at that end. Their main purposes and important results are reviewed in this chapter and the recommendations essential for further studies are summarized as follows.

In Chapter 3, the accelerated corrosion test of reinforcing steel in concrete was carried out under raised temperatures. The influences of salt concentration in mixing water, of crack width in concrete cover and of surface condition of reinforcing steel on the corrosion rate and mechanism were investigated.

(1) The accelerated corrosion test at higher temperature (40 - 60^{o}C) and high humidity (90% R.H.) is very effective in shortening the time of testing.

(2) The cracks of width less than 0.06 mm scarecely influence on the whole corrosion, but have significant effects just around the cracks.

(3) The corroded area of reinforcing steel embedded horizontally in concrete is much larger on the lower surface than on the upper surface.

(4) According to the accelerated corrosion test used here, the critical chloride content inducing severe corrosion is 2.5 kg/m^3.

In Chapters 4 and 5, the chloride corrosion of reinforcing steel in cracked concrete was investigated. The rate of crack corrosion and mechanism of crack corrosion were discussed in Chapters 4 and 5, respectively.

(1) Wide cracks in the reinforced concrete structures will form the macrocell corrosion of the reinforcing steel.

(2) As the ratio of Ac/Aa increases, both the macrocell current density and corrosion rate at cracks become larger.

(3) According to the experimental method used in this study, the critical crack width is between 0.1-0.2 mm from the view point of reinforcement corrosion.

(4) Water cement ratio influences significantly both the macrocell corrosion rate at cracks and mechanism of corrosion.

(5) As water cement ratio of concrete increases, the half cell potential of reinforcing steel becomes less noble and the electric resistance of cover concrete becomes lower due to high permeability, resultng in acceleration of reinforcing steel corrosion.

In Chapter 6, influences of cover concrete on chloride corrosion of reinforcing steel were discussed.

(1) Each of the water cement ratio of concrete, thickness of concrete cover and arrangement of reinforcing steel in concrete has significant influences on the absorption of chloride solution by concrete and pore size distribution of cover concrete, and finally on the mechanism of chloride corrosion.

(2) Both the water absorption by capillarity and height of capillary rise in concrete increase with an increase in water cement ratio, especially, when $W/C > 0.40$.

(3) Both the diameter of reinforcing steel (ϕ) and thickness of cover (c) should be taken into account in a combined form as expressed by, for instance, c/ϕ ratio to assure effective corrosion protection by concrete.

(4) The environmental condition, such as wetting and drying condition of concrete, is one of the major factors on reinfocement corrosion.

Chapter 7 discussed the corrosion monitoring method for reinforced concrete together with the numerical analysis.

(1) The half cell potential method can be effectively used to assess the progres of reinforcing steel corrosion.

(2) The water content of concrete is a major factor influencing the measured half cell potential.

(3) The macrocell corrosion rate can be estimated considerably well by the numerical model analysis proposed in this study.

In the future, it is strongly hoped that the systematic investigations on the following three items will be carried out to complete the works of this study.

(a) Establishment of corrosion monitoring method for various types of reinforced concrete structures under wide ranges of environmental conditions (8.1 and 8.2).

(b) Maintenance and repair of reinforced concrete structures damaged due to reinforcement corrosion (8.3 and 8.4).

(c) Assessment of environmental condition from a view point of reinforcement corrosion (8.5 and 8.6).

References

(8.1) Okada, K., Kobayashi, K. and Miyagawa, T., "Corrosion monitoring method of reinforcing steel in off-shore concrete structures", ACI SP-82, pp. 703-720, Oct. 1984

(8.2) Miyagawa, T., "Tentative method for measurement of half cell potential of reinforcing steel in concrete", Recommendations for Prevention against Deterioration of Offshre Concrete Structures", pp. 93-97, Feb. 1983

(8.3) Okada, K., Kobayashi, K., Miyagawa, T., Kutomi, O. and Noi, T., "Corrosion protection of reinforcing steel by using epoxy resin", Cement & Concrete, No. 444, pp. 20-27, Feb. 1984

(8.4) Kume, T., Miyagawa, T. and Okada, K., "Synsetic resin lining on concrete surface", Annual Meeting of JSCE, Vol. 39-5, pp. 53-54, Oct. 1984

(8.5) Okada, K., Kobayashi, K., Miyagawa, T. and Honda, S., "Corrosion monitoring system for reinforcing steel using polarization resistance method", Trans. of JCI, Vol. 5, pp. 83-90, Dec. 1983

(8.6) Sano, M., Miyagawa, T. and Kobayashi, K., "Corrosion monitoring of reinforcement in concrete", Annual Meeting of JSCE, Vol. 39-5, pp. 33-34, Oct. 1984

ACKNOWLEDGEMENT

The author is deeply grateful to Prof. Dr. Kiyoshi Okada for suggesting the topic of this thesis, for his valuable guidance and also his patience and perseverence in the author's work.

The author wishes to thank for Dr. Wataru Koyanagi, Prof. of Civil Engineering at Gifu University and Dr. Kazuo Kobayashi, Assoc. Professor of Civil Engineering at Kyoto University, who offered helpful advice and valuable discussions.

The author is indebted to Dr. Takayuki Kojima, Professor of Civil Engineering at Ritsumeikan University, Dr. Kiyoshi Yamura, Assoc. Professor of Civil Engineering at Tottori University and Dr. Keitetsu Rokugo, Assoc. Professor of Civil Engineering at Gifu University, for their discussions and experimental assistance. A debt of gratitude is expressed to Dr. Koji Yamakawa, Professor of Metallurgical Engineering at University of Osaka Prefecture, for his advice and encouragement.

Thanks are also due to Mr. Toshihide Toyofuku, Assistant at Kagawa University, Dr. Muhammad A. Azimi, Mr. Junichiro Katsuragi, Mr. Michiya Ohura, Mr. Satoshi Honda, Mr. Haruo Tomiyama, Mr. Susumu Inoue, Mr. Osamu Kutomi, Mr. Tatsuya Ohno, Mr. Yoshio Kiuchi, Mr. Takeo Noi, Mr. Masaaki Sano, Mr. Takahiro Kume and Mr. Shiro Fujii for their help in experiments.

The assistance in drawing Tables and Figures in this thesis by Miss Masako Kawase and Mr. Akira Tsuda is appreciated.